

Defense - 13/11/2023

Exactly modeling the unitary dynamics of quantum interfaces with collision models

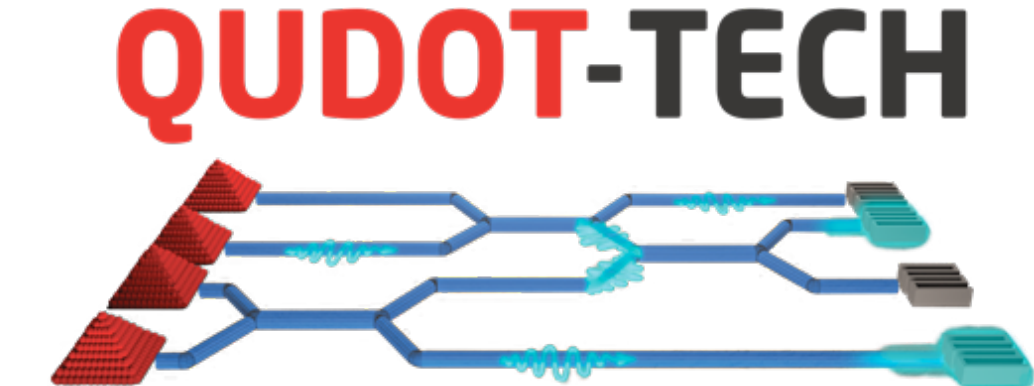
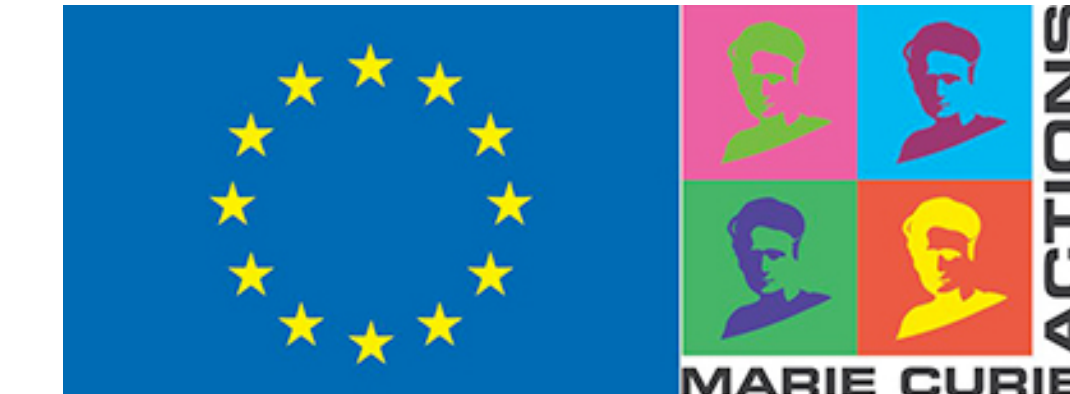
Bruno O. Goes

Université Grenoble Alpes, CNRS, Institut Néel, France

Supervisor: Alexia Auffèves

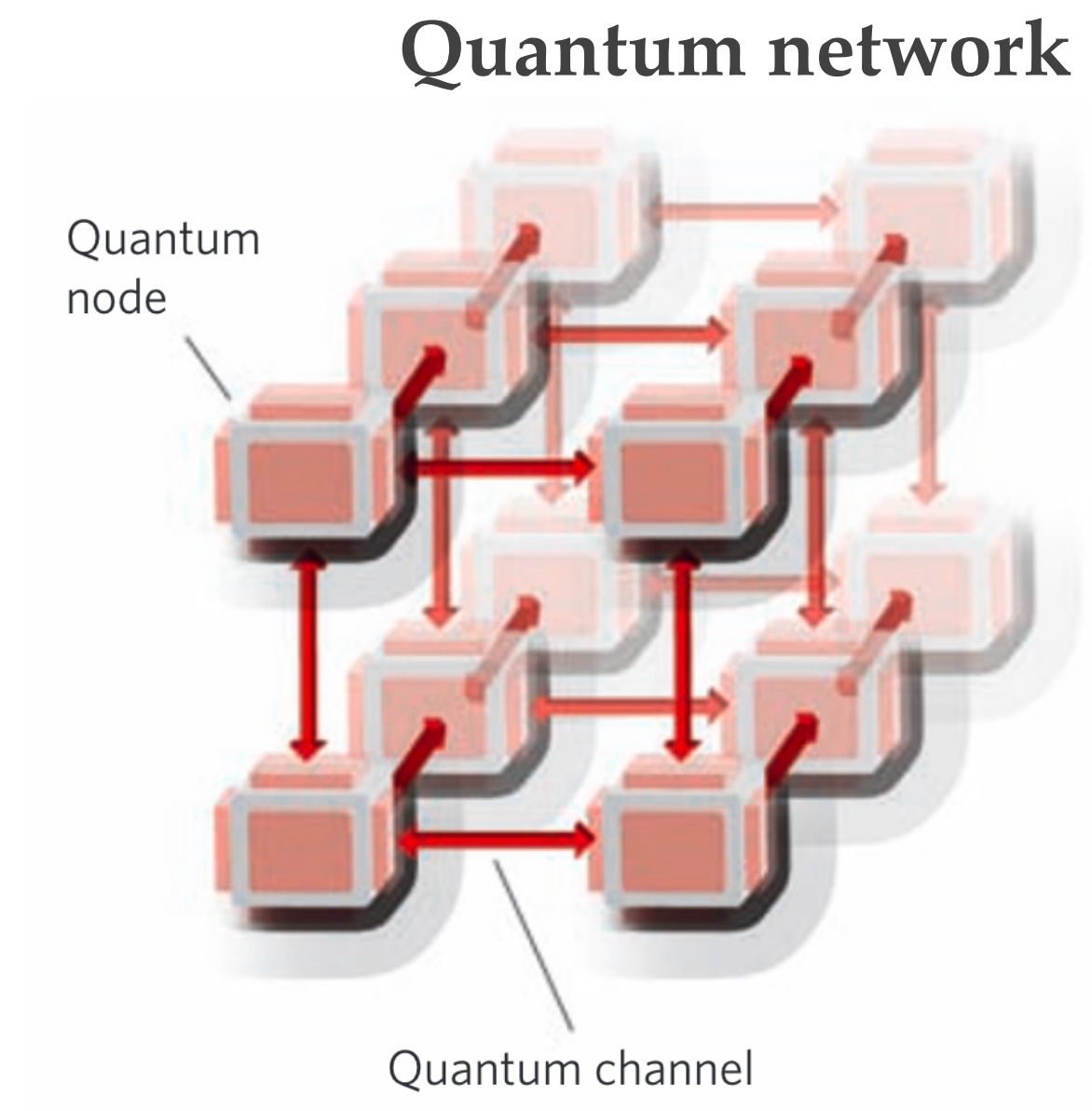
MajuLab, CNRSUCA-SU-NUS-NTU

International Joint Research Laboratory



Introduction

- ❖ Quantum interfaces → transfer of information between light and matter via their interaction
- ❖ Quantum networks, memory based quantum repeaters
- ❖ Artificial atoms & waveguides
 - ❖ Quantum dots (QDs)



Quantum dot in a micropillar

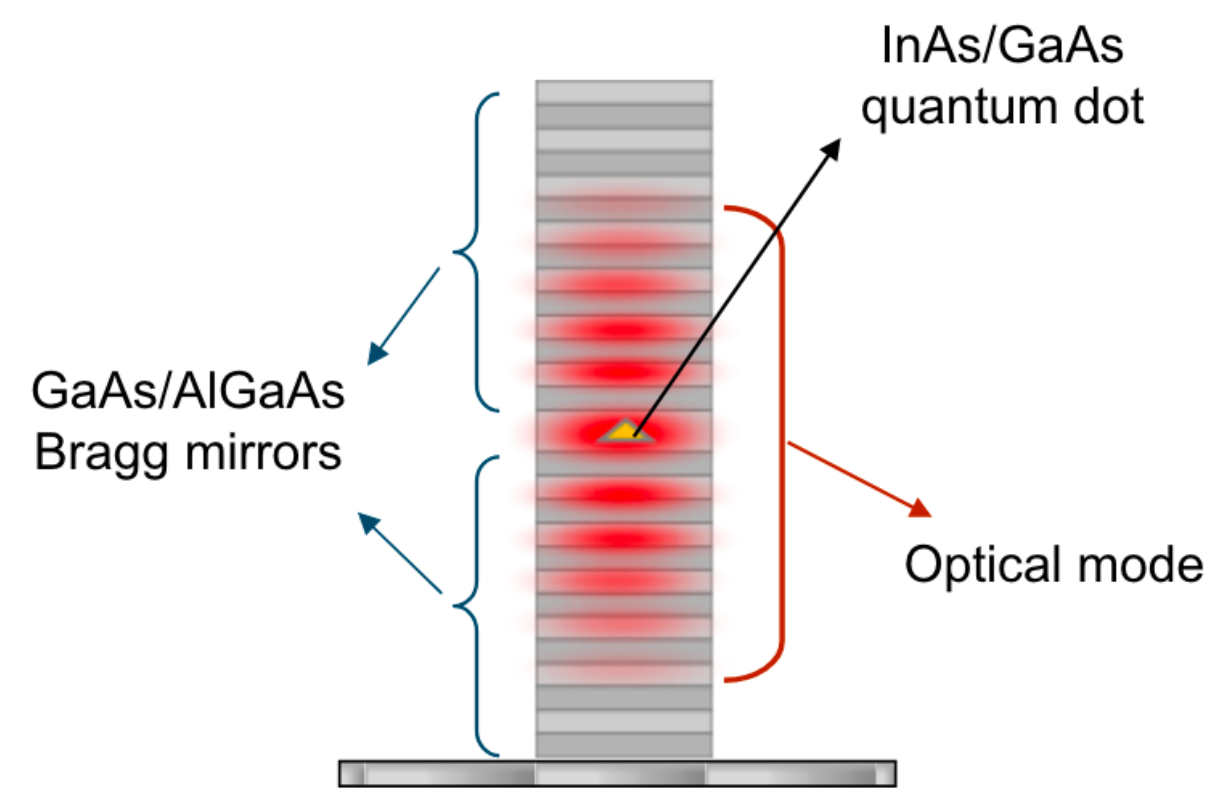


Figure taken from Ref. [2]

- [1] Lanço, L. & Senellart, P. A highly efficient single photon-single quantum dot interface. arXiv:1502.01062 (2015)
[2] Kimble, H. J. The quantum internet. Nature 453, 1023–1030 (2008).

Scope of the thesis

Quantum measurement

Fundamental

- ❖ Emergence of non-classical features of the scattered field (Not discussed today)
- ❖ Non-destructive measurement of a spin in a QD?

Technological applications

- ❖ Photon-photon gate & error analysis
- ❖ Model for experiment that implements the Lindner-Rudolph protocol (LRP)

Theoretical tool: Collisional model → Full-information about the entangled state of light and matter

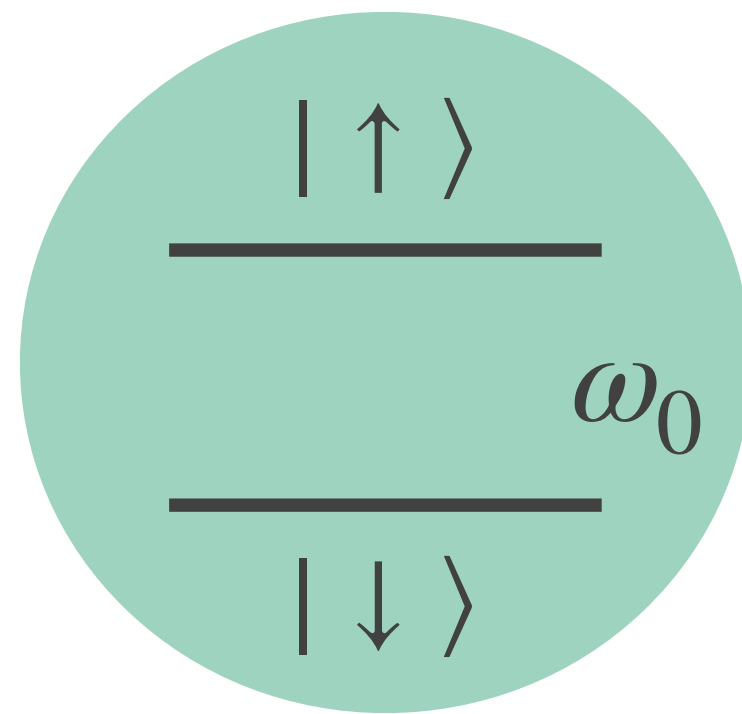
Outline

- ❖ Preliminaries
 - ❖ von Neumann measurement model
 - ❖ Collisional model or how to close open systems
- ❖ Main results
 - ❖ Energy efficient entanglement generation and readout in a spin-photon interface
 - ❖ Photon-photon controlled phase-gate and error analysis
 - ❖ The SPI subjected to an in-plane magnetic field
- ❖ Conclusions and perspectives

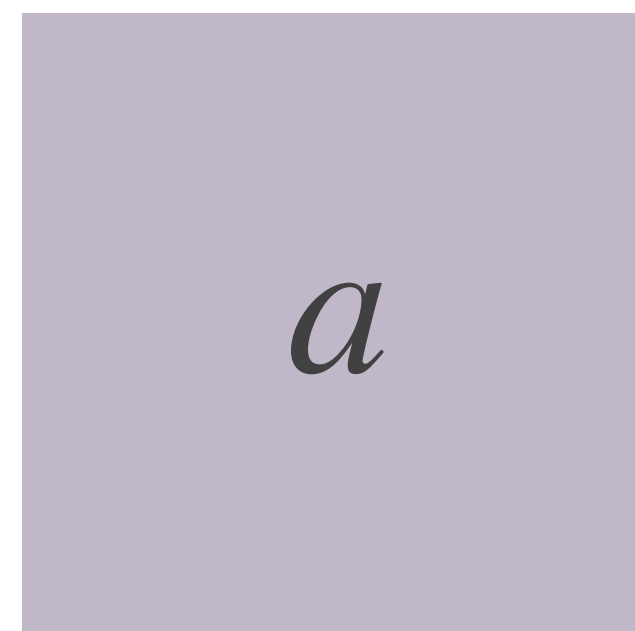
How can we measure the state of a qubit?

Measured system (or target): S

$$|\psi_S(0)\rangle = \left(\frac{|\uparrow\rangle + |\downarrow\rangle}{\sqrt{2}} \right)$$



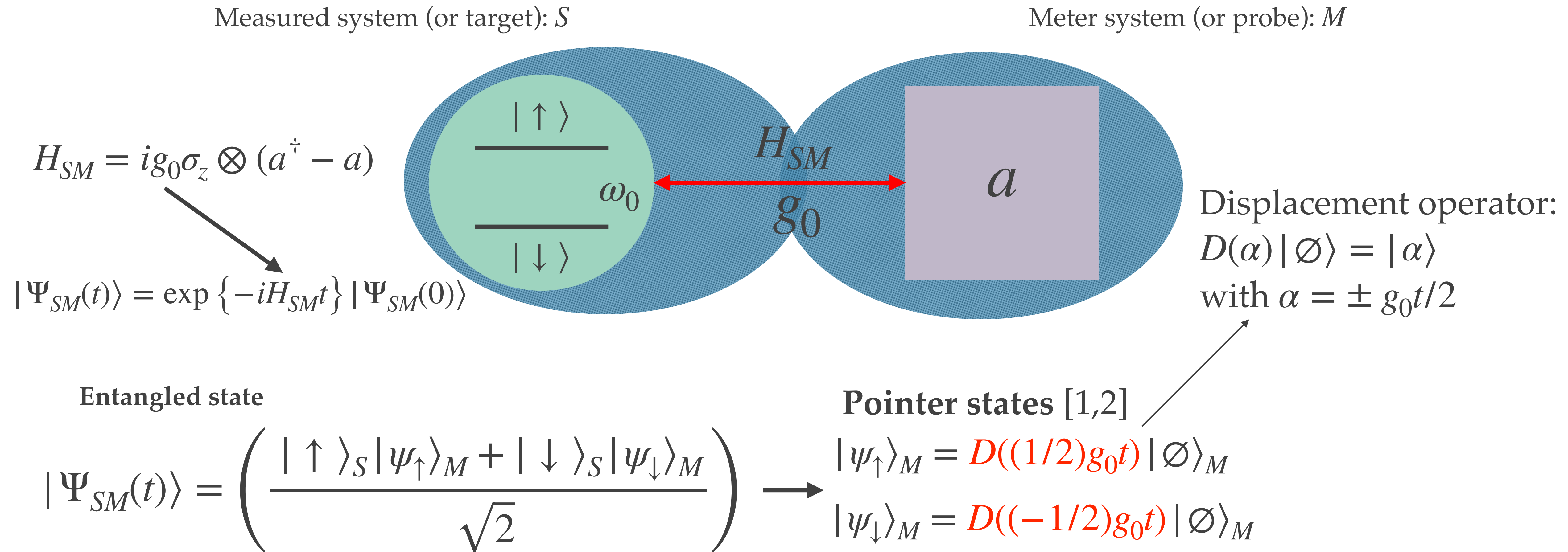
Meter system (or probe): M



$$\begin{aligned} |\psi_M(0)\rangle &= |\emptyset\rangle \\ [a, a^\dagger] &= 1 \\ a |\emptyset\rangle &= 0 \end{aligned}$$

$$|\Psi_{SM}(0)\rangle = \left(\frac{|\uparrow\rangle + |\downarrow\rangle}{\sqrt{2}} \right) \otimes |\emptyset\rangle_M$$

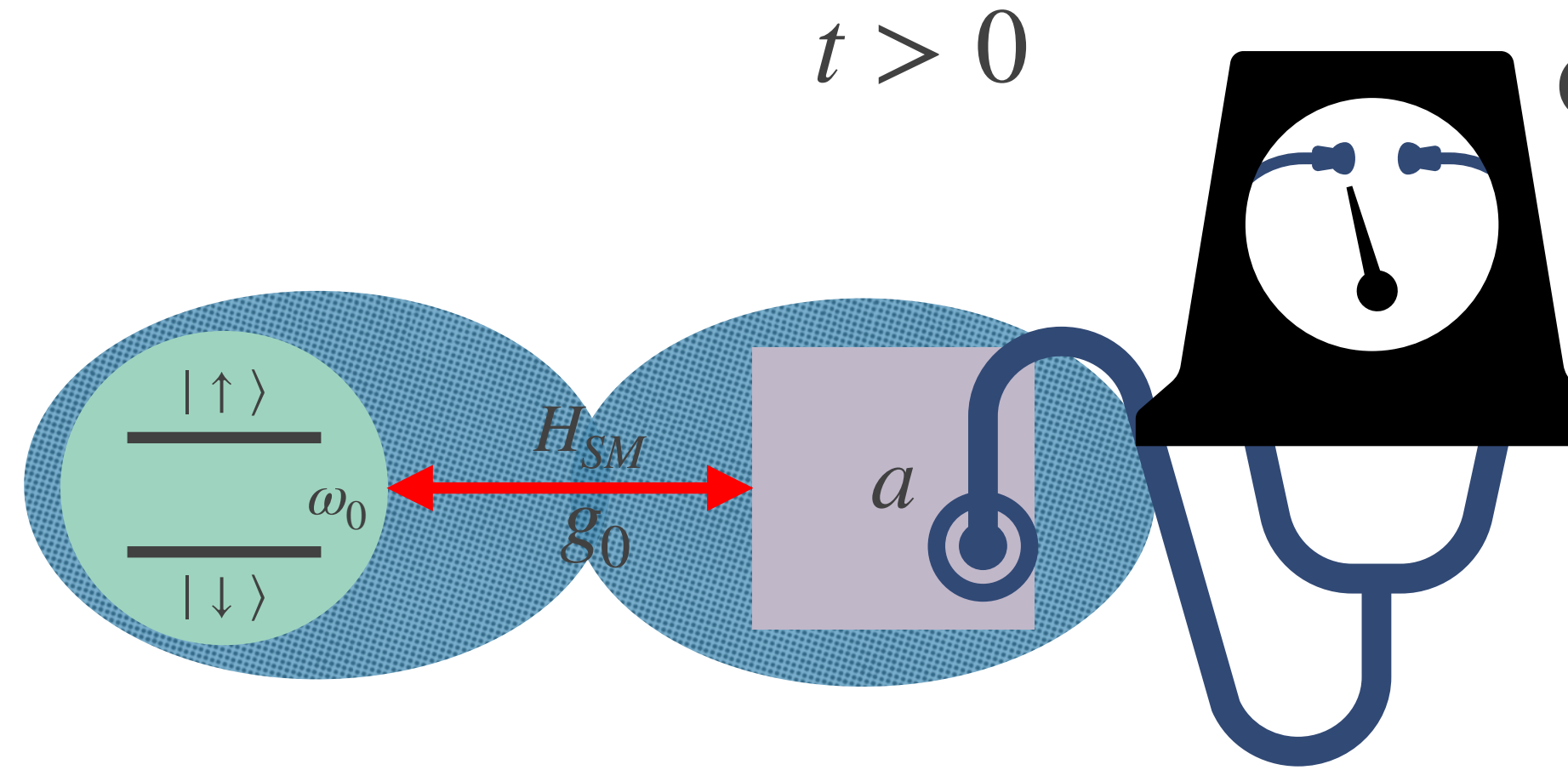
Pre-measurement is the process that generates entanglement between the target and probe.



[1] J. von Neumann, Mathematical Foundations of Quantum Mechanics: New Edition. Princeton University Press, 2018.

[2] W. H. Zurek, “Decoherence, einselection, and the quantum origins of the classical,” Rev. Mod. Phys., vol. 75, no. 3, pp. 715–775, May 2003

Measurement happens when the state of the meter is collapsed with a classical apparatus.



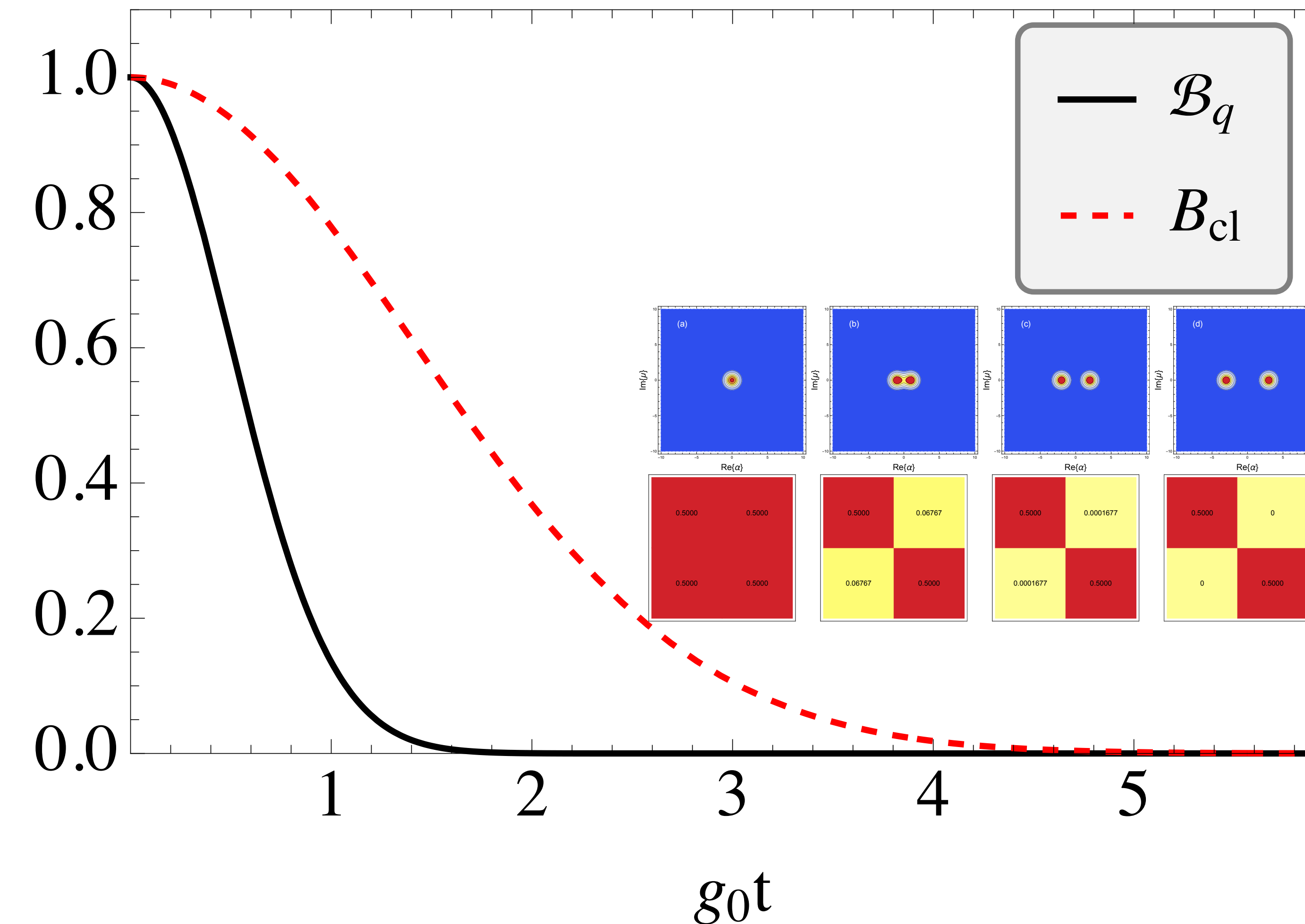
$$|\Psi_{SM}(t)\rangle = \left(\frac{|\uparrow\rangle_S |\psi_\uparrow\rangle_M + |\downarrow\rangle_S |\psi_\downarrow\rangle_M}{\sqrt{2}} \right)$$

- ❖ Projection of the meter in $|\psi_\uparrow\rangle$:
 - ❖ $\langle \psi_\uparrow | \Psi_{SM}(t) \rangle = \left(\frac{|\uparrow\rangle_S + |\downarrow\rangle_S \langle \psi_\uparrow | \psi_\downarrow \rangle_M}{\sqrt{2}} \right)$
- ❖ One can infer the target is in state $|\uparrow\rangle_S$ if $\langle \psi_\uparrow | \psi_\downarrow \rangle_M = 0$
- ❖ **Information about the system is fully encoded in the meter.**

[1] J. von Neumann, Mathematical Foundations of Quantum Mechanics: New Edition. Princeton University Press, 2018.

[2] W. H. Zurek, “Decoherence, einselection, and the quantum origins of the classical,” Rev. Mod. Phys., vol. 75, no. 3, pp. 715–775, May 2003

Quantifying the quality of pre-measurement and collapse



Bhattacharyya coefficients

Quantum Bhattacharyya coefficient (qBhat)

$$\mathcal{B}_q(t) = |\langle \psi_\uparrow(t) | \psi_\downarrow(t) \rangle|$$

Classical Bhattacharyya coefficient (cBhat)

$$B_{cl}(p_\uparrow, p_\downarrow) = \sum_{x \in \mathcal{X}} \sqrt{p_\uparrow(x)p_\downarrow(x)}$$

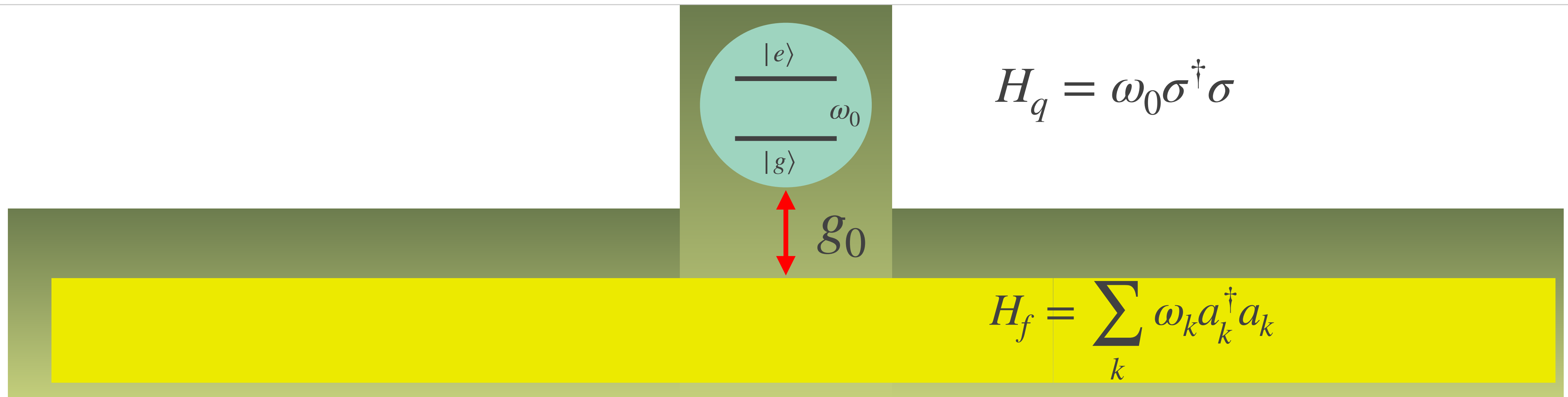
Relation between the coefficients

$$\mathcal{B}_q(t) \leq B_{cl}(p_i, p_j)$$

Outline

- ❖ Preliminaries
 - ❖ von Neumann measurement model
 - ❖ Collisional model or how to close open systems
- ❖ Main results
 - ❖ Energy efficient entanglement generation and readout in a spin-photon interface
 - ❖ Photon-photon controlled phase-gate and error analysis
 - ❖ The SPI subjected to an in-plane magnetic field
- ❖ Conclusions and perspectives

Qubit + multimode electromagnetic field in a 1D waveguide



$$V_{qf} = ig_0 \sum_{k=0}^{\infty} (\sigma^\dagger a_k - a_k^\dagger \sigma)$$

The emitter interacts with **all the modes** at the same time.

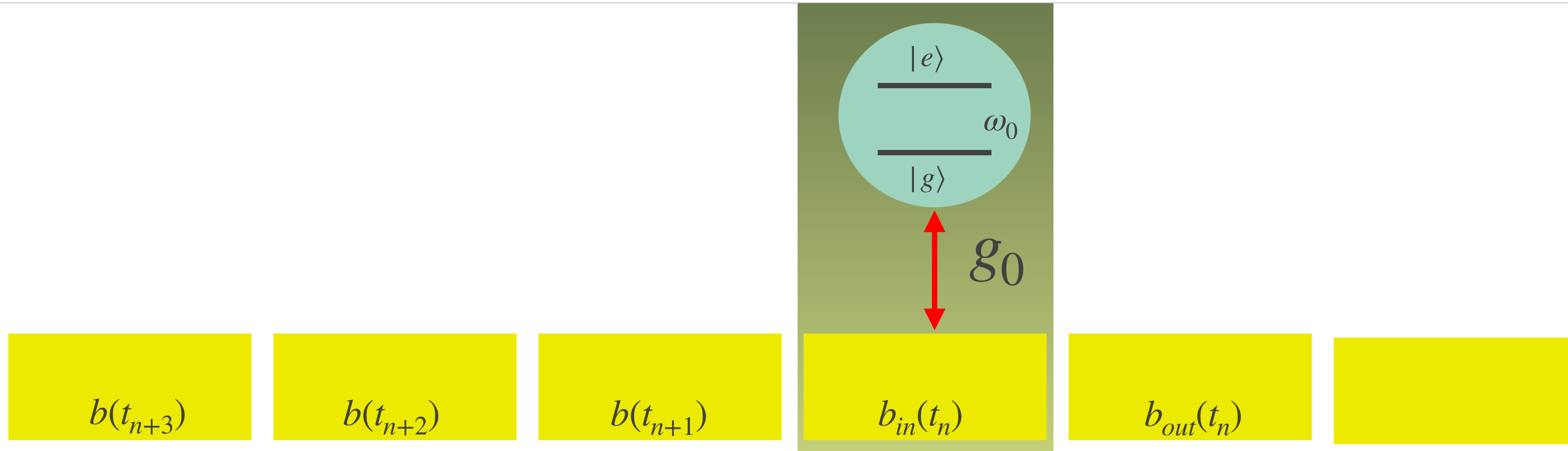
$$H = H_0 + V_{qf} = \omega_0 \sigma^\dagger \sigma + \sum_k \omega_k a_k^\dagger a_k + ig_0 \sum_k (\sigma^\dagger a_k - \sigma a_k^\dagger)$$

How to solve the joint dynamics?
[1,2]

[1] F. Ciccarello, S. Lorenzo, V. Giovannetti, and G. M. Palma, "Quantum collision models: open system dynamics from repeated interactions," *arXiv:2106.11974 [quant-ph]*

[2] F. Ciccarello, "Collision models in quantum optics," doi: [10.1515/qmetro-2017-0007](https://doi.org/10.1515/qmetro-2017-0007).

Interaction picture & time discretization: The emitter interacts with one *temporal mode* at a time, repeatedly → Collisional model interpretation.



$$V_{qf} \xrightarrow{H_0} V_{qf}(t) = ig_0 \sum_{k=0}^{\infty} \left(\sigma^\dagger(t) e^{-i\omega_k t} a_k - e^{i\omega_k t} a_k^\dagger \sigma(t) \right) \xrightarrow{t_n = n\Delta t} V_{qf}(t_n) = V_n = i\sqrt{\frac{\gamma}{\Delta t}} [\sigma^\dagger(t_n) b(t_n) - b^\dagger(t_n) \sigma(t_n)]$$

Wave-function solution

- ❖ Suzuki-Trotter formula

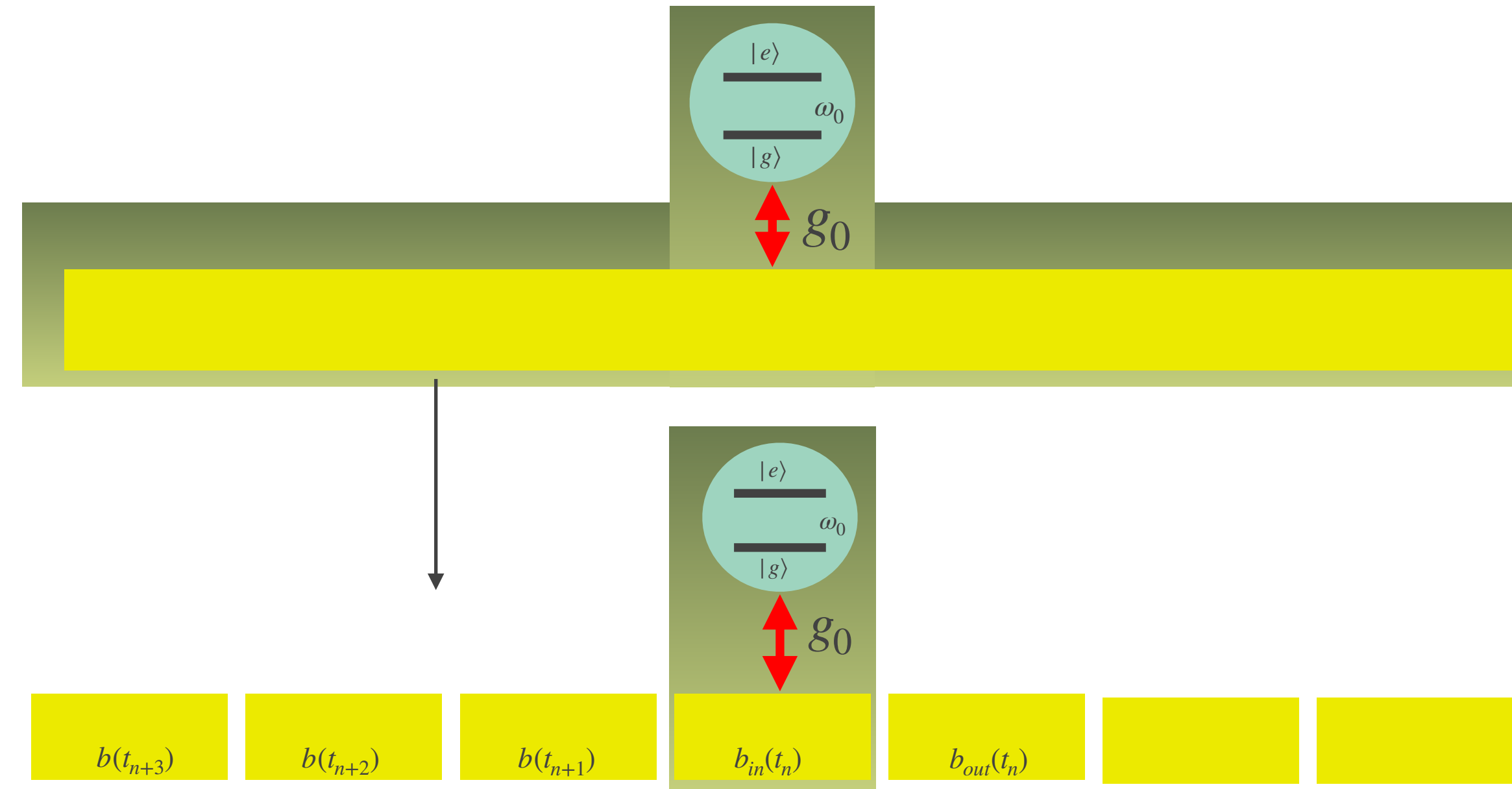
$$|\Psi_N\rangle = e^{-i(N-1)\Delta t V_{N-1}} e^{-i(N-2)\Delta t V_{N-2}} \dots e^{-iM\Delta t V_M} |\Psi_0\rangle$$

- ❖ Joint emitter+field wave-function solution

- ❖ Input-output relation for the average values

- ❖ $\langle b_{out} \rangle = \langle b_{in} \rangle - \sqrt{\gamma} \langle \sigma \rangle$

- ❖ Similar to the known textbook [3]: $b_{out} = b_{in} - \sqrt{\gamma} \sigma$.



- [1] M. Suzuki, “Generalized Trotter’s formula and systematic approximants of exponential operators and inner derivations with applications to many-body problems,” Commun.Math. Phys., vol. 51, no. 2, pp. 183–190, Jun. 1976
- [2] M. Maffei, P. A. Camati, and A. Auffèves, “Closed-System Solution of the 1D Atom from Collision Model,” Entropy, vol. 24, no. 2, p. 151, Jan. 2022
- [3] Gardiner, C. W. & Collett, M. J. Input and output in damped quantum systems: Quantum stochastic differential equations and the master equation. Phys. Rev. A 31, 3761–3774 (1985).

Coherent field & Single photon solutions

Coherent input field

$$|\Psi_{CS}(0)\rangle = \bigotimes_{n=0}^N D(\beta_n) |\emptyset\rangle \otimes |\zeta\rangle, \zeta = g, e$$

$$|\Psi_{\beta}^{\zeta}(t_N)\rangle = \sqrt{P_g(t)} |g\rangle |\phi_g(t)\rangle + \sqrt{P_e(t)} |e\rangle |\phi_e(t)\rangle$$

$$|\phi_e\rangle = \frac{1}{\sqrt{P_e(t)}} \left[\sqrt{p_{0,e}} \tilde{f}_{\varepsilon,\zeta}^{(0)}(t) + \sum_{m=1}^{\infty} \sqrt{p_{m,e}(t)} \int_0^t ds_m \tilde{f}_{\varepsilon,\zeta}^{(m)}(t,s) \prod_{i=1}^m b_i^\dagger \right] |\emptyset\rangle$$

Suffices to find the coefficients: possible to do analytically.

Single photon input field

$$|\Psi_{SP}(0)\rangle = \sum_{n=0}^{\infty} \sqrt{\Delta t} \beta(t_n) b_n^\dagger |\emptyset\rangle \otimes |g\rangle \quad \sum_{n=0}^{\infty} \Delta t |\beta(t_n)| = 1$$

$$|\Psi_{SP}(t_N)\rangle = \left(\sqrt{\gamma \Delta t} e^{-\frac{\gamma}{2} t_N} \sum_{n=0}^{N-1} \sqrt{\Delta t} e^{(\frac{\gamma}{2} + i\omega_0)t_n} \xi(t_n) |\emptyset\rangle \right) \otimes |e\rangle$$

$$+ \left(\sum_{n=0}^{N-1} \sqrt{\Delta t} \Upsilon(t_n) b_n^\dagger |\emptyset\rangle \right) \otimes |g\rangle$$

$$+ \left(\sum_{n=N}^{\infty} \sqrt{\Delta t} \beta(t_n) b_n^\dagger |\emptyset\rangle \right) \otimes |g\rangle.$$

Already interacted.

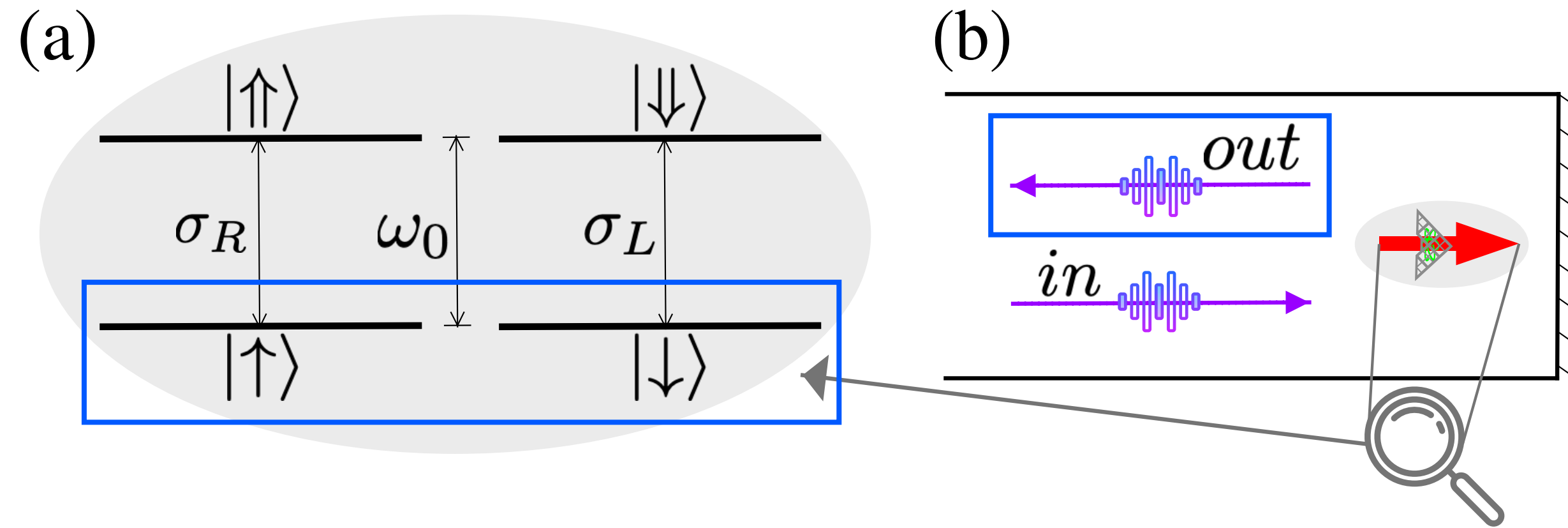
Part that is yet to interact.

Outline

- ❖ Preliminaries
 - ❖ von Neumann measurement model
 - ❖ Collisional model or how to close open systems
- ❖ Main results
 - ❖ Energy efficient entanglement generation and readout in a spin-photon interface
 - ❖ Photon-photon controlled phase-gate and error analysis
 - ❖ The SPI subjected to an in-plane magnetic field
 - ❖ Conclusions and perspectives

Measuring the spin state

- ❖ Set-up:



- ❖ Questions:

- ❖ Budget: 1 quanta → Get entanglement between spin state and output field.
 - ❖ Comparison: Superposition of **number states** vs. low energy **coherent pulses**
 - ❖ **1) WHICH ONE ENTANGLES BETTER? (qBhat)**
 - ❖ **2) DOES BETTER ENTANGLEMENT TRANSLATE INTO BETTER READOUT? (cBhat)**

[1] M. Maffei, B. O. Goes, S. C. Wein, A. N. Jordan, L. Lanço, and A. Auffèves, “Energy-efficient quantum non-demolition measurement with a spin-photon interface,” *Quantum*, vol. 7, p. 1099, Aug. 2023, doi: 10.22331/q-2023-08-31-1099.

Pointer states for the different initial fields

- ❖ Long-time limit state:

$$|\Psi(t \rightarrow \infty)\rangle = c_{\uparrow} |\psi_{\uparrow}\rangle |\uparrow\rangle + c_{\downarrow} |\psi_{\downarrow}\rangle |\downarrow\rangle$$

Coherent state

$$|\psi^{cs}(0)\rangle_H = |\beta\rangle_H$$



$$|\psi_{\uparrow(\downarrow)}^{cs}\rangle = D_H(\beta) \left[\sqrt{p_0} + \sqrt{p_1} \int dt f^{(1)}(t) b_{R(L)}^{\dagger}(t) + \dots \right] |\emptyset\rangle$$

Superposition of vacuum and single

$$|\psi^{qs}(0)\rangle_H = c_{\emptyset} |\emptyset\rangle + c_1 |1\rangle_H$$



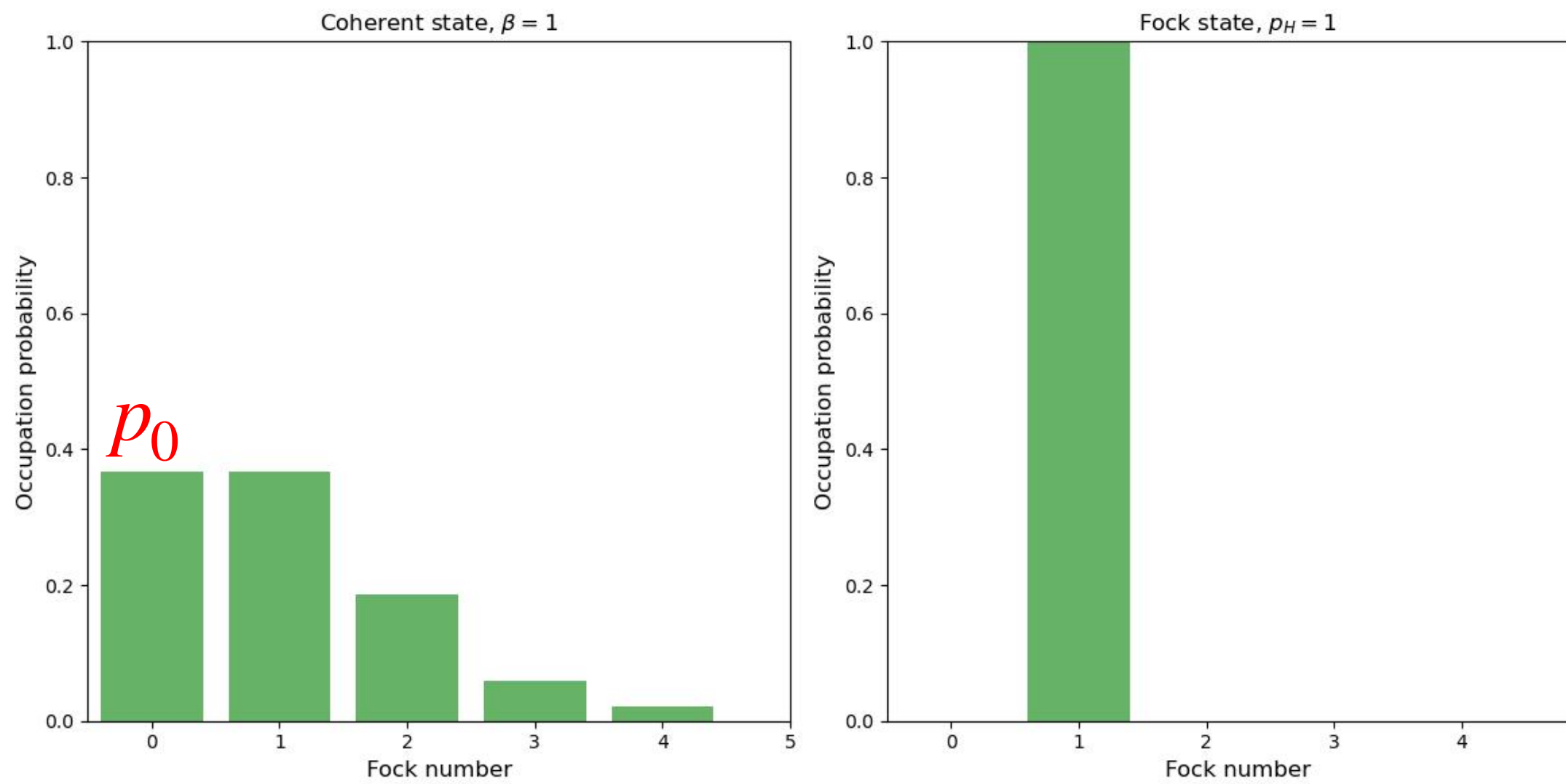
$$|\psi_{\uparrow(\downarrow)}^{qs}(t)\rangle = \left[c_{\emptyset} + \frac{c_1}{\sqrt{2}} \int dt \left[Y(t) b_{R(L)}^{\dagger}(t) + \beta(t) b_{L(R)}^{\dagger}(t) \right] \right] |\emptyset\rangle$$

1st main result: quantum light may produce orthogonal pointer states. We have quantum advantage at the pre-measurement level.

Coherent state

$$\mathcal{B}_q^{cs} = p_0$$

- ❖ $p_0 \rightarrow$ no photon re-emission probability
- ❖ Fundamental limitation for the coherent state



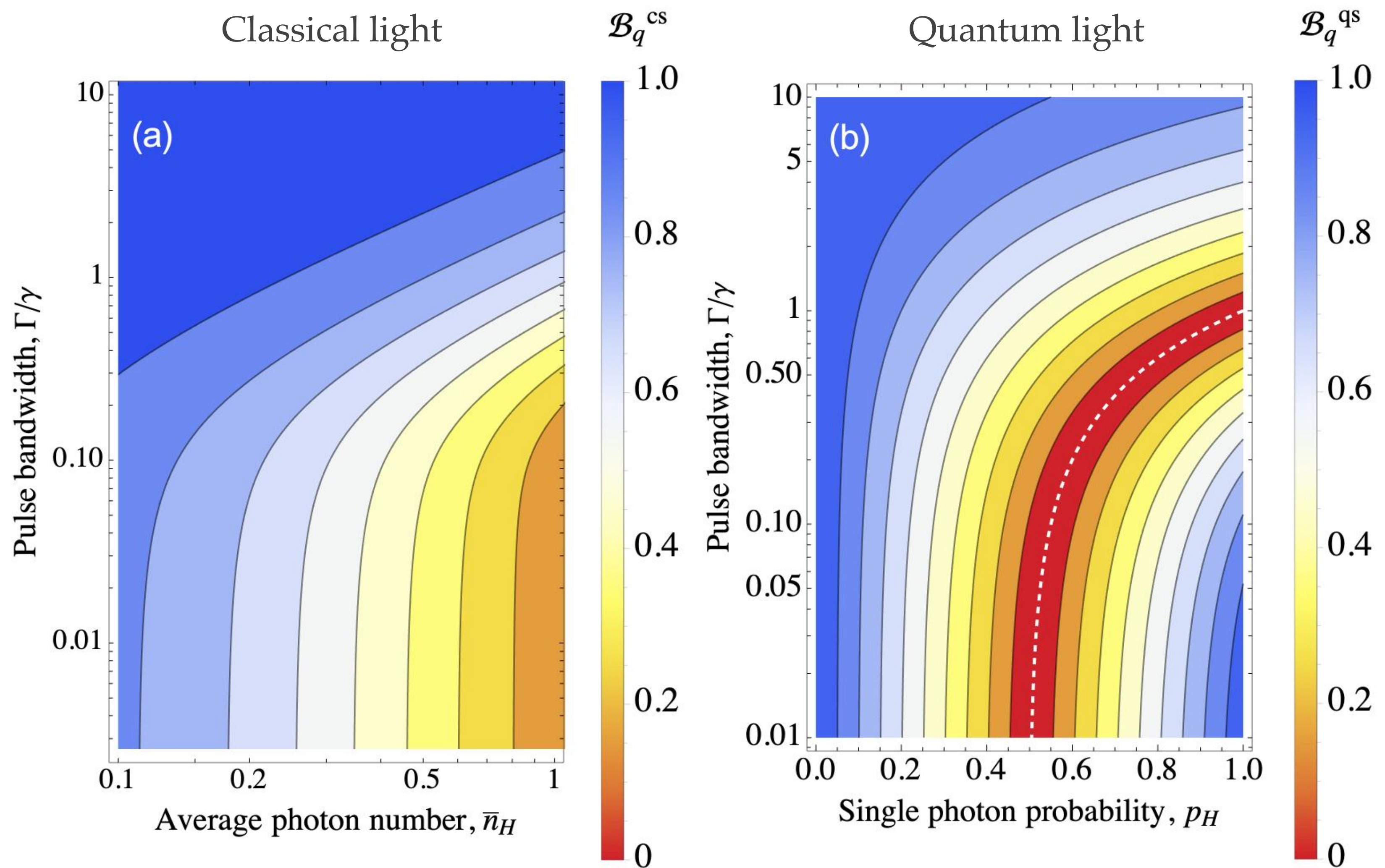
Superposition of vacuum and single photon

$$\mathcal{B}_q^{qs} = \left| 1 - \gamma p_H \int dt \Re \left\{ \beta(t) \tilde{\beta}(t) \right\} \right|$$

$$p_H = |c_1|^2$$

- ❖ For a given β it is possible to tune p_H to vanish the qBhat.

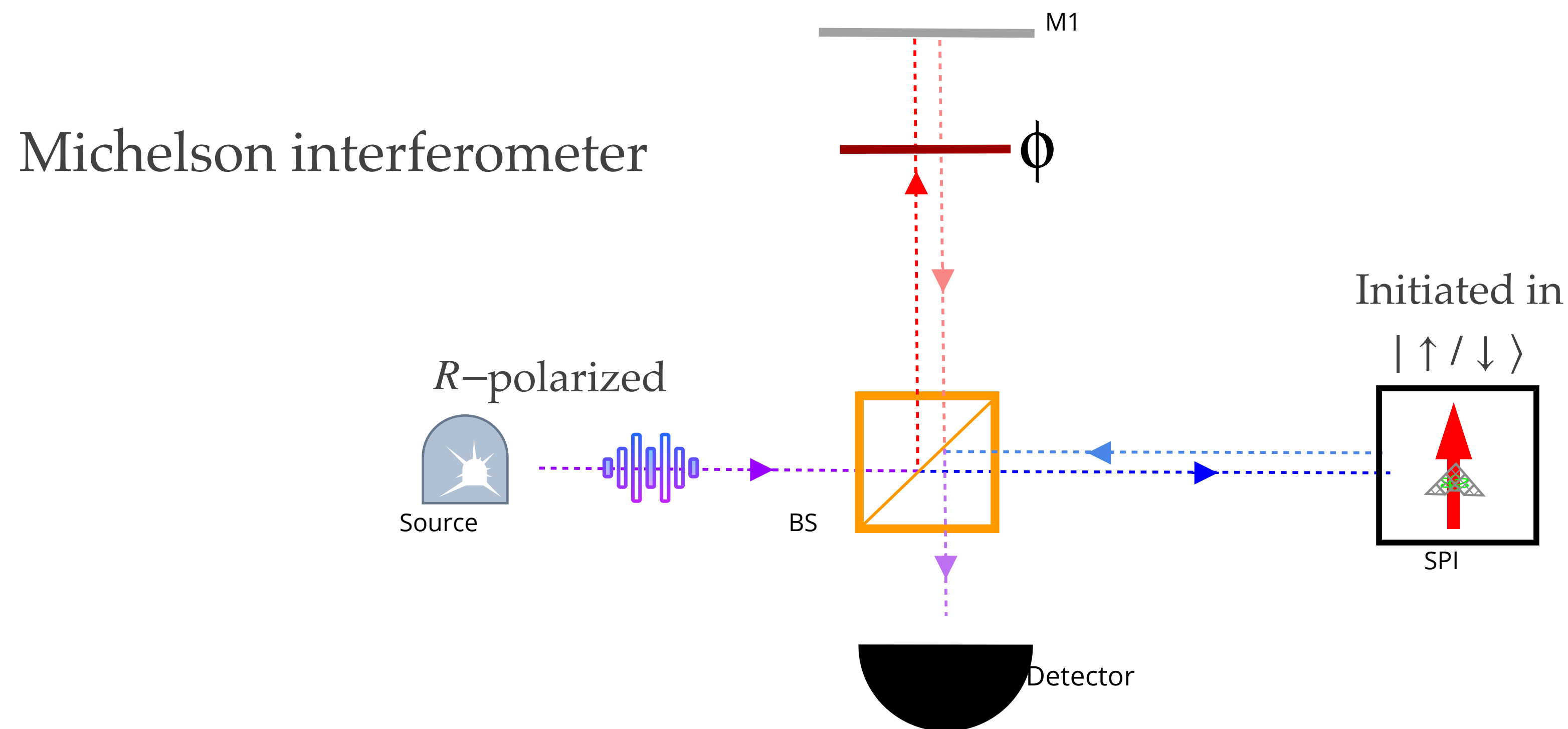
Visualization of the quantum advantage: the superposition of number states creates orthogonal pointer states of the meter.



Quantum advantage:
 $\mathcal{B}_q = 0 \rightarrow$ Superposition of
number states
 $p_H = (1 + \Gamma/\gamma)/2$

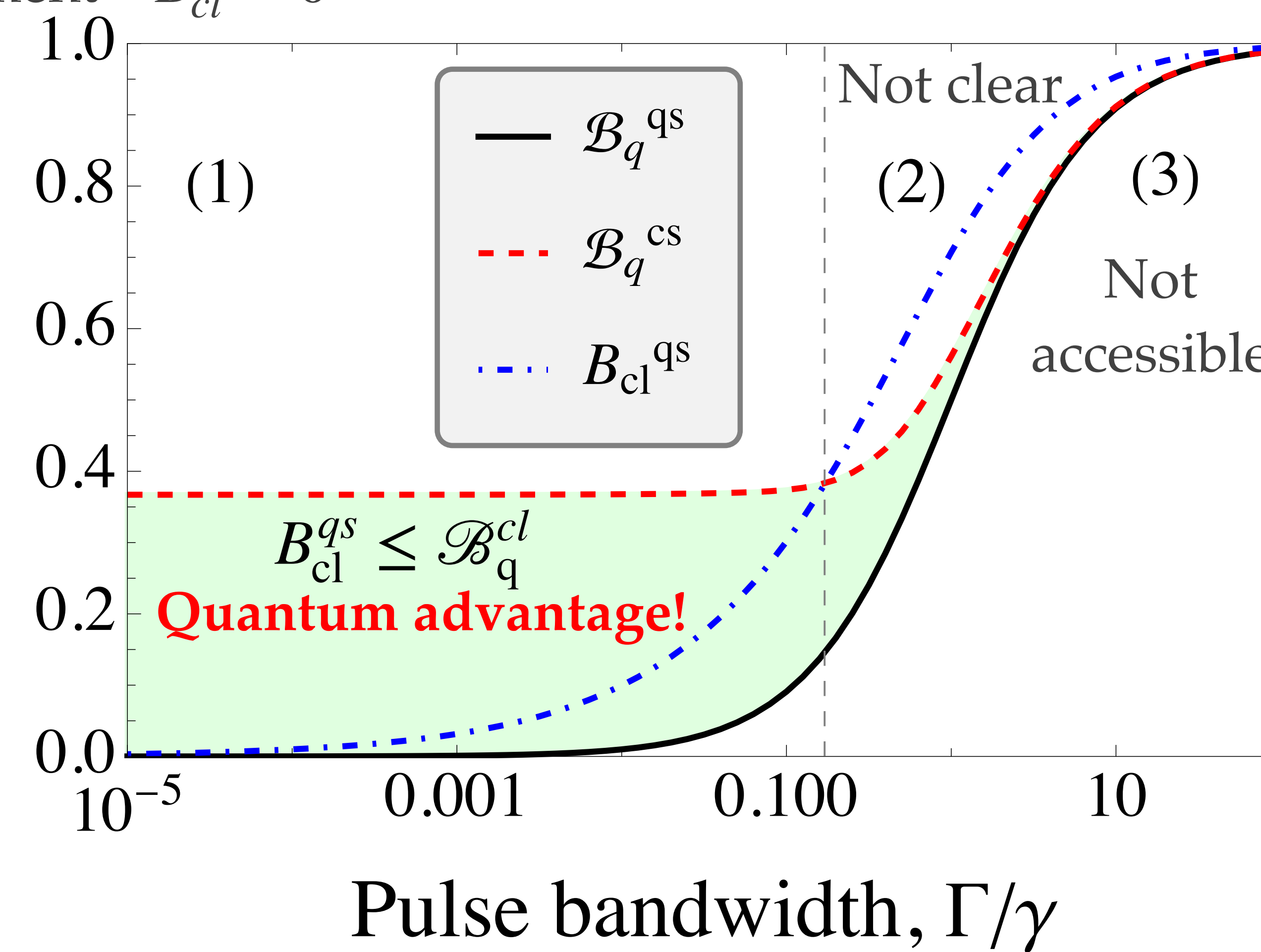
Measuring the phase with a Michelson interferometer

- ❖ Regime: $\bar{n}_H = p_H = 0.5$, and $\rightarrow | \uparrow, 1_R \rangle \rightarrow -| \uparrow, 1_R \rangle$
- ❖ $\Gamma = 10^{-2}\gamma$ $| \downarrow, 1_R \rangle \rightarrow | \downarrow, 1_R \rangle$



2nd main result: quantum advantage at the readout level

- ❖ Perfect measurement $\rightarrow B_{cl} = 0$

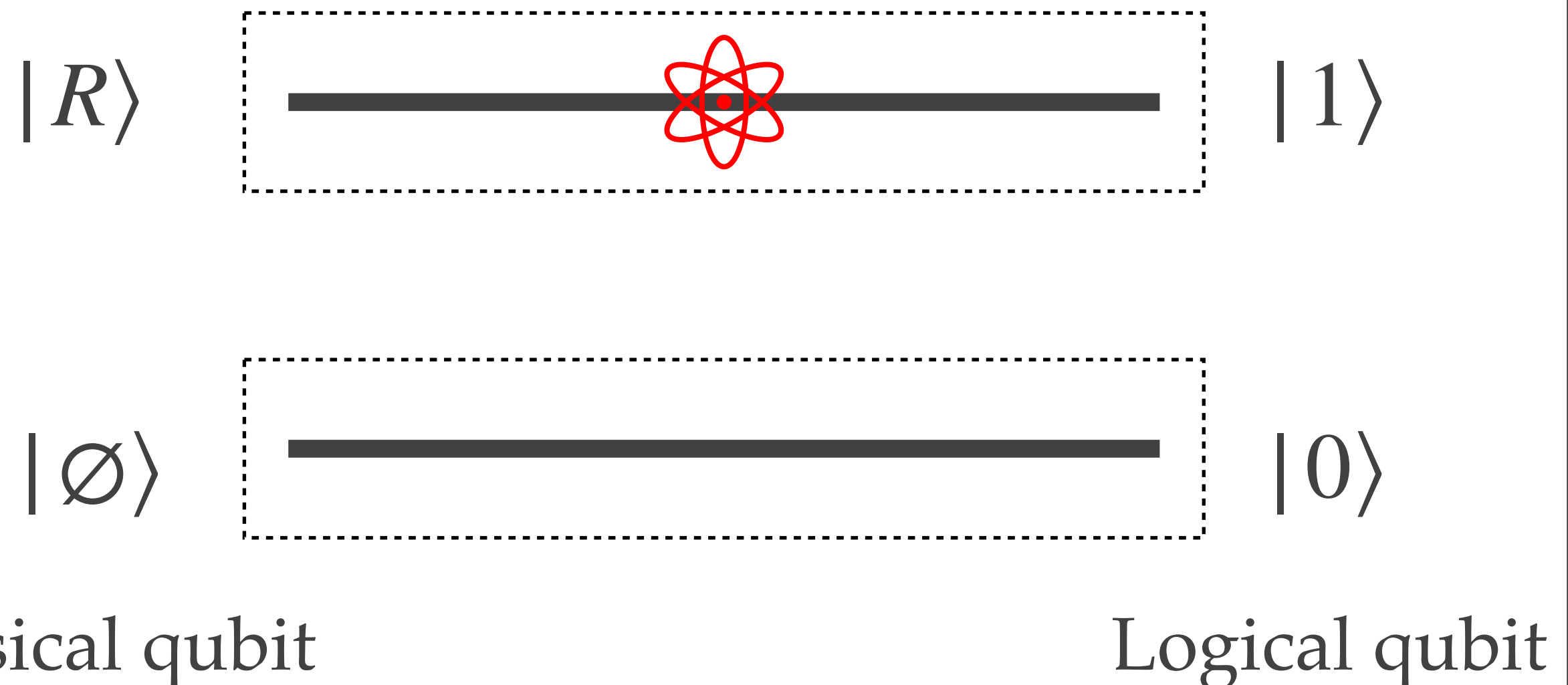


Outline

- ❖ Preliminaries
 - ❖ von Neumann measurement model
 - ❖ Collisional model or how to close open systems
- ❖ Main results
 - ❖ Energy efficient entanglement generation and readout in a spin-photon interface
 - ❖ Photon-photon controlled phase-gate and error analysis
 - ❖ The SPI subjected to an in-plane magnetic field
- ❖ Conclusions and perspectives

C-Phase gate and Error

- ❖ Goal: perform a controlled phase gate [1] and characterize the error induced solely due to the finite duration of the pulse.
 - ❖ Single rail basis:



$$\begin{aligned}
 |\emptyset\rangle |\uparrow\rangle &\rightarrow |\emptyset\rangle |\uparrow\rangle \\
 |\emptyset\rangle |\downarrow\rangle &\rightarrow |\emptyset\rangle |\downarrow\rangle \\
 |R\rangle |\uparrow\rangle &\rightarrow -|\tilde{R}\rangle |\uparrow\rangle \xrightarrow{\text{Monochromatic}} -|R\rangle \\
 |R\rangle |\downarrow\rangle &\rightarrow |R\rangle |\downarrow\rangle
 \end{aligned}$$

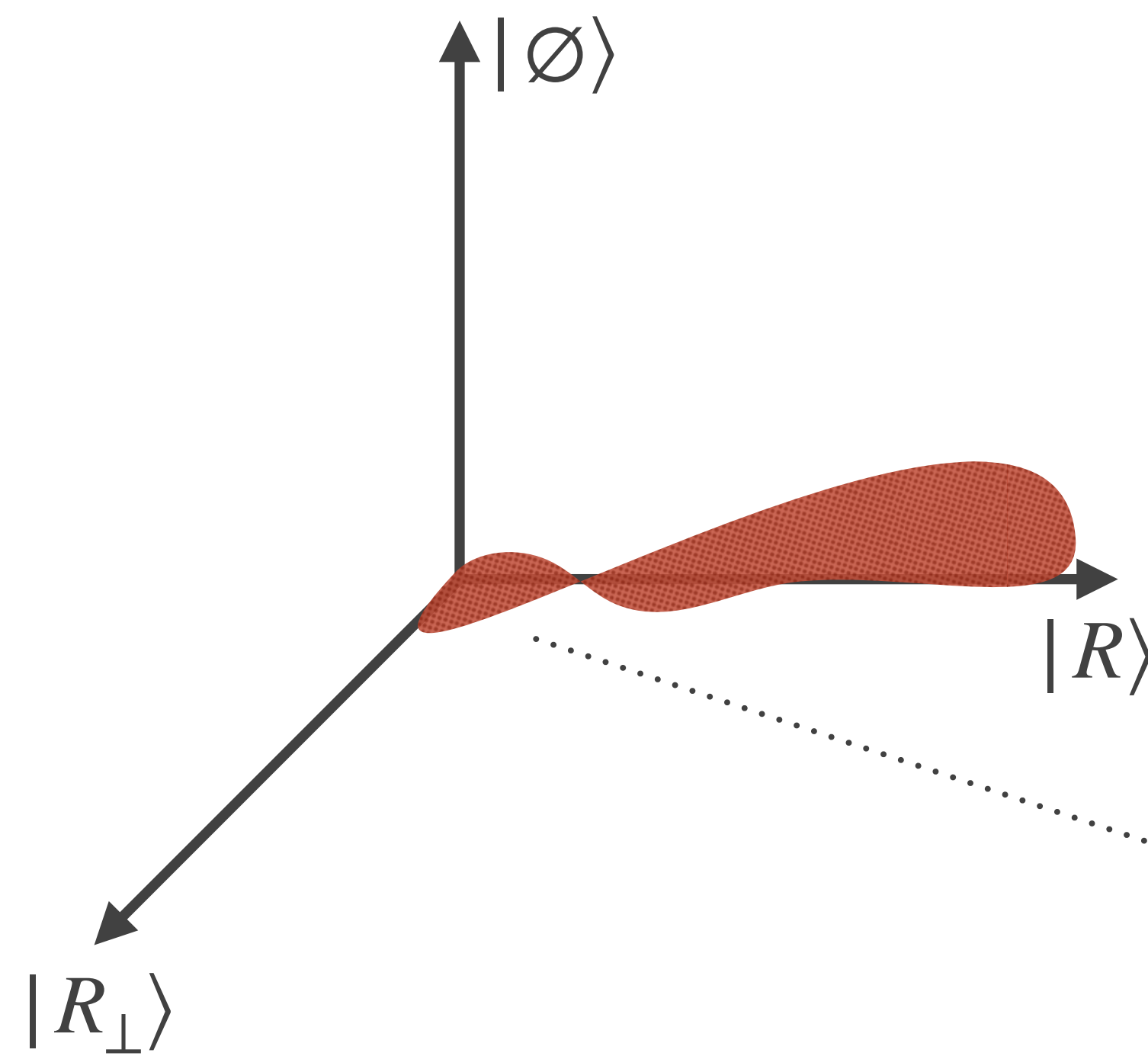
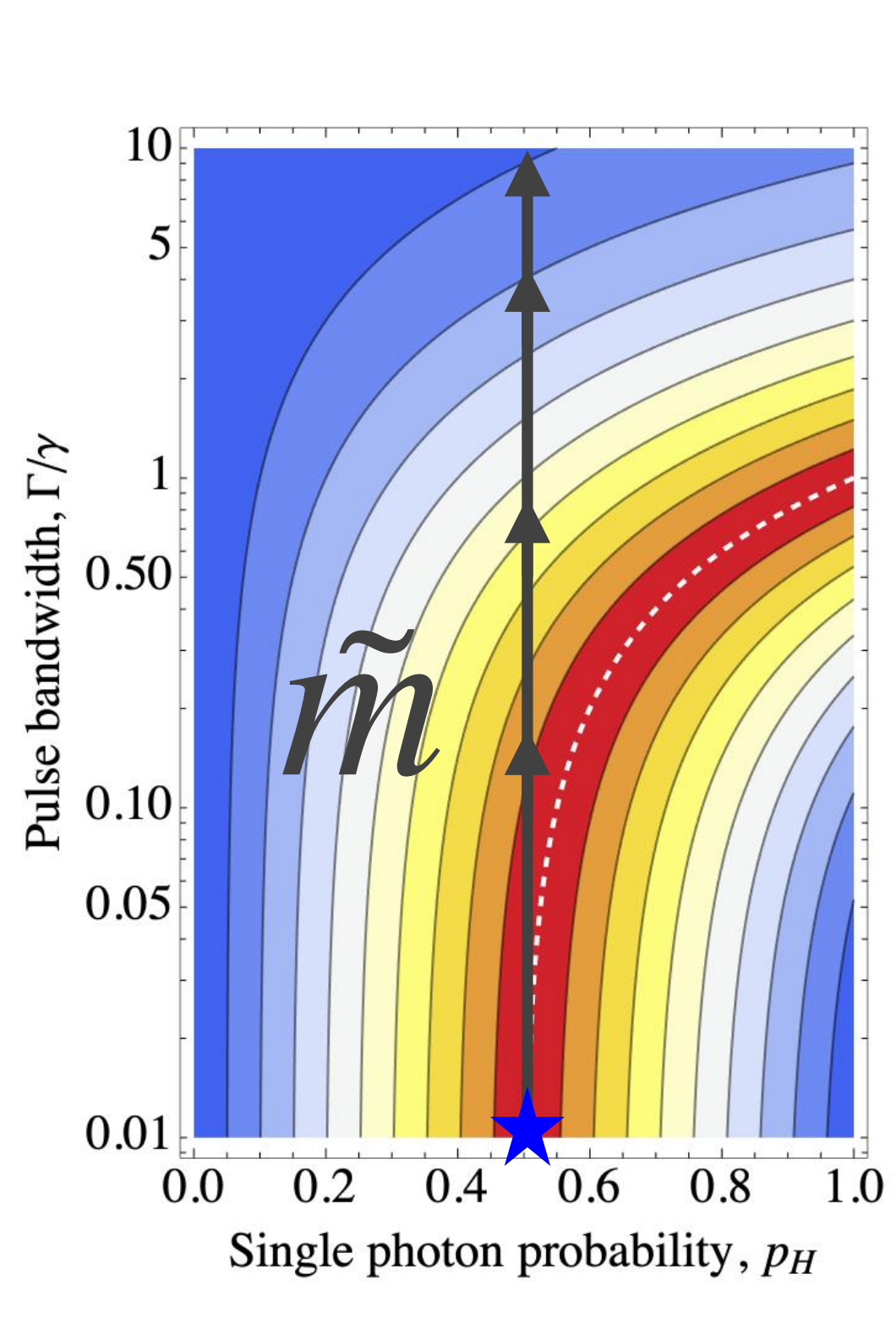
Collisional model provides:

$$|\mathbf{R}\rangle = \int dt \beta(t) b_{\mathbf{R}}^\dagger(t) |0\rangle \rightarrow |\tilde{\mathbf{R}}\rangle = \int dt \Upsilon(t) b_{\mathbf{R}}^\dagger(t) |0\rangle$$

[1] M. A. Nielsen and I. L. Chuang, "Quantum Computation and Quantum Information: 10th Anniversary Edition".

Leakage out of the logical basis due to pulse finite duration

- ❖ The protocol works in the quasi-monochromatic regime.
- ❖ What is the effect of a finite pulse duration?

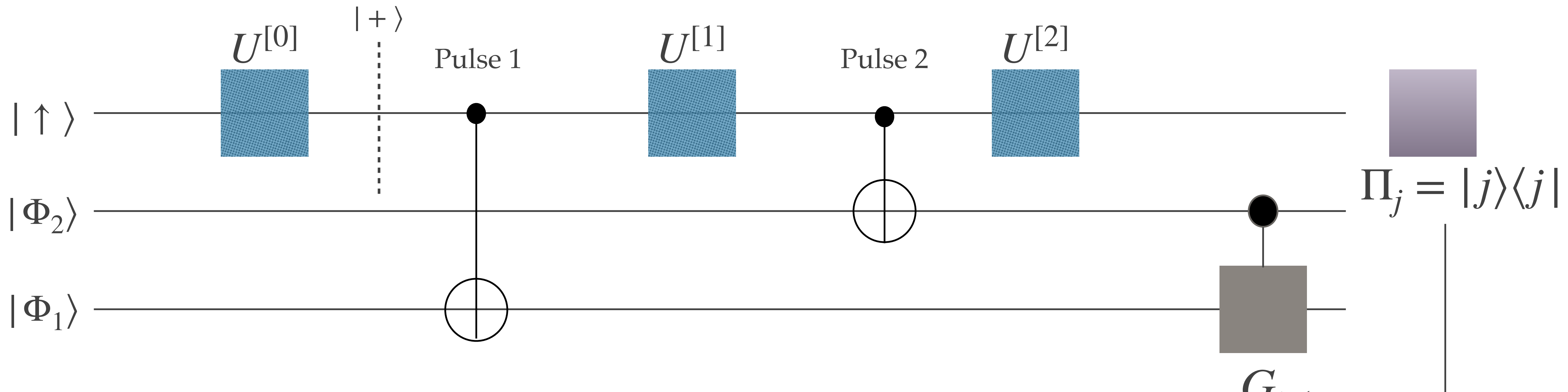


$$\tilde{m}(\beta, \Upsilon) = \langle R | \tilde{R} \rangle$$

$$|\tilde{R}\rangle = \boxed{\sqrt{1 - |\tilde{m}|^2} |R_{\perp}\rangle + \tilde{m} |R\rangle}$$

→ Leak out of the logical space.

Gate protocol



Light-pulses

$$|\Phi_1\rangle = |\Phi_2\rangle = \left(\frac{|\emptyset\rangle + |R\rangle}{\sqrt{2}} \right)$$

Spin rotations

$$U^{[n]} = R_y\left(\frac{\pi}{2}\right) = \exp\left\{-i\frac{\pi}{4}\sigma_y\right\}$$

$$|\Phi_f^j\rangle = G_j(|\Phi_2\rangle \otimes |\Phi_1\rangle)$$

3rd main result: possible to implement the c-phase gate, and access to the coherent error associated with the finite pulse duration

Gate action for $| \uparrow \rangle$:

Ideal	Real
$ 01\rangle \xrightarrow{G_{\uparrow}^{[1]}} - 01\rangle$	$ 01\rangle \xrightarrow{\tilde{m}<1} 01\rangle \xrightarrow{G_{\uparrow}^{[1]}} -\tilde{m} 01\rangle \equiv -e^{i\varepsilon_{\uparrow}} 01\rangle$
$ 11\rangle \xrightarrow{G_{\uparrow}^{[1]}} 11\rangle$	$ 11\rangle \xrightarrow{G_{\uparrow}^{[1]}} \frac{1}{2}(\tilde{m}^2 + 1) 11\rangle \equiv e^{i\delta_{\uparrow}} 11\rangle$

Rotation errors:

$$\varepsilon_{\uparrow} = 2\pi - i\text{Log} \left\{ -\frac{(\tilde{m}^2 + 2\tilde{m} - 1)}{2} \right\}$$

$$\delta_{\uparrow} = 2\pi - i\text{Log} \left\{ \frac{\tilde{m} + 1}{2} \right\}$$

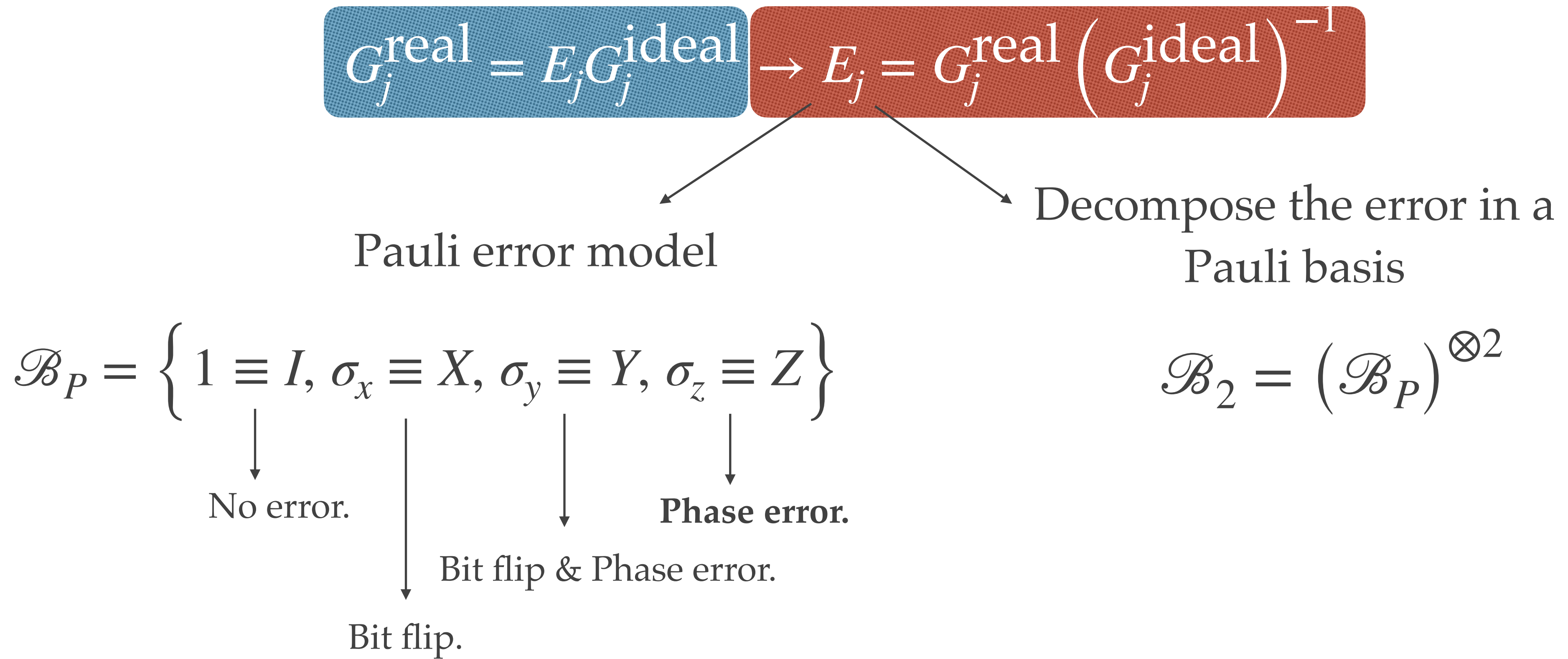
Gate action for $| \downarrow \rangle$:

Ideal	Real
$ 11\rangle \xrightarrow{G_{\uparrow}^{[1]}} - 11\rangle$	$ 11\rangle \xrightarrow{\tilde{m}<1} 11\rangle \xrightarrow{G_{\uparrow}^{[1]}} \frac{1}{2}(\tilde{m}^2 + 2\tilde{m} - 1) 11\rangle \equiv -e^{i\varepsilon_{\downarrow}} 11\rangle$

Rotation error:

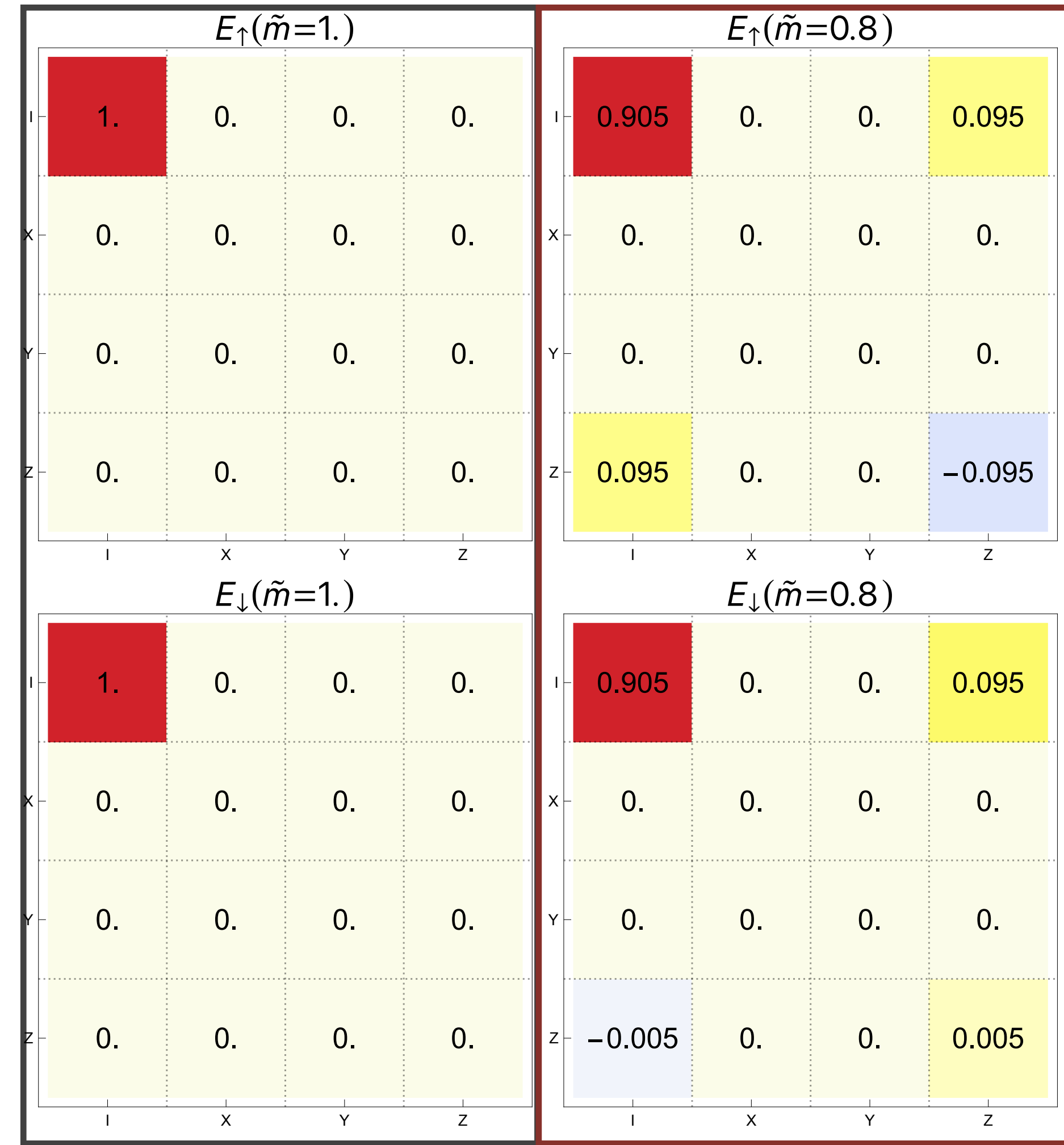
$$\varepsilon_{\downarrow} = 2\pi - i\text{Log} \{-\tilde{m}\}$$

Error matrix: The real process is a composition of the ideal process with some error on the top of it.



4th main result: Coherent error characterization with error matrix

Ideal process:
only one peak [3]

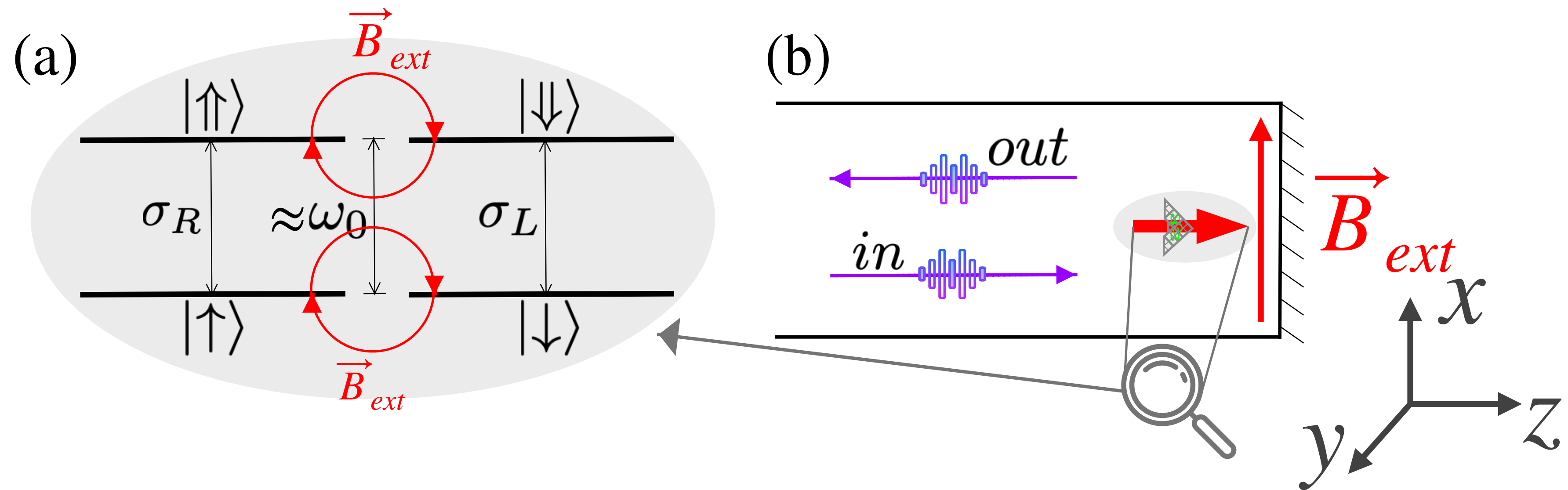


Imperfect process

Outline

- ❖ Preliminaries
 - ❖ von Neumann measurement model
 - ❖ Collisional model or how to close open systems
- ❖ Main results
 - ❖ Energy efficient entanglement generation and readout in a spin-photon interface
 - ❖ Photon-photon controlled phase-gate and error analysis
 - ❖ SPI under a magnetic field
- ❖ Conclusions and perspectives

SPI under a magnetic field



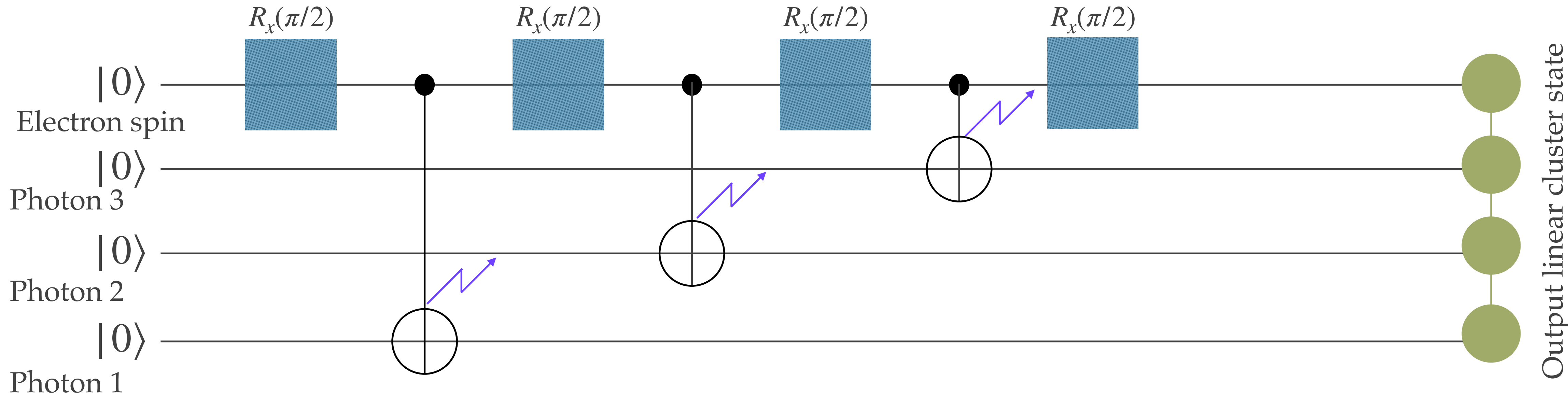
- ❖ **Set-up:** Same as before + perpendicular magnetic field (Voigt configuration)
- ❖ Necessary to perform the **Lindner Rudolph protocol (LRP)** [1] → Generation of highly entangled photonic states

[1] Lindner, N. H. & Rudolph, T. Proposal for Pulsed On-Demand Sources of Photonic Cluster State Strings. *Phys. Rev. Lett.* 103, 113602 (2009).

[2] Coste, N. et al. High-rate entanglement between a semiconductor spin and indistinguishable photons. *Nat. Photon.* (2023) doi:10.1038/s41566-023-01186-0.

What is the LRP and how does it work?

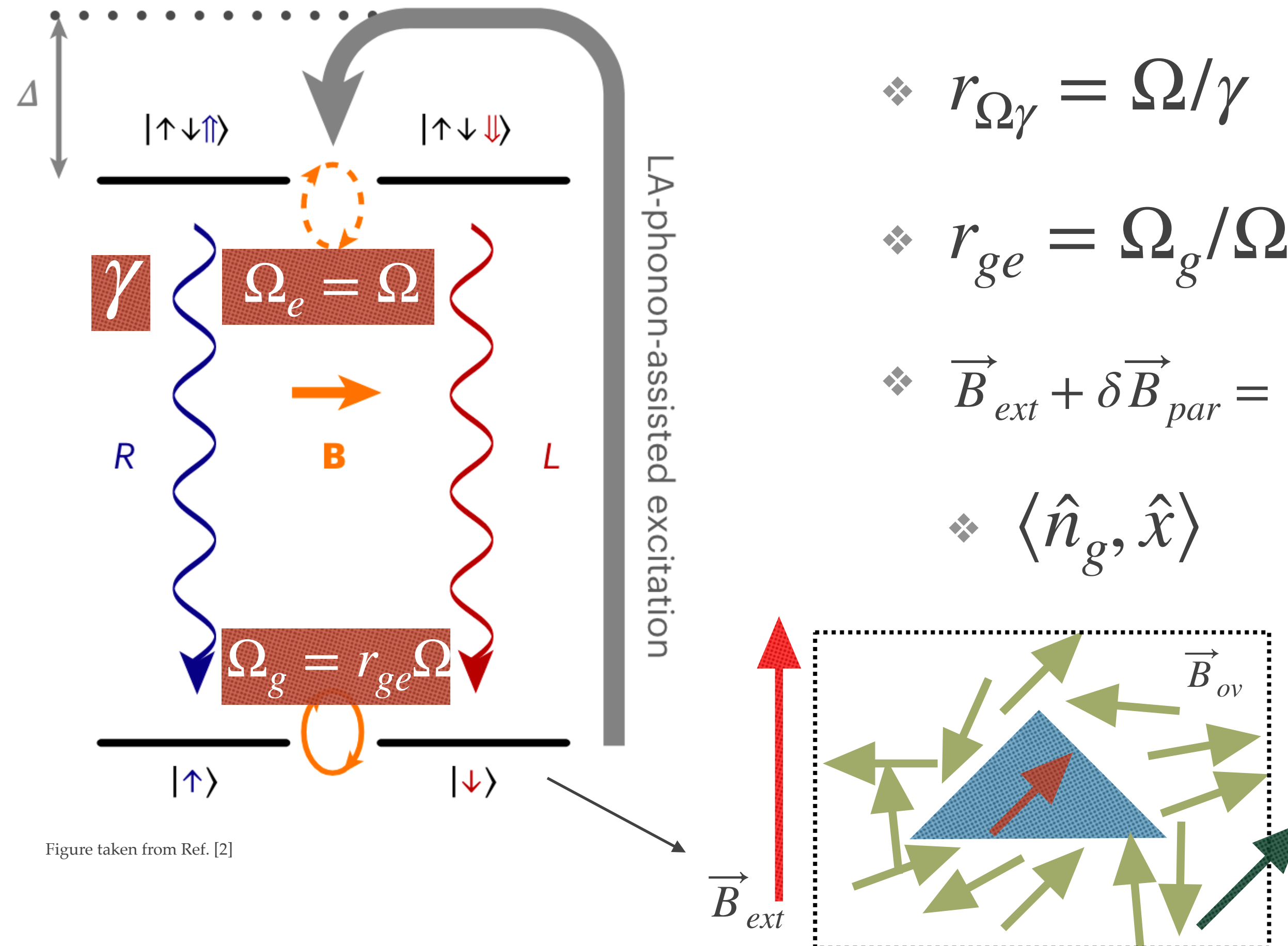
- ❖ Two ingredients:
 - ❖ π -pulses
 - ❖ Spin rotations



[1] Lindner, N. H. & Rudolph, T. Proposal for Pulsed On-Demand Sources of Photonic Cluster State Strings. *Phys. Rev. Lett.* 103, 113602 (2009).

[2] Coste, N. et al. High-rate entanglement between a semiconductor spin and indistinguishable photons. *Nat. Photon.* (2023) doi:10.1038/s41566-023-01186-0.

Experimental implementation



- ❖ $r_{\Omega\gamma} = \Omega/\gamma$

- ❖ $r_{ge} = \Omega_g/\Omega$

- ❖ $\vec{B}_{ext} + \delta\vec{B}_{par} = \vec{B}_g = B_g \hat{n}_g$

- ❖ $\langle \hat{n}_g, \hat{x} \rangle$

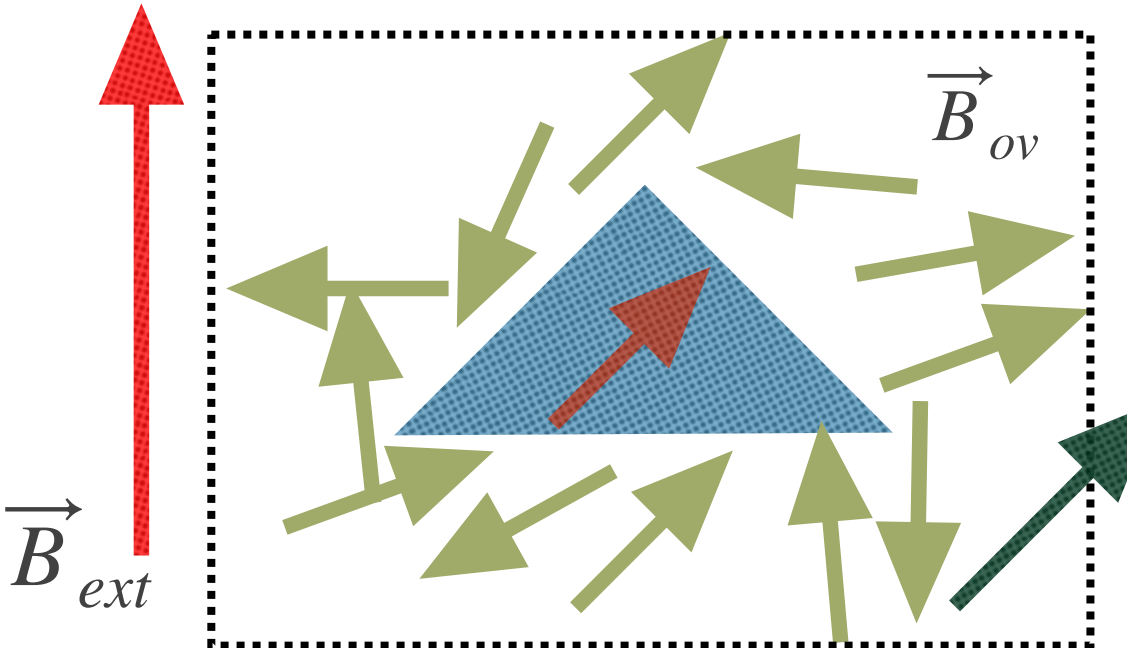
- ❖ Ideal scenario:

- ❖ $r_{\Omega\gamma} \ll 1$

- ❖ $r_{ge} = 1$

- ❖ $\langle \hat{n}_g, \hat{x} \rangle = 1$

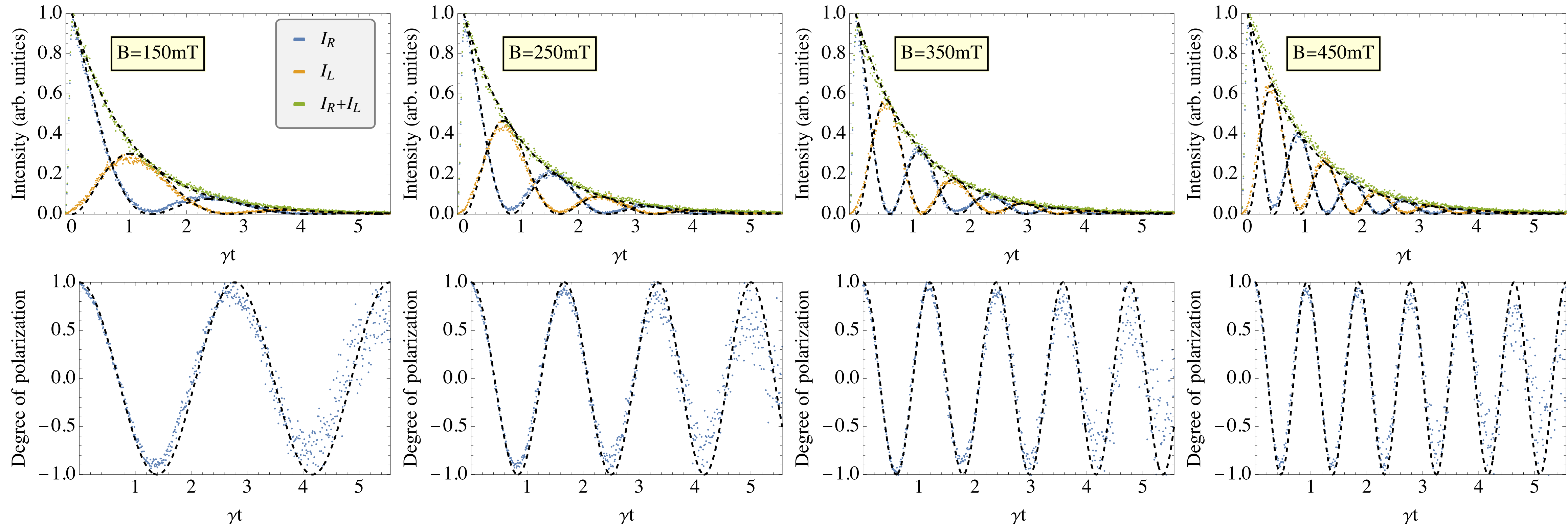
The analytical wave-function $|\Psi^\zeta(t)\rangle$ is found as a function of all these parameters.



[1] Lindner, N. H. & Rudolph, T. Proposal for Pulsed On-Demand Sources of Photonic Cluster State Strings. Phys. Rev. Lett. 103, 113602 (2009).

[2] Coste, N. et al. High-rate entanglement between a semiconductor spin and indistinguishable photons. Nat. Photon. (2023) doi:10.1038/s41566-023-01186-0.

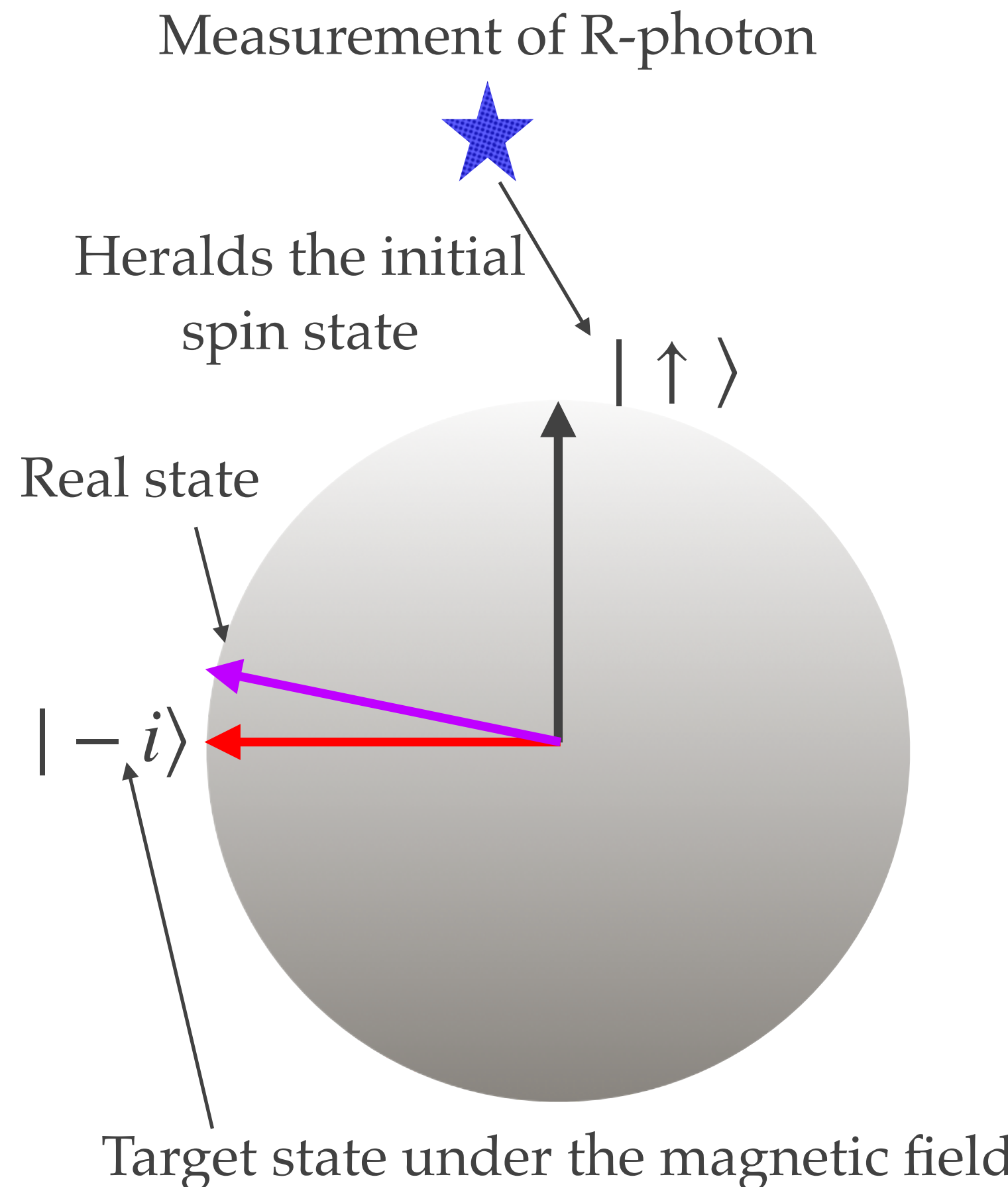
Model validation: The analytical solution (dashed black lines) fits experimental data points.



The closed dynamics solution replicates experimental data from Ref. [1] (provided by the authors)

[1] Coste, N. et al. Probing the dynamics and coherence of a semiconductor hole spin via acoustic phonon-assisted excitation. Preprint at <http://arxiv.org/abs/2207.05981> (2022).

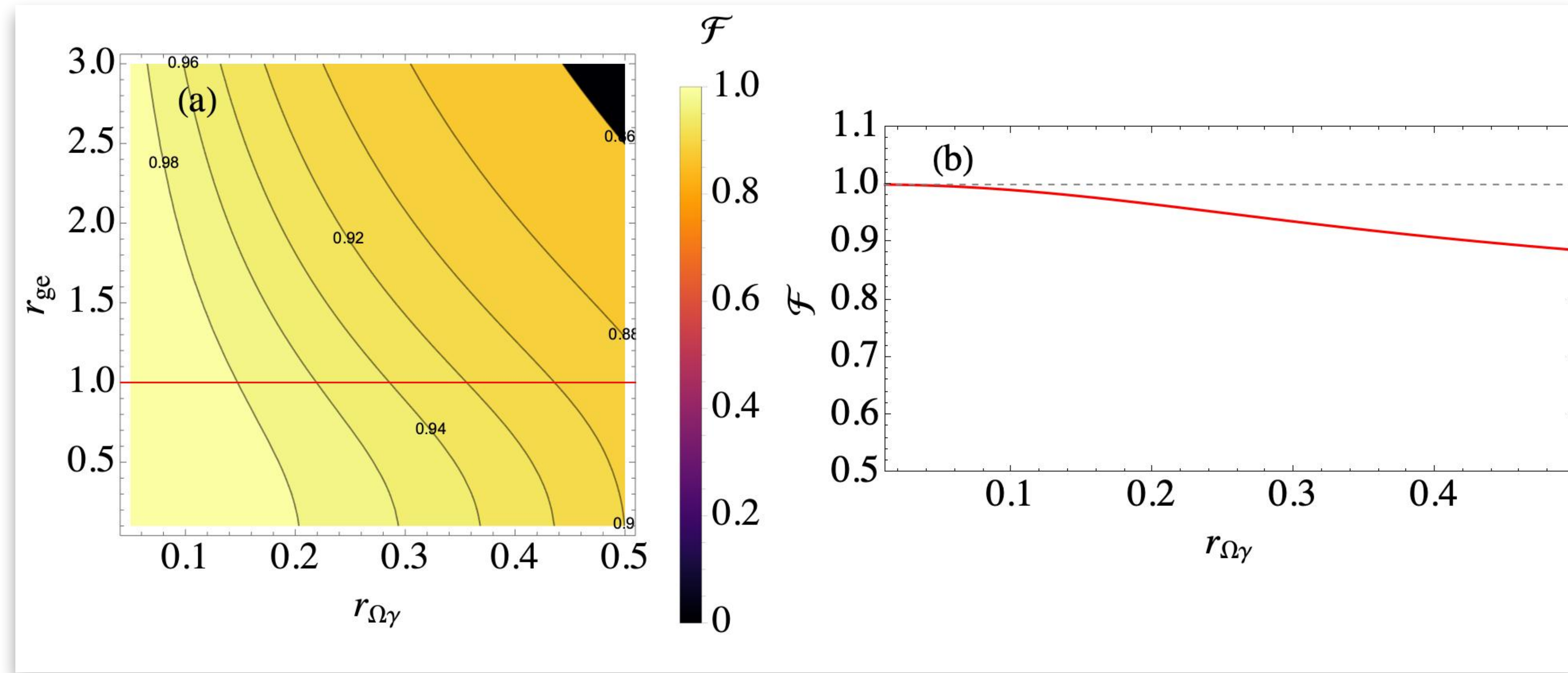
How do deviations from the ideal scenario impact the rotation?



$$\begin{aligned}\mathcal{F}(\rho_{tar}, \rho_{real}) &= \text{tr}\{\sqrt{\sqrt{\rho_{tar}}\rho_{real}\sqrt{\rho_{tar}}}\} \\ &= \frac{1}{2} + \text{Im}\{\rho_{\downarrow\uparrow}^{\uparrow}\}\end{aligned}$$

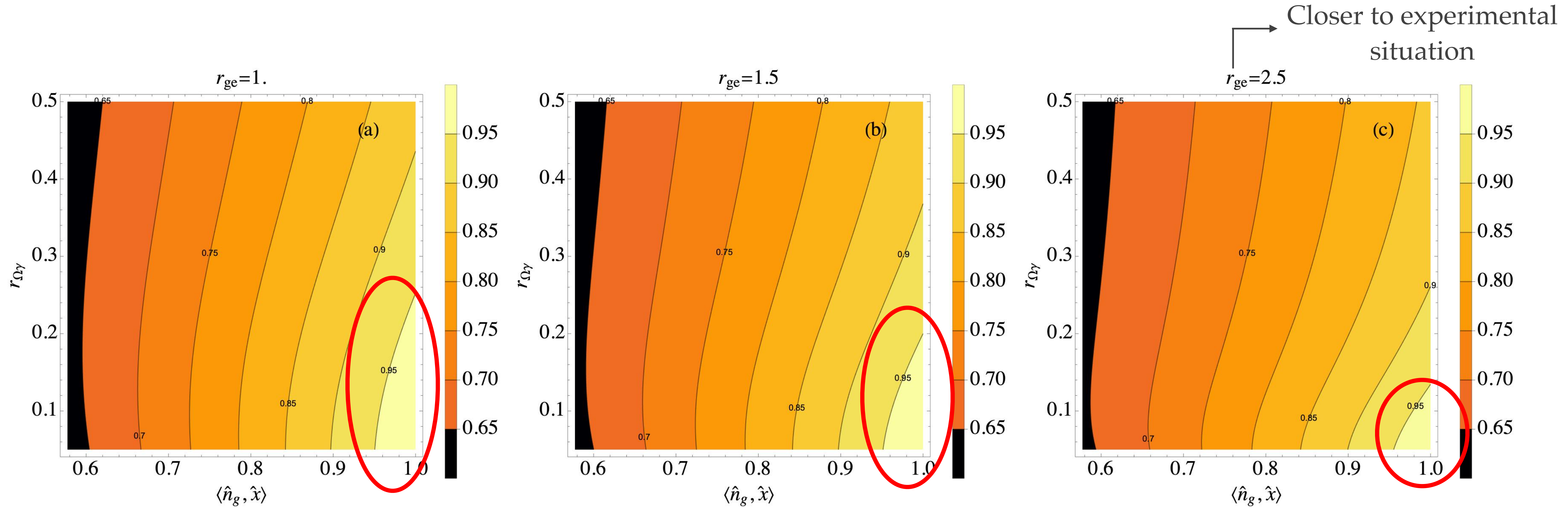
- ❖ Ideal scenario:
- ❖ $r_{\Omega\gamma} = \Omega/\gamma \ll 1$
- ❖ $r_{ge} = 1$
- ❖ $\langle \hat{n}_g, \hat{x} \rangle = 1$

Fidelity analysis: impact of finite pulse duration $r_{\Omega\gamma}$ and different precession frequencies r_{ge}



Perfect aligned magnetic field: overall we have a high fidelity.
 $r_{\Omega\gamma}$ plays a bigger role.

Fidelity analysis for different r_{ge} : impact of finite decay $r_{\Omega\gamma}$ and imperfect alignment of the magnetic field $\langle \hat{n}_g, \hat{x} \rangle$



Tilted magnetic field: the region of high fidelity **shrinks** as the r_{ge}

Outline

- ❖ Preliminaries
 - ❖ von Neumann measurement model
 - ❖ Collisional model or how to close open systems
- ❖ Main results
 - ❖ Energy efficient entanglement generation and readout in a spin-photon interface
 - ❖ Photon-photon controlled phase-gate and error analysis
 - ❖ SPI under a magnetic field
- ❖ Conclusions and perspectives

Conclusions

- ❖ **Collisional model solution:** The technique closes systems that are usually treated as open quantum systems or within cQED, providing **complete information about the light-matter entangled state.**
- ❖ **Contributions:**
 - ❖ **Spin-Photon Entanglement:** Achieved quantum advantage in non-destructive spin state measurements in both, pre-measurement and collapse, steps of the von Neumann measurement model
 - ❖ **Photon-Photon Gate:** Proposed a single-rail photon-photon gate c-phase gate, and analyzed error characterization leveraging the dynamics resolution.
 - ❖ **Modeling the LRP:** Extended solutions to include in-plane magnetic fields to model state-of-art experimental platform implementing the LRP.

Some perspectives

- ❖ Investigate **spin-spin entanglement** generation via the spin-photon entanglement studied.
- ❖ Study the characterization of the scattered field and investigate protocols that generates **non-classical states of light**.
- ❖ Gain insights from **thermodynamics concepts in the quantum regime** leveraging the closed dynamics solution and using quantum optics settings.

Thank you!



This project received funding from the European Union's Horizon 2020 Research and Innovation Program under the Marie Skłodowska-Curie grant agreement No. 861097.

Publications

PHYSICAL REVIEW A 107, 023710 (2023)

Anomalous energy exchanges and Wigner-function negativities in a single-qubit gate

Maria Maffei¹, Cyril Elouard², Bruno O. Goes¹, Benjamin Huard³, Andrew N. Jordan^{4,5}, and Alexia Auffèves^{1,6}

¹Université Grenoble Alpes, CNRS, Grenoble INP, Institut Néel, 38000 Grenoble, France

²Inria, ENS Lyon, LIP, F-69342, Lyon Cedex 07, France

³Ecole Normale Supérieure de Lyon, CNRS, Laboratoire de Physique, F-69342 Lyon, France

⁴Institute for Quantum Studies, Chapman University, 1 University Drive, Orange, California 92866, USA

⁵Department of Physics and Astronomy, University of Rochester, Rochester, New York 14627, USA

⁶MajuLab, International Joint Research Unit UMI 3654, CNRS, Université Côte d'Azur, Sorbonne Université, National University of Singapore, Nanyang Technological University, Singapore



(Received 26 October 2022; accepted 30 January 2023; published 13 February 2023)

nature photonics

Article

<https://doi.org/10.1038/s41566-023-01186-0>

High-rate entanglement between a semiconductor spin and indistinguishable photons

Received: 22 November 2022

N. Coste¹✉, D. A. Fioretto¹, N. Belabas¹, S. C. Wein^{1,2,3}, P. Hilaire^{2,4},

Accepted: 21 February 2023

R. Frantzeskakis⁵, M. Gundin¹, B. Goes^{1,3}, N. Somaschi², M. Morassi¹,

Published online: 10 April 2023

A. Lemaitre¹, I. Sagnes¹, A. Harouri¹, S. E. Economou^{1,6}, A. Auffèves³,

O. Krebs¹, L. Lanco^{1,7} & P. Senellart¹✉

Check for updates

Quantum
the open journal for quantum science

PAPERS

Energy-efficient quantum non-demolition measurement with a spin-photon interface

Maria Maffei¹, Bruno O. Goes², Stephen C. Wein^{2,3}, Andrew N. Jordan^{4,5}, Loïc Lanco⁶, and Alexia Auffèves^{7,8}

¹Dipartimento di Fisica, Università di Bari, I-70126 Bari, Italy

²Université Grenoble Alpes, CNRS, Grenoble INP, Institut Néel, 38000 Grenoble, France

³Quandela SAS, 10 Boulevard Thomas Gobert, 91120 Palaiseau, France

⁴Institute for Quantum Studies, Chapman University, 1 University Drive, Orange, CA 92866, USA

⁵Department of Physics and Astronomy, University of Rochester, Rochester, New York 14627, USA

⁶Université Paris Cité, Centre for Nanoscience and Nanotechnology (C2N), F-91120 Palaiseau, France

⁷MajuLab, CNRS-UCA-SU-NUS-NTU International Joint Research Laboratory

⁸Centre for Quantum Technologies, National University of Singapore, 117543 Singapore, Singapore

Published: 2023-08-31, volume 7, page 1099

Eprint: arXiv:2205.09623v4

Doi: <https://doi.org/10.22331/q-2023-08-31-1099>

Citation: Quantum 7, 1099 (2023).

Participation in events

- ❖ QUDOT-TECH + QCLUSTER workshop! - Palaiseau. Talk. 2023. (Workshop)
- ❖ QUDOT-TECH 3rd summer school - Oxford. Poster presentation. 2023. (School).
- ❖ (Post)modern thermodynamics school + workshop - Luxembourg. Poster presentation. Dec. 2022 (School & workshop).
- ❖ QUDOT-TECH 2nd summer school - Denmark. Poster presentation. 2022. (School).
- ❖ QUDOT-TECH 1st summer school - Online. Poster presentation. 2021. (School).
- ❖ Quantum Thermodynamics Summer School - Switzerland. (Summer school).
- ❖ Quantum nanophotonics - Centro de Ciencias de Benasque Pedro Pascual - Online. Poster presentation. 2021. (Workshop)

Bonus

- ❖ All the codes used for the thesis and some extra material is publicly available on a dedicated GitHub directory:

The screenshot shows a GitHub repository page for 'PhDThesisSPI'. The repository is public and has 1 branch and 0 tags. The commit history lists 76 commits from the 'main' branch, all made by 'BrunoOGoess'. The commits are organized into several folders: 'Bonus material', 'Chapter1', 'Chapter2', 'Chapter3', 'Chapter4', 'Chapter5', '.DS_Store', '.gitattributes', and 'README.md'. The most recent commit is 'Update README.md' from 2 months ago. The repository has 1 watch, 0 forks, and 0 stars. The 'About' section describes the repository as a comprehensive collection of codes utilized to generate plots and analytical expressions for the PhD thesis.

Commit	Message	Date
548941e	Took off unnecessary notebooks.	2 weeks ago
	Organized chapters 2 and 3 folders.	2 months ago
	Organized chapters 2 and 3 folders.	2 months ago
	Organized chapters 2 and 3 folders.	2 months ago
	.	2 weeks ago
	.	2 weeks ago
	Organized chapters 2 and 3 folders.	2 months ago
	Initial commit	4 months ago
	Update README.md	2 months ago

About

This repository is dedicated to the comprehensive collection of codes utilized to generate the plots and/or analytical expressions showcased within the pages of my PhD thesis.

Readme
Activity
0 stars
1 watching
0 forks

Releases

No releases published
[Create a new release](#)

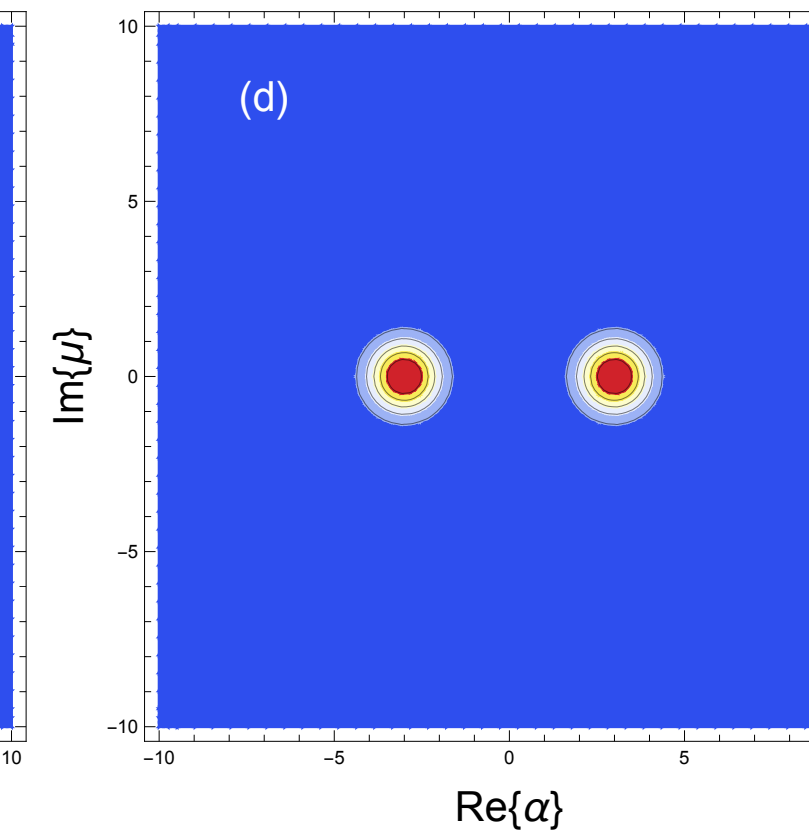
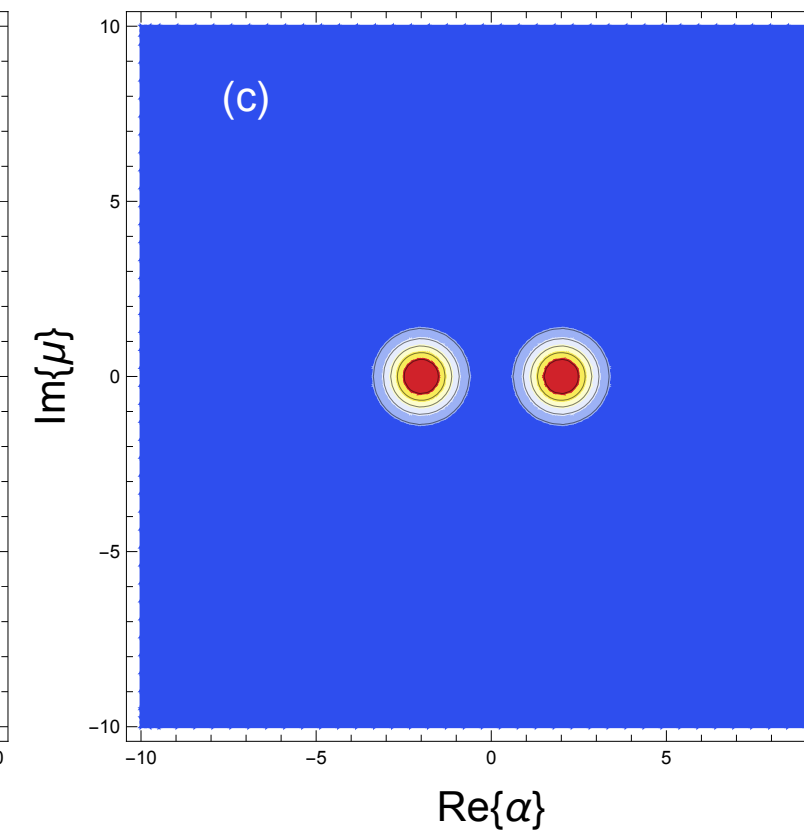
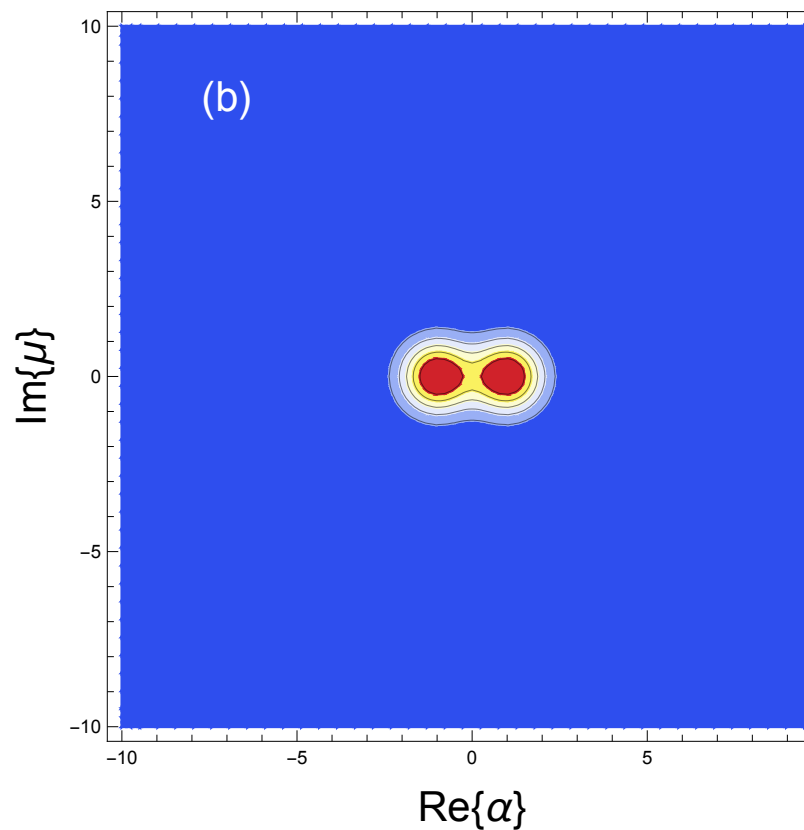
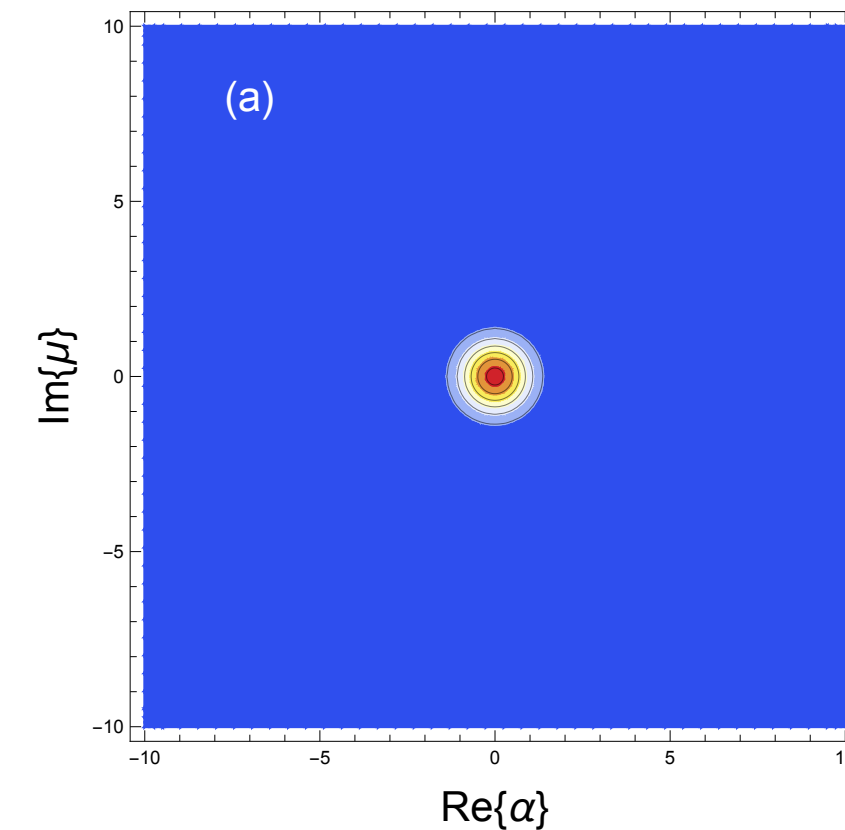
Backup slides

Chapter 1

Example: measuring the spin of a 1/2 particle

- ❖ System density matrix:

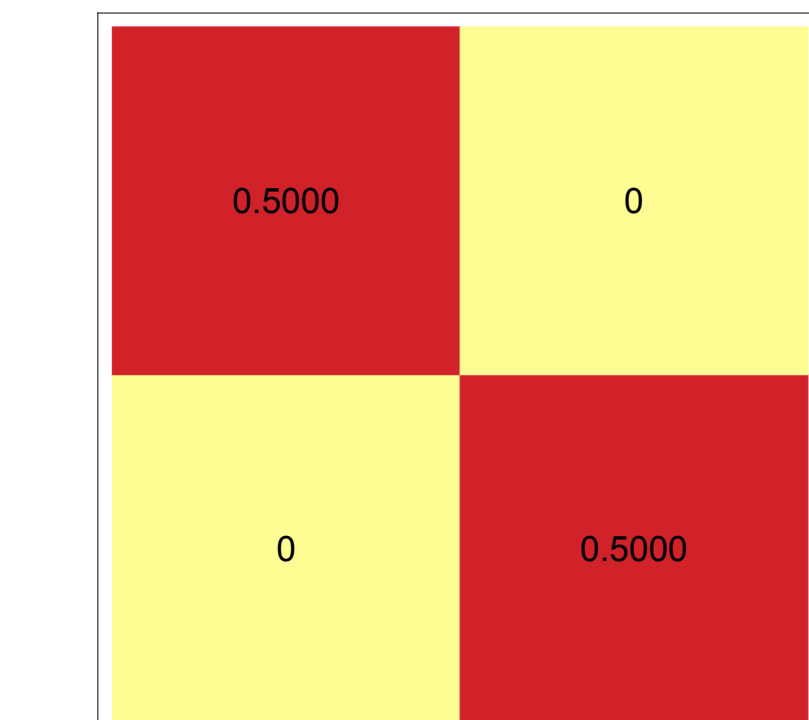
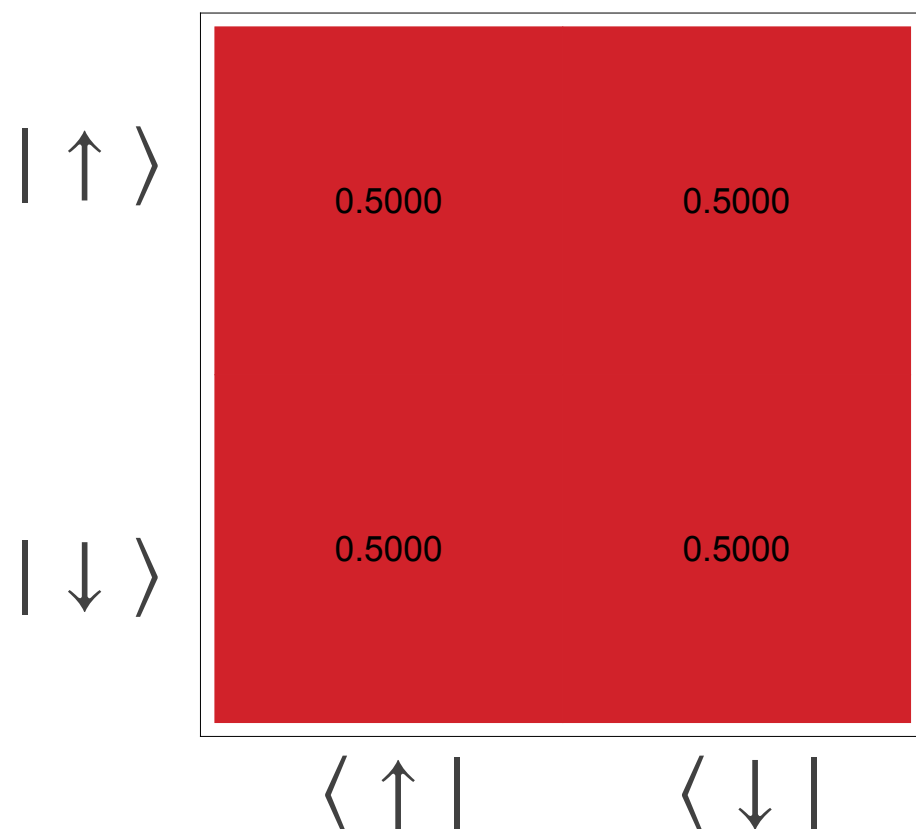
$$\rho_S = \sum_{k,q} c_k c_q^* \exp \left\{ -\frac{(g_0 t)^2}{2} (k - q)^2 \right\} |k\rangle_S \langle q|$$



- ❖ Meter density matrix:

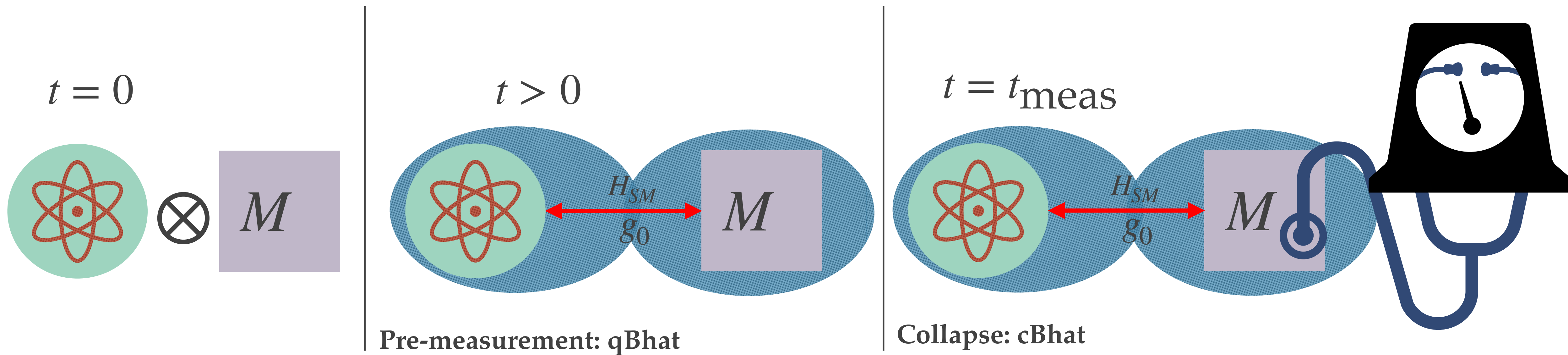
$$\rho_M = \sum_k |c_k|^2 |g_0 k t\rangle_M \langle g_0 k t| \longrightarrow Q_M(\mu, \bar{\mu}) = \frac{1}{\pi} \langle \mu | \rho_M | \mu \rangle$$

→ Disjoint probability distributions.



→ Mixed state.

Take away messages 1



- ❖ When measurement is concerned, having access to the joint wave-function a **valuable information** (here enters the Collisional Model to be discussed next).

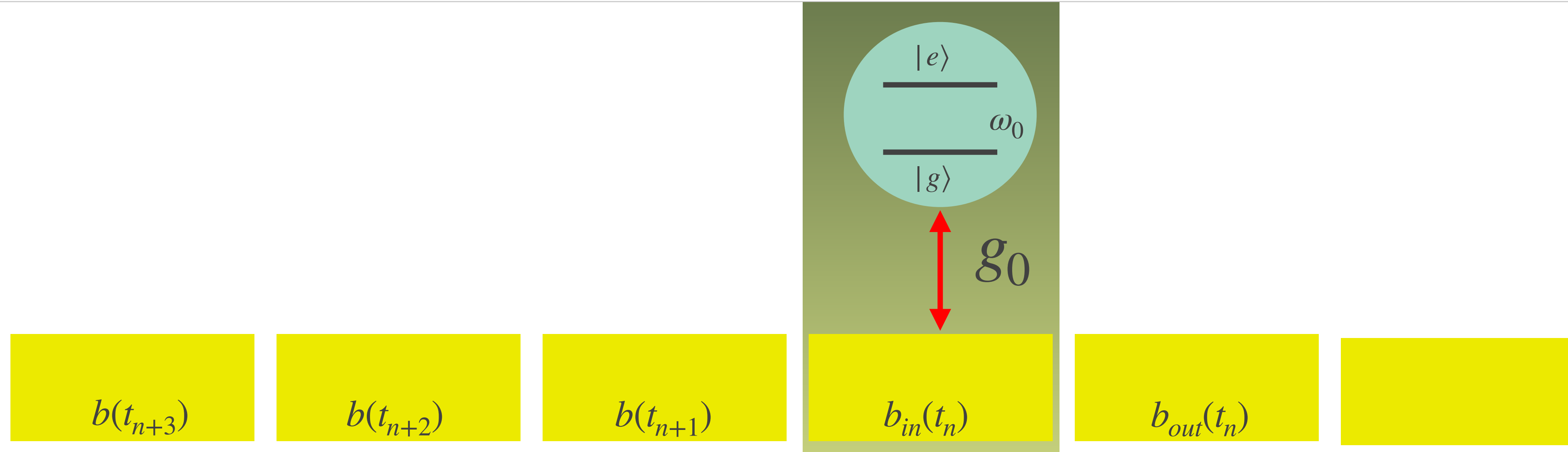
[1] J. von Neumann, Mathematical Foundations of Quantum Mechanics: New Edition. Princeton University Press, 2018.

[2] W. H. Zurek, “Decoherence, einselection, and the quantum origins of the classical,” Rev. Mod. Phys., vol. 75, no. 3, pp. 715–775, May 2003

[3] Fuchs, C. A. & Caves, C. M. Mathematical techniques for quantum communication theory. Open Syst Inf Dyn 3, 345–356 (1995).

Chapter 2

Interaction picture & time discretization



$$V_{qf}(t_n) = V_n = i\sqrt{\frac{\gamma}{\Delta t}} [\sigma^\dagger(t_n)b(t_n) - b^\dagger(t_n)\sigma(t_n)]$$

The emitter interacts with one *temporal mode* at a time, repeatedly → Collisional model interpretation.

[3] M. Maffei, P. A. Camati, and A. Auffèves, "Closed-System Solution of the 1D Atom from Collision Model," Entropy, vol. 24, no. 2, p. 151, Jan. 2022

[4] Gross, J. A., Caves, C. M., Milburn, G. J. & Combes, J. Qubit models of weak continuous measurements: markovian conditional and open-system dynamics. Quantum Sci. Technol. 3, 024005 (2018).

Coherent field solution

$$|\Psi_{CS}(0)\rangle = D(\alpha_d)|\zeta\rangle \otimes |\emptyset\rangle, \zeta = g, e$$



Initially uncorrelated: Markovian dynamics
(Lindblad)

$$|\Psi_\beta^\zeta(t_N)\rangle = \sqrt{P_g(t)}|g\rangle|\phi_g(t)\rangle + \sqrt{P_e(t)}|e\rangle|\phi_e(t)\rangle$$

→ Technical detail: displaced frame.

$$|\phi_\epsilon\rangle = \frac{1}{\sqrt{P_\epsilon(t)}} \left[\sqrt{p_{0,\epsilon}} \tilde{f}_{\epsilon,\zeta}^{(0)}(t) + \sum_{m=1}^{\infty} \sqrt{p_{m,\epsilon}(t)} \int_0^t ds_m \tilde{f}_{\epsilon,\zeta}^{(m)}(t,s) \prod_{i=1}^m b_m^\dagger \right] |\emptyset\rangle$$



Suffices to find the coefficients: possible to do analytically.

Single photon solution

$$|1\rangle = \sum_{n=0}^{\infty} \sqrt{\Delta t} \xi(t_n) b_n^\dagger |\emptyset\rangle \quad \sum_{n=0}^{\infty} \Delta t |\xi(t_n)| = 1$$

↓

Initially correlated: Non-markovian dynamics

$$|\Psi_{SP}(t_N)\rangle = \left(\sqrt{\gamma} \sqrt{\Delta t} e^{-\frac{\gamma}{2}t_N} \sum_{n=0}^{N-1} \sqrt{\Delta t} e^{(\frac{\gamma}{2} + i\omega_0)t_n} \xi(t_n) |\emptyset\rangle \right) \otimes |e\rangle$$

$$+ \left(\sum_{n=0}^{N-1} \left[\sqrt{\Delta t} \xi(t_n) - \gamma \Delta t e^{-(\frac{\gamma}{2} + i\omega_0)t_n} \sum_{m=0}^n \left(e^{(\frac{\gamma}{2} + i\omega_0)t_m} \sqrt{\Delta t} \xi(t_m) \right) \right] b_n^\dagger |\emptyset\rangle \right) \otimes |g\rangle + \left(\sum_{n=N}^{\infty} \sqrt{\Delta t} \xi(t_n) b_n^\dagger |\emptyset\rangle \right) \otimes |g\rangle.$$

Already interacted.

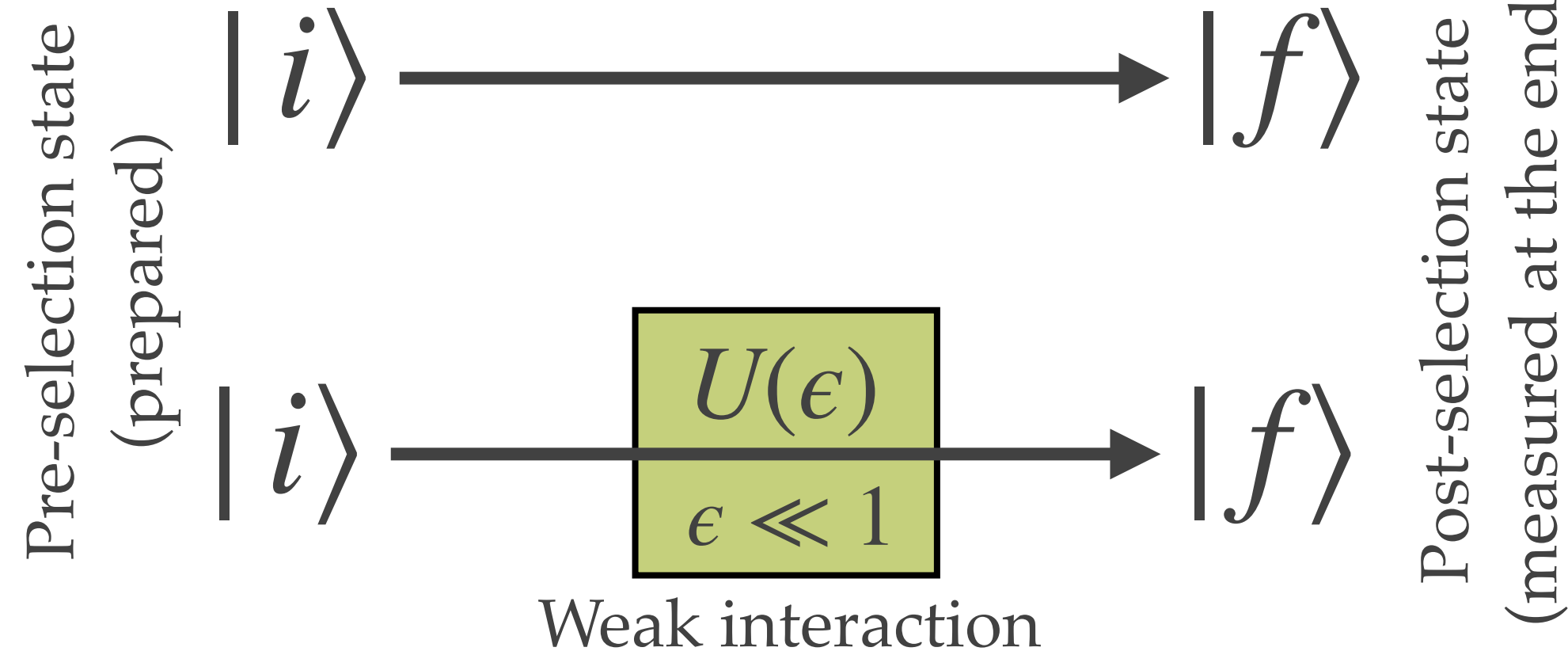
Part that is yet to interact.

Take away messages 2

- ❖ The collisional model allows to solve the the unitary dynamics of the 1D waveguide and emitter.
- ❖ Analytical light-matter wave functions are derived.

Chapter 3

Quantum weak values



Post-selection state (measured at the end)

$$P_{i \rightarrow f} = |\langle f | i \rangle|^2$$

$$P_{i \rightarrow f}(\epsilon) = |\langle f | U(\epsilon) | i \rangle|^2$$

$$\frac{P_{i \rightarrow f}(\epsilon)}{P_{i \rightarrow f}} = 1 + 2\epsilon \Im\{A_w^1\} + \mathcal{O}(\epsilon^2)$$

The nth order weak value of A has the form:

$$A_w^n = \frac{\langle f | A^n | i \rangle}{\langle f | i \rangle}$$

❖ Weak measurements → **minimal disturbance to the system.**

$$U(\epsilon) = \exp\{-i\epsilon A\} \approx 1 - i\epsilon A + \dots$$

$$P_{i \rightarrow f}(\epsilon) = |\langle f | U(\epsilon) | i \rangle|^2 = P_{i \rightarrow f} + 2\epsilon \Im\{\langle i | f \rangle \langle f | A | i \rangle\} + \mathcal{O}(\epsilon^2)$$

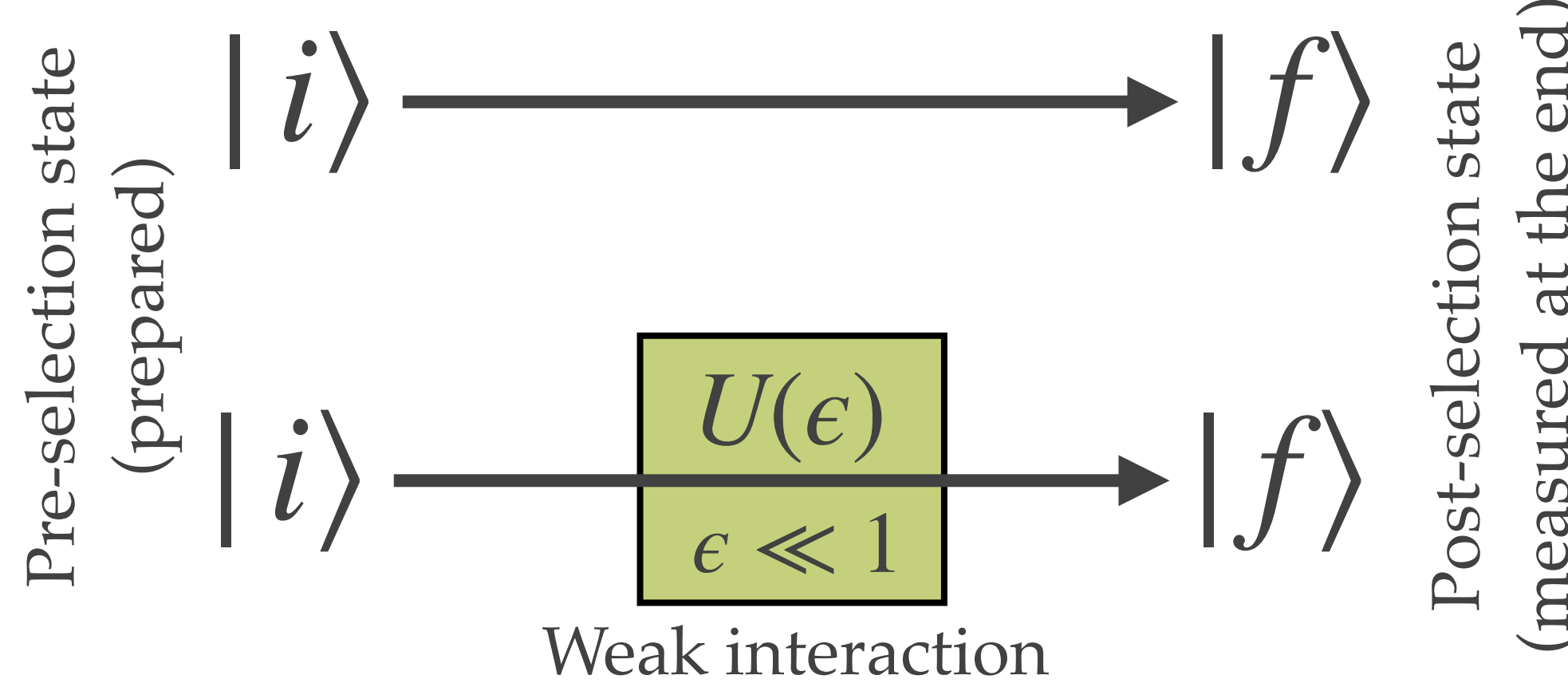
$|i\rangle$ =pre-selection state

$|f\rangle$ =post-selection state

Y. Aharonov, D. Albert, and L. Vaidman, "How the result of a measurement of a component of the spin of a spin-1/2 particle can turn out to be 100," Physical Review Letters 60, 1351 (1988).

J. Dressel, M. Malik, F. M. Miatto, A. N. Jordan, and R. W. Boyd, "Colloquium: Understanding quantum weak values: Basics and applications," Rev. Mod. Phys., vol. 86, no. 1, pp. 307–316, Mar. 2014

Quantum weak values



$$P_{i \rightarrow f} = |\langle f | i \rangle|^2$$

$$\frac{P_{i \rightarrow f}(\epsilon)}{P_{i \rightarrow f}} = 1 + 2\epsilon \Im\{A_w^1\} + \mathcal{O}(\epsilon^2)$$

$$P_{i \rightarrow f}(\epsilon) = |\langle f | U(\epsilon) | i \rangle|^2$$

$$A_w^n = \frac{\langle f | A^n | i \rangle}{\langle f | i \rangle}$$

$|i\rangle$ =pre-selection state

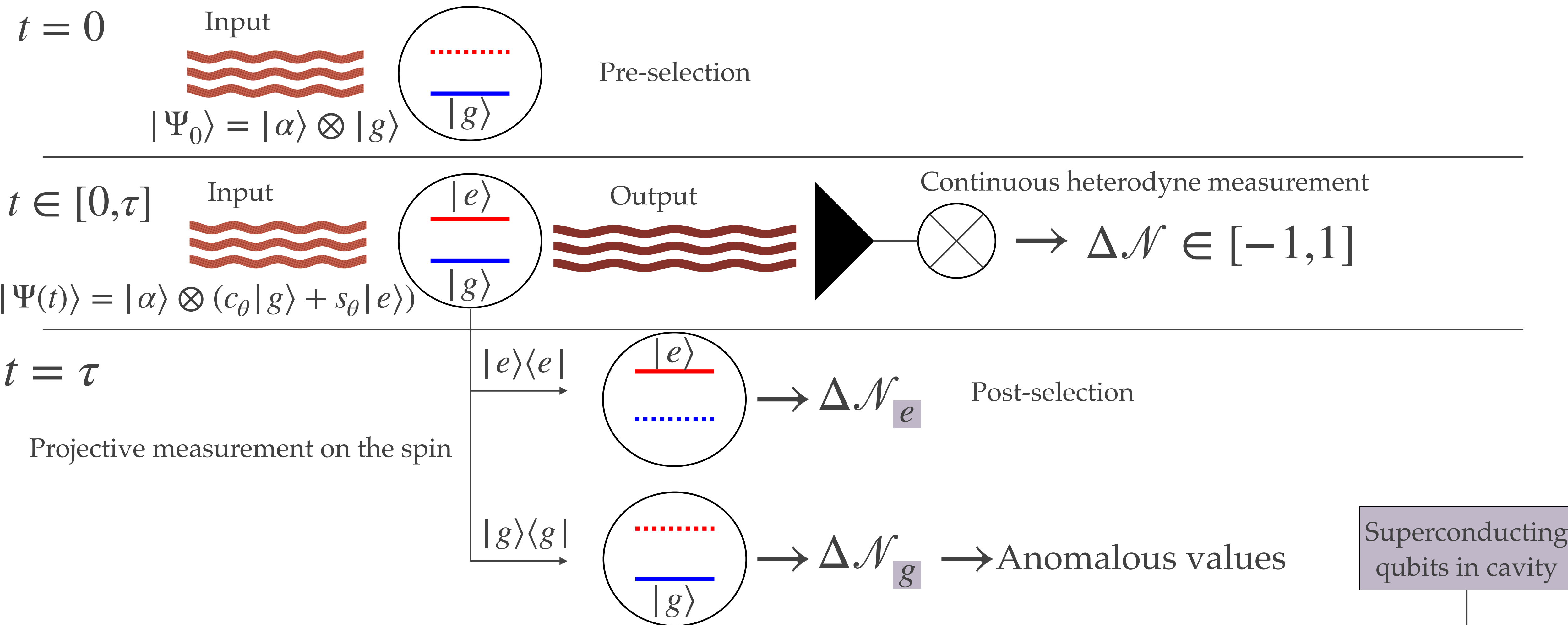
$|f\rangle$ =post-selection state

- ❖ The weak value → **shift in the measured value** of the observable due to a weak measurement
- ❖ They can be:
 - ❖ **Outside the range of eigenvalues**→**Anomalous weak values**→**nonclassical effect** .
 - ❖ Complex Values

Y. Aharonov, D. Albert, and L. Vaidman, "How the result of a measurement of a component of the spin of a spin-1/2 particle can turn out to be 100," Physical Review Letters 60, 1351 (1988).

J. Dressel, M. Malik, F. M. Miatto, A. N. Jordan, and R. W. Boyd, "Colloquium: Understanding quantum weak values: Basics and applications," Rev. Mod. Phys., vol. 86, no. 1, pp. 307–316, Mar. 2014

Measurement protocol



Experimental background

PHYSICAL REVIEW LETTERS 129, 110601 (2022)

Energetics of a Single Qubit Gate

J. Stevens¹, D. Szombati,¹ M. Maffei,² C. Elouard³, R. Assouly¹, N. Cottet¹, R. Dassonneville¹, Q. Ficheux,¹ S. Zeppetzauer¹, A. Bienfait,¹ A. N. Jordan,^{4,5} A. Auffèves,² and B. Huard¹

¹*Ecole Normale Supérieure de Lyon, CNRS, Laboratoire de Physique, F-69342 Lyon, France*

²*CNRS and Université Grenoble Alpes, Institut Néel, F-38042 Grenoble, France*

³*QUANTIC team, INRIA de Paris, 2 Rue Simone Iff, 75012 Paris, France*

⁴*Institute for Quantum Studies, Chapman University, 1 University Drive, Orange, California 92866, USA*

⁵*Department of Physics and Astronomy, University of Rochester, Rochester, New York 14627, USA*

(Received 21 October 2021; revised 19 August 2022; accepted 24 August 2022; published 9 September 2022)

Qubits are physical, a quantum gate thus not only acts on the information carried by the qubit but also on its energy. What is then the corresponding flow of energy between the qubit and the controller that implements the gate? Here we exploit a superconducting platform to answer this question in the case of a quantum gate realized by a resonant drive field. During the gate, the superconducting qubit becomes entangled with the microwave drive pulse so that there is a quantum superposition between energy flows. We measure the energy change in the drive field conditioned on the outcome of a projective qubit measurement. We demonstrate that the drive's energy change associated with the measurement backaction can exceed by far the energy that can be extracted by the qubit. This can be understood by considering the qubit as a weak measurement apparatus of the driving field.

DOI: [10.1103/PhysRevLett.129.110601](https://doi.org/10.1103/PhysRevLett.129.110601)

- ❖ Anomalous weak values appear when post-selected on the ground state
- ❖ Continuous monitoring of the scattered field
- ❖ The joint dynamics of the system is obtained via collisional model
- ❖ **qubit+waveguide with intense coherent state**

Theoretical background

PRL 113, 200401 (2014)

PHYSICAL REVIEW LETTERS

week ending
14 NOVEMBER 2014

Anomalous Weak Values Are Proofs of Contextuality

Matthew F. Pusey*

Perimeter Institute for Theoretical Physics, 31 Caroline Street North, Waterloo, Ontario N2L 2Y5, Canada

(Received 5 September 2014; published 12 November 2014)

The average result of a weak measurement of some observable A can, under postselection of the measured quantum system, exceed the largest eigenvalue of A . The nature of weak measurements, as well as the presence of postselection and hence possible contribution of measurement disturbance, has led to a long-running debate about whether or not this is surprising. Here, it is shown that such “anomalous weak values” are nonclassical in a precise sense: a sufficiently weak measurement of one constitutes a proof of contextuality. This clarifies, for example, which features must be present (and in an experiment, verified) to demonstrate an effect with no satisfying classical explanation.

DOI: [10.1103/PhysRevLett.113.200401](https://doi.org/10.1103/PhysRevLett.113.200401)

PACS numbers: 03.65.Ta, 03.67.-a

PHYSICAL REVIEW LETTERS 129, 230401 (2022)

Contextuality and Wigner Negativity Are Equivalent for Continuous-Variable Quantum Measurements

Robert I. Booth^{1,2,3,*}, Ulysse Chabaud,^{4,†} and Pierre-Emmanuel Emeriau^{5,‡}

¹School of Informatics, University of Edinburgh, Edinburgh EH8 9AB, United Kingdom

²LORIA CNRS, Inria-MOCQUA, Université de Lorraine, F-54000 Nancy, France

³Sorbonne Université, CNRS, LIP6, F-75005 Paris, France

⁴Institute for Quantum Information and Matter, Caltech, Pasadena, California 91125, USA

⁵Quandela, 10 Boulevard Thomas Gobert, 91120, Palaiseau, France

(Received 10 February 2022; accepted 24 October 2022; published 29 November 2022)

Quantum computers promise considerable speedups with respect to their classical counterparts. However, the identification of the innately quantum features that enable these speedups is challenging. In the continuous-variable setting—a promising paradigm for the realization of universal, scalable, and fault-tolerant quantum computing—contextuality and Wigner negativity have been perceived as two such distinct resources. Here we show that they are in fact equivalent for the standard models of continuous-variable quantum computing. While our results provide a unifying picture of continuous-variable resources for quantum speedup, they also pave the way toward practical demonstrations of continuous-variable contextuality and shed light on the significance of negative probabilities in phase-space descriptions of quantum mechanics.

DOI: [10.1103/PhysRevLett.129.230401](https://doi.org/10.1103/PhysRevLett.129.230401)

- [1] Aharonov, Y., Albert, D. Z. & Vaidman, L. How the result of a measurement of a component of the spin of a spin- 1/2 particle can turn out to be 100. Phys. Rev. Lett. 60, 1351–1354 (1988).
- [2] Dressel, J., Malik, M., Miatto, F. M., Jordan, A. N. & Boyd, R. W. Colloquium : Understanding quantum weak values: Basics and applications. Rev. Mod. Phys. 86, 307–316 (2014).
- [3] Kenfack, A. & Yczkowski, K. Negativity of the Wigner function as an indicator of non-classicality. J. Opt. B: Quantum Semiclass. Opt. 6, 396–404 (2004).

Anomalous energy exchanges and Wigner-function negativities in a single qubit gate

- ❖ **Question:** Two hallmarks of non-classicality:
 - ❖ Anomalous weak values → Contextuality
 - ❖ Contextuality → Negativity of the Wigner function (for some set of measurements)
 - ❖ **DO THE PRESENCE OF ANOMALOUS WEAK VALUES INDICATE THE NEGATIVITY OF THE CONDITIONED WIGNER FUNCTION?**
- ❖ **Tool:** Analytical calculation of the field's weak values from the joint-state solution
 - ❖ → CM spot how the weak values appear analytically
 - ❖ → Compute the conditional Wigner function

Change of the field's number of excitations vs. time

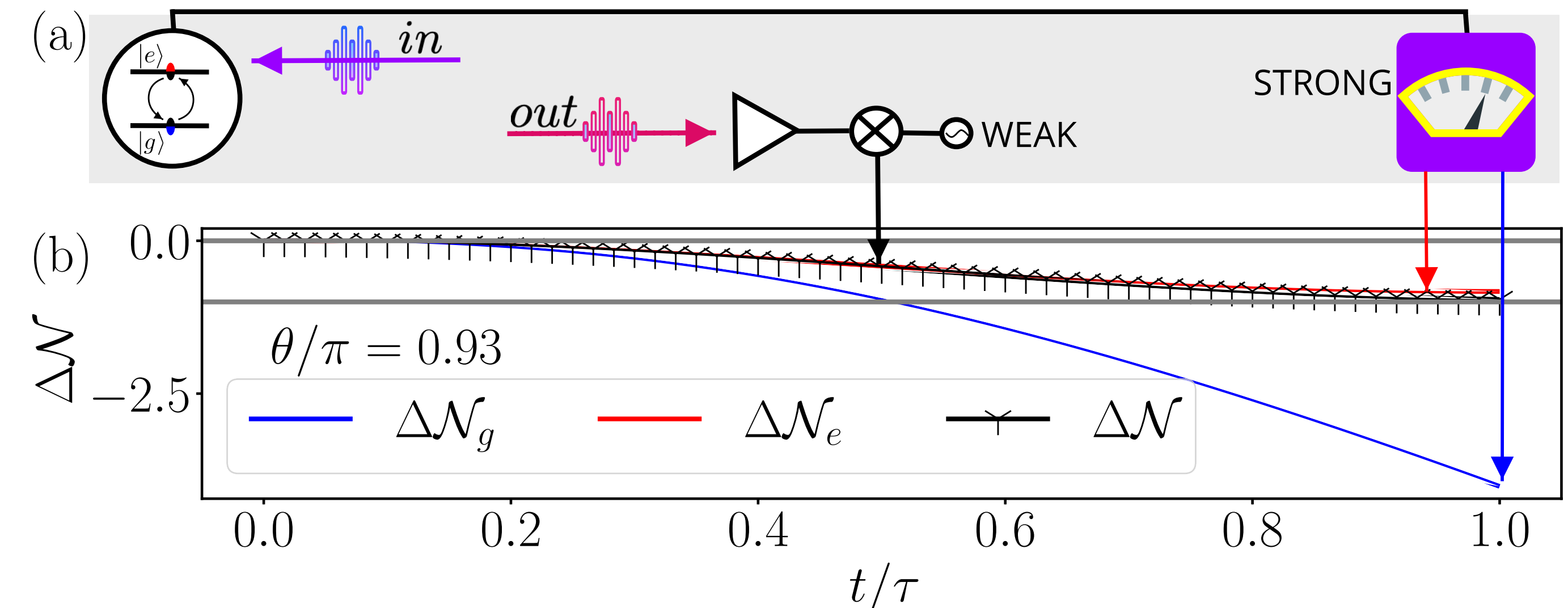
- ❖ Anomalous weak values when conditioned on the ground state.

$$\Delta\mathcal{N}_\epsilon = \int_0^\tau dt \left(\gamma \mathcal{J}_\epsilon(t) - \Omega \text{Re}\{\langle \sigma(t) \rangle_\epsilon\} \right).$$

Total probability
of spontaneous
emission along
the evolution

$$|g\rangle \rightarrow |\epsilon\rangle$$

Interference between input and
emitter's fluorescence post-
selected over $|\epsilon\rangle \rightarrow$ module can
exceed 1 → Anomalous values!

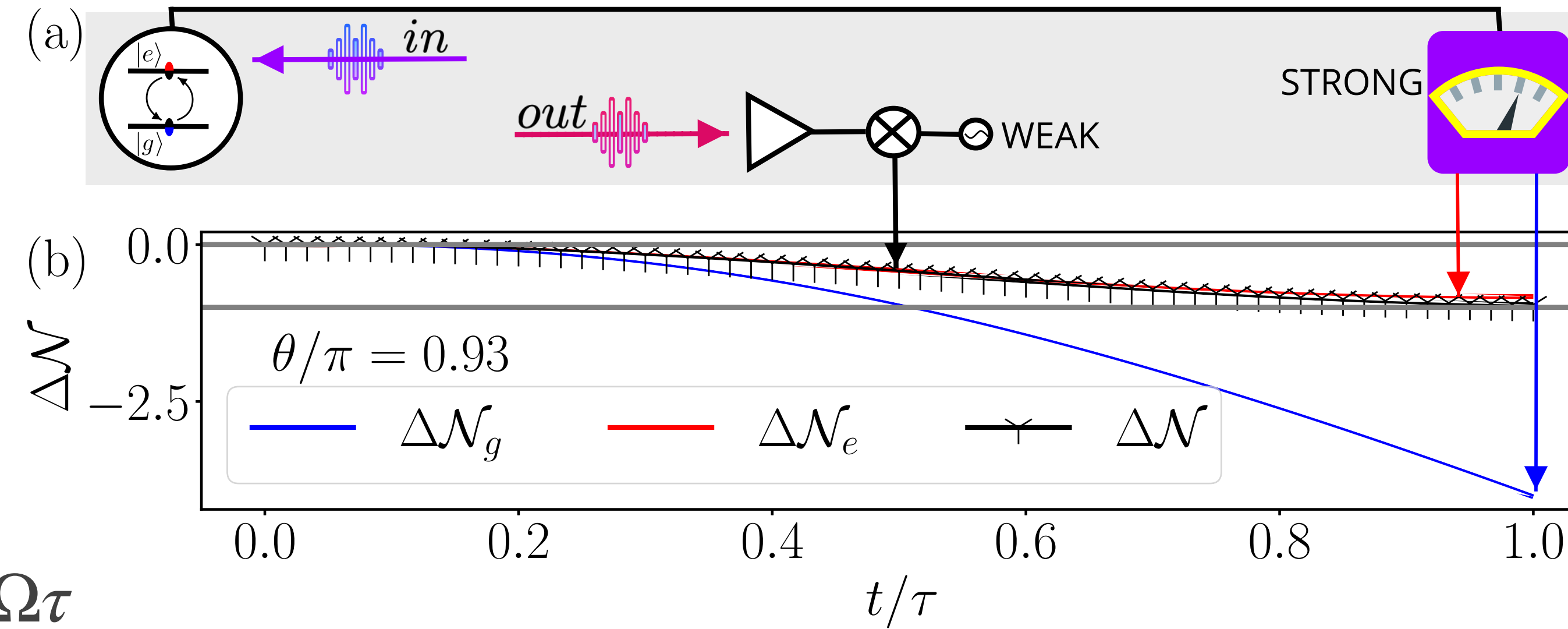


Weak value interpretation

Intense coherent
drive

$$H_D(t) = -\frac{\Omega}{2}\sigma_y$$

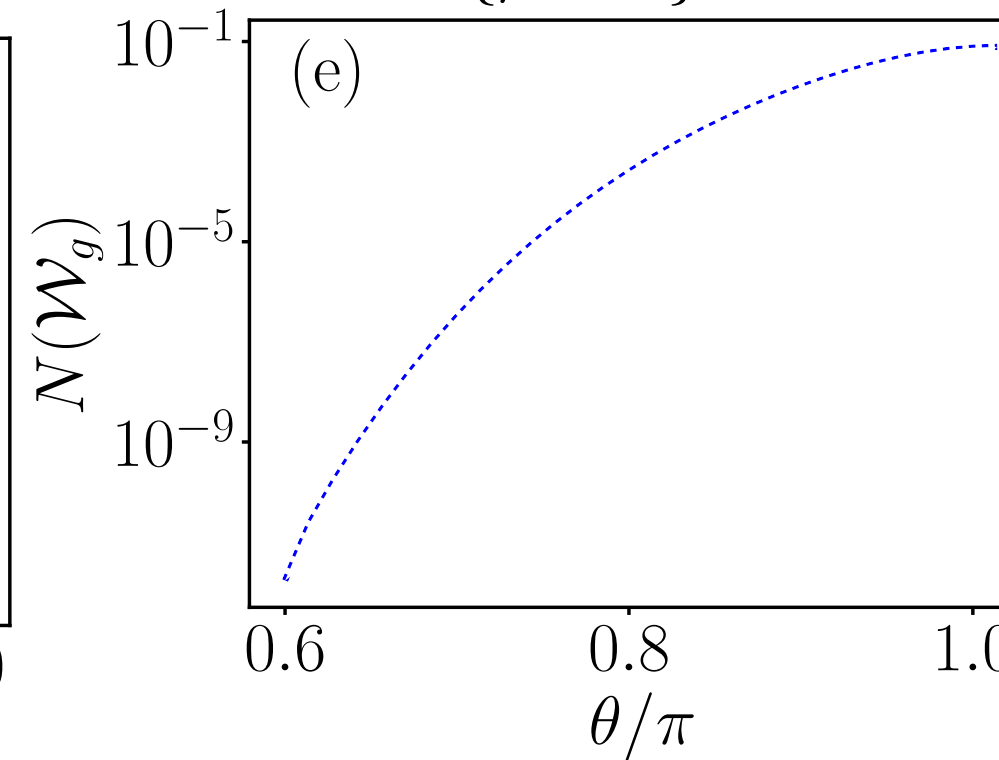
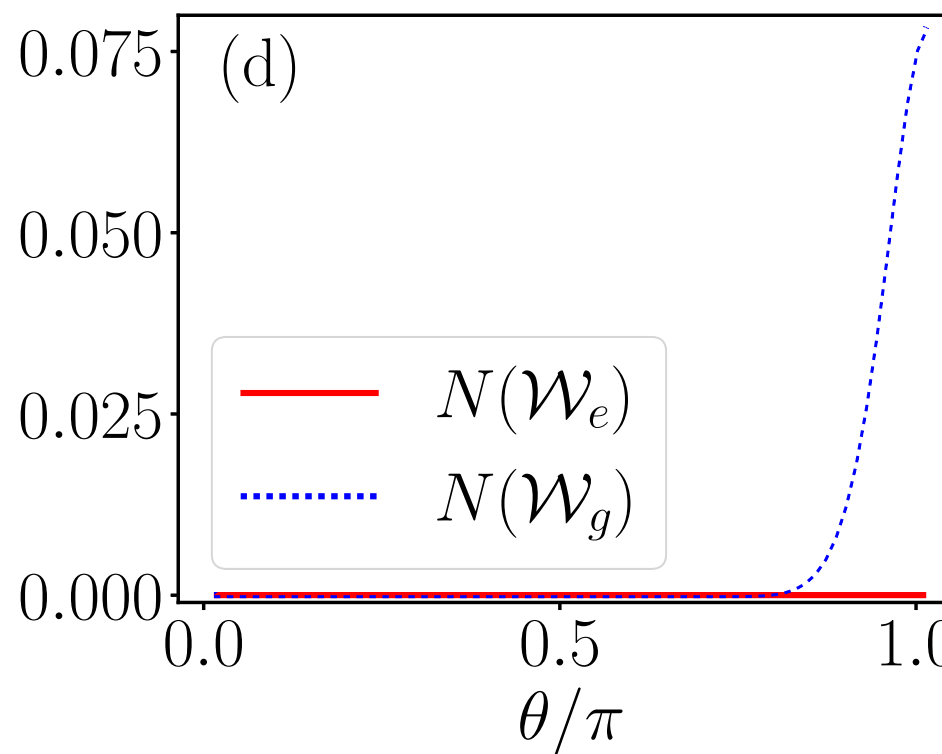
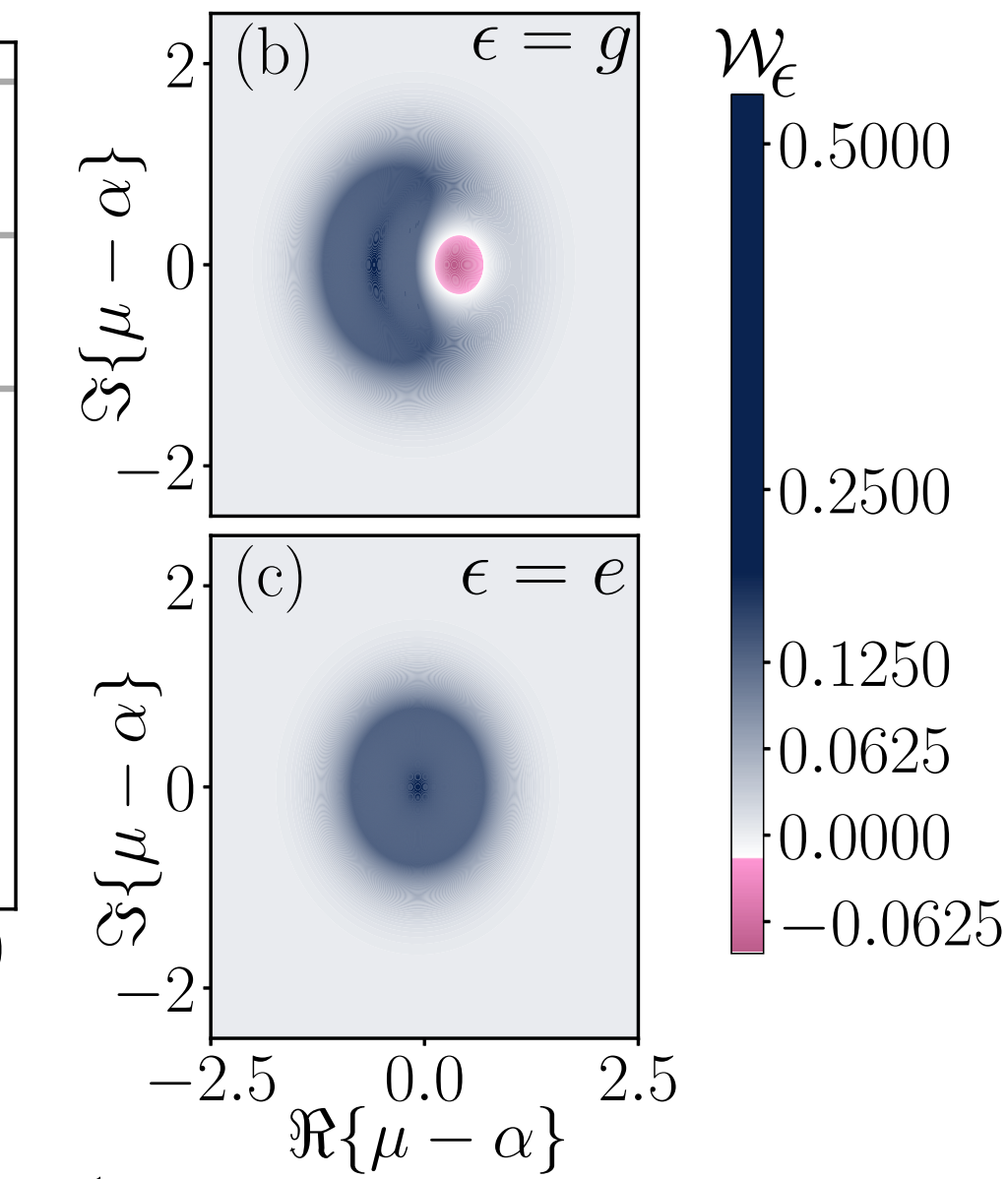
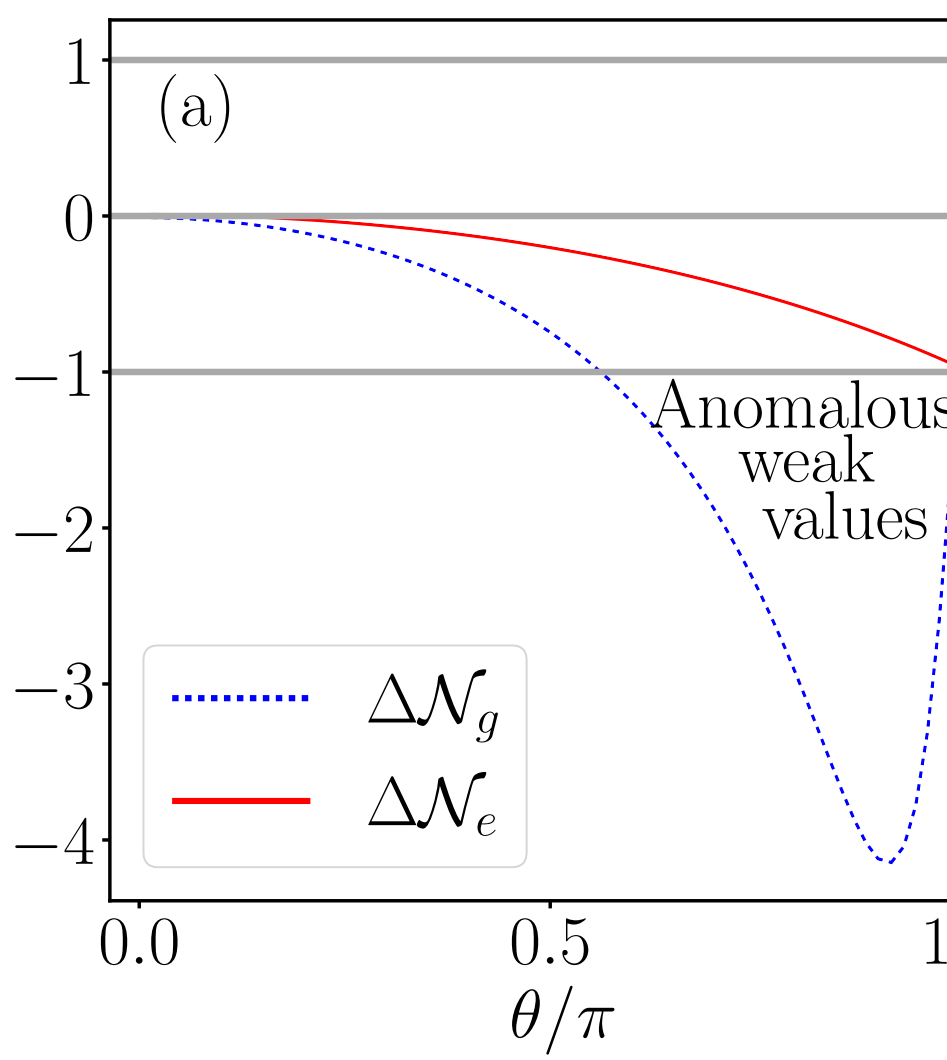
$$\Omega = g\alpha \longrightarrow \theta = \Omega\tau$$



- ❖ $|g\rangle \otimes |\alpha\rangle \xrightarrow{\text{int}(\tau)} [\cos(\theta/2)|g\rangle + \sin(\theta/2)|e\rangle] \otimes |\alpha\rangle$,
- ❖ $\theta < \pi$, rotation around y-axis — **single qubit gate**.
- ❖ **Weak values interpretation:**
- ❖ **unlikeness** of finding the qubit in the post-selected state: $|g\rangle$

Wigner function negativity

$t = \tau$

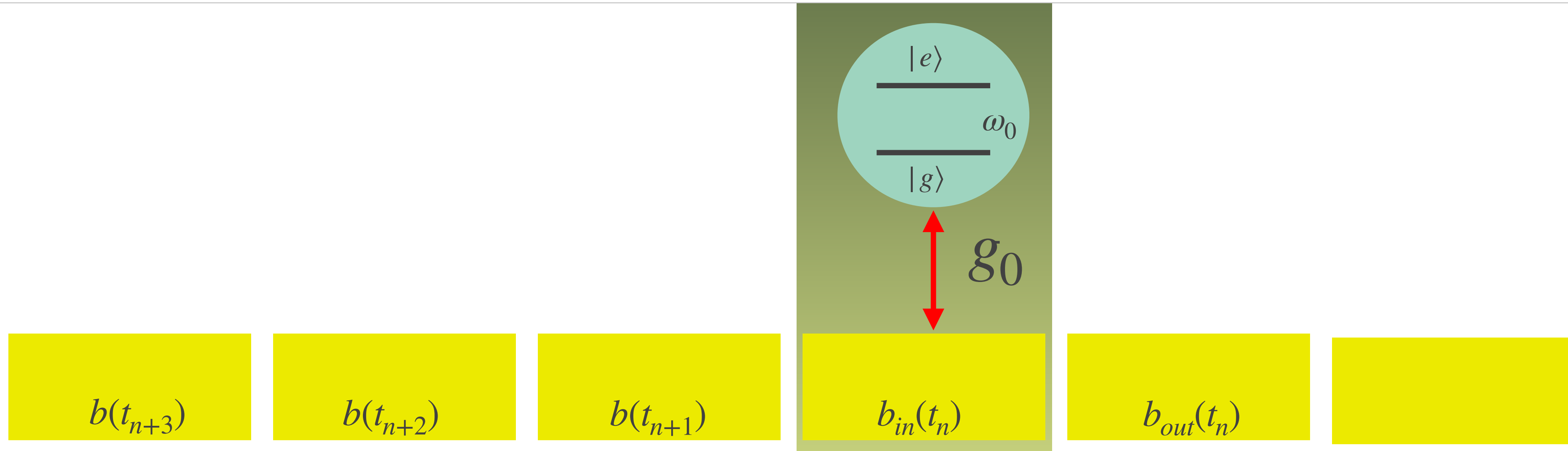


Take away messages 3

- ❖ Analytical expression of atom-field wave-function → Weak value of field's energy change & field's conditional Wigner functions
- ❖ Weak value **exceeding single quantum** → anomalous values → **contextuality**
- ❖ Anomalous weak values of energy change → Wigner negativity

Chapter 4: SPI

Interaction picture & time discretization: The emitter interacts with one *temporal mode* at a time, repeatedly → Collisional model interpretation.



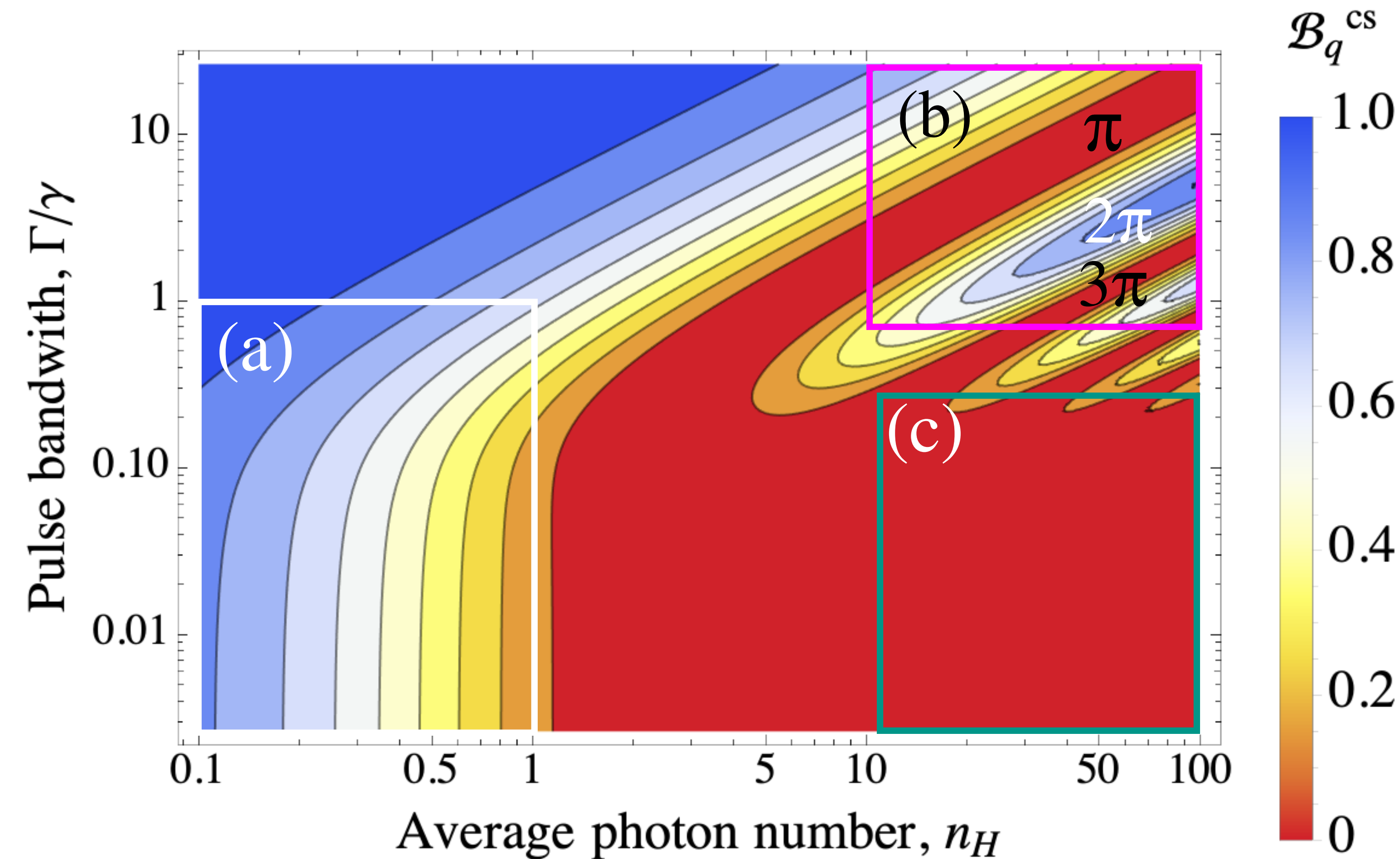
$$V_{qf} \xrightarrow{H_0} V_{qf}(t) = i g_0 \sum_{k=0}^{\infty} \left(\sigma^\dagger(t) e^{-i\omega_k t} a_k - e^{i\omega_k t} a_k^\dagger \sigma(t) \right)$$

$$\xrightarrow{t_n = n\Delta t} V_{qf}(t_n) = i \sqrt{\frac{\gamma}{\Delta t}} (\sigma^\dagger(t_n) b(0, t_n) - \sigma(t_n) b^\dagger(0, t_n))$$

$$\text{With } b(0, t_n) = b(t_n) \equiv \frac{b_n}{\sqrt{\Delta t}} = \sqrt{\frac{\Delta t}{\gamma}} \sum_{k=0}^{\infty} e^{-i\omega_k t_n} a_k$$

$$V_{qf}(t_n) = V_n = i \sqrt{\frac{\gamma}{\Delta t}} [\sigma^\dagger(t_n) b(t_n) - b^\dagger(t_n) \sigma(t_n)]$$

Spin-light entanglement: Coherent state

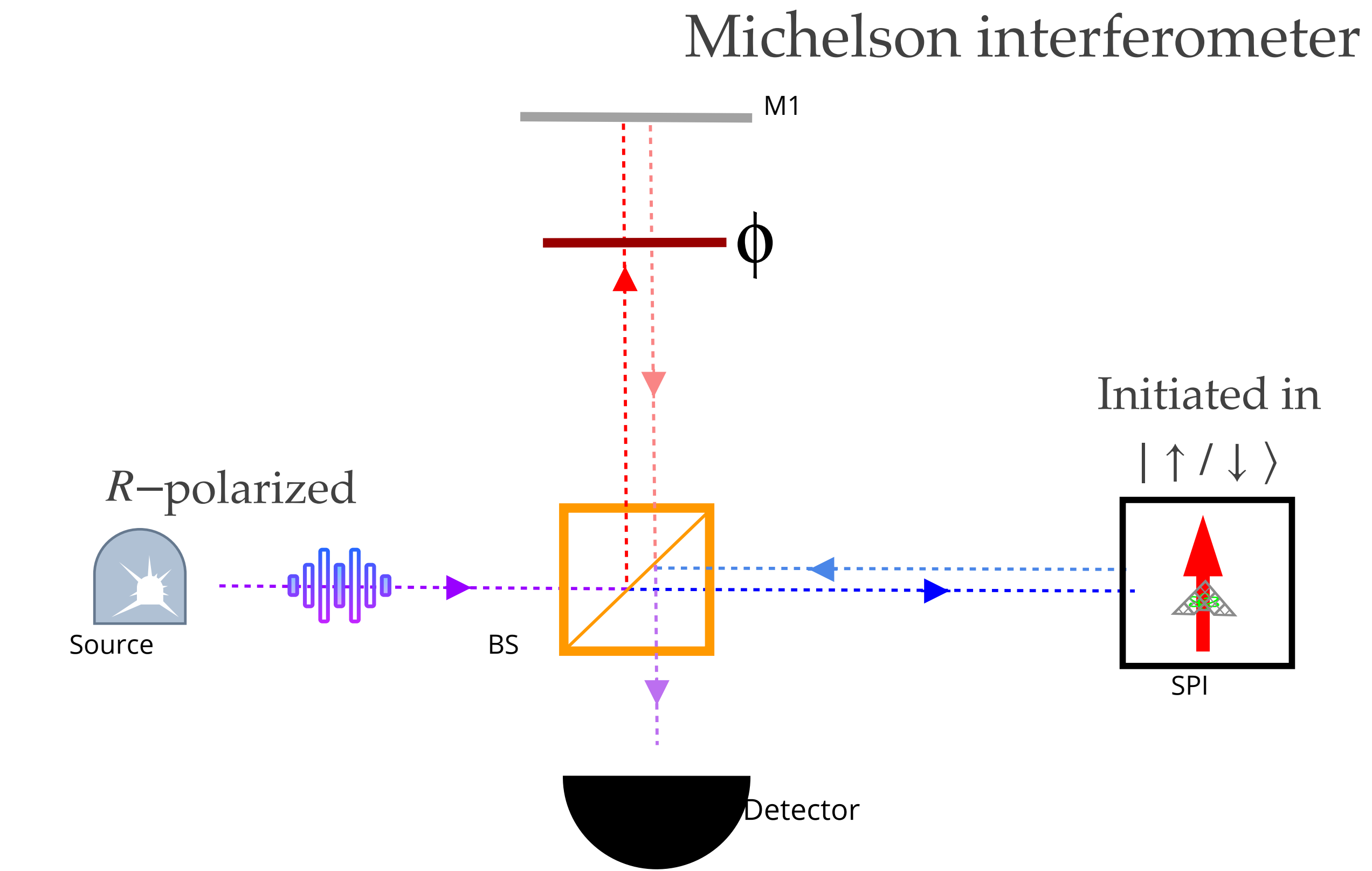
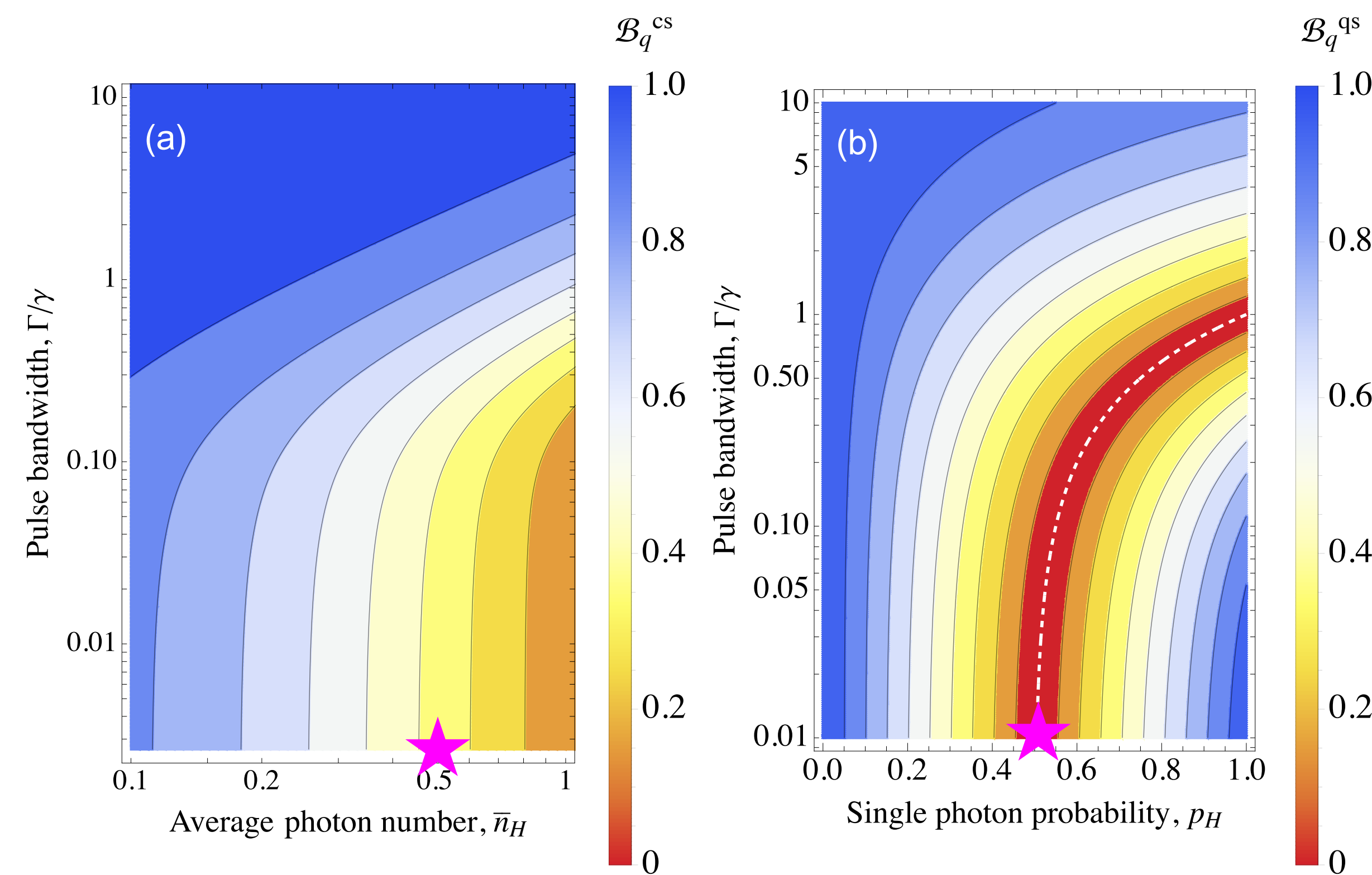


Phase measurement

- ❖ Regime: $\bar{n}_H = p_H = 0.5$, and
- ❖ $\Gamma = 10^{-2}\gamma$

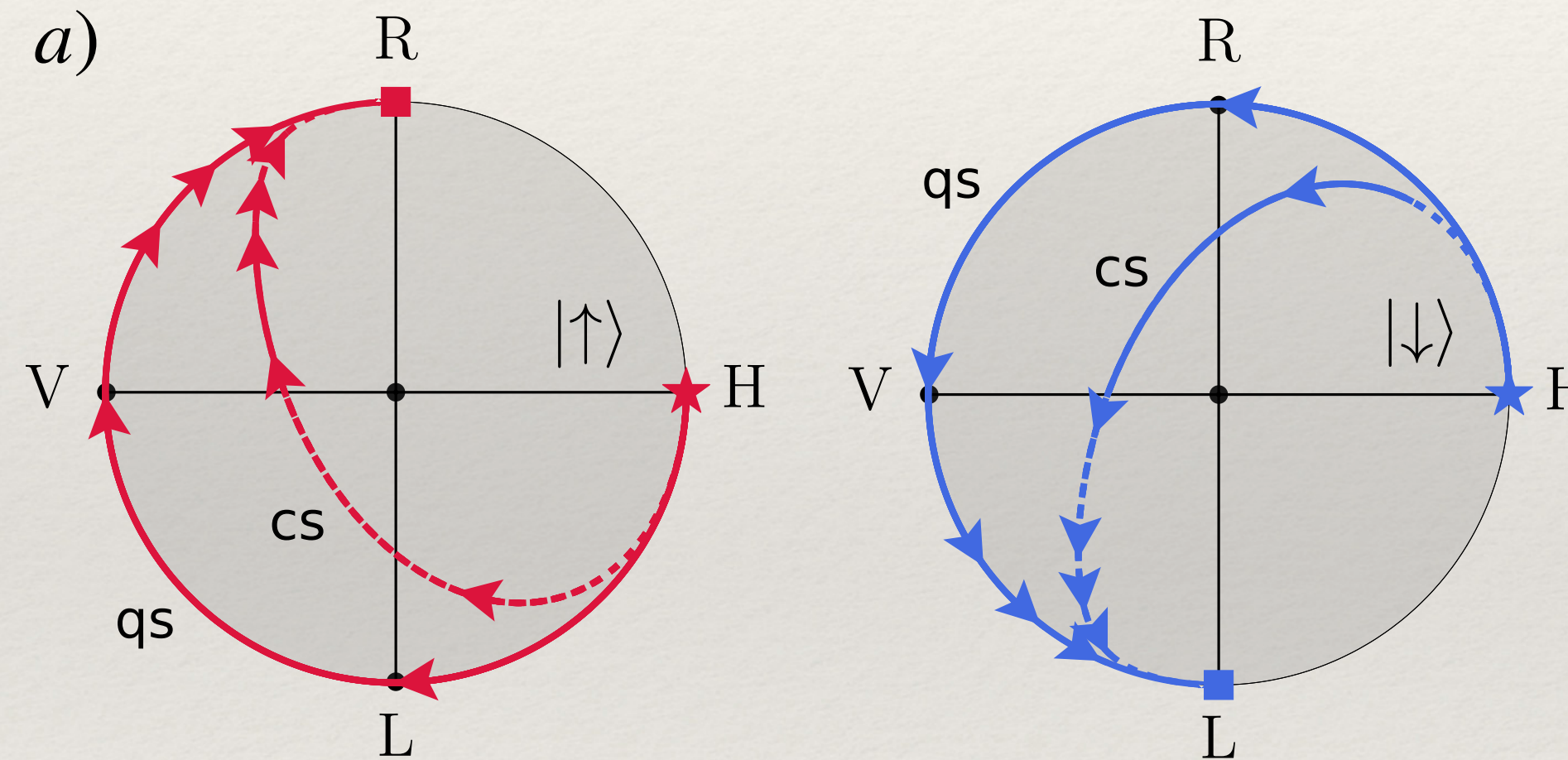
$$|\uparrow(\downarrow),1_{R(L)}\rangle \rightarrow -|\uparrow(\downarrow),1_{R(L)}\rangle$$

$$|\downarrow(\uparrow),1_{R(L)}\rangle \rightarrow |\downarrow(\uparrow),1_{R(L)}\rangle$$

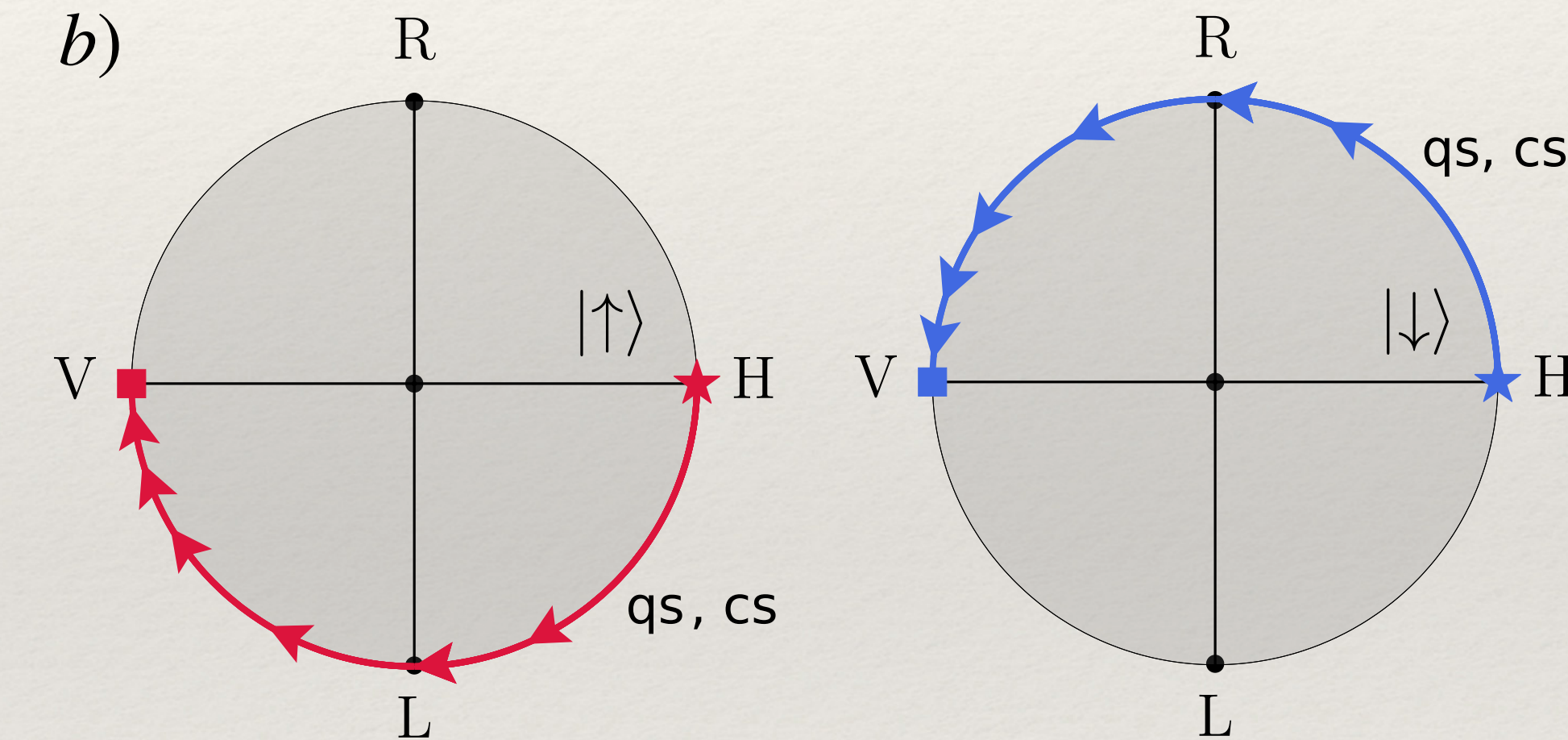


Polarization evolution in the Poincaré spheres

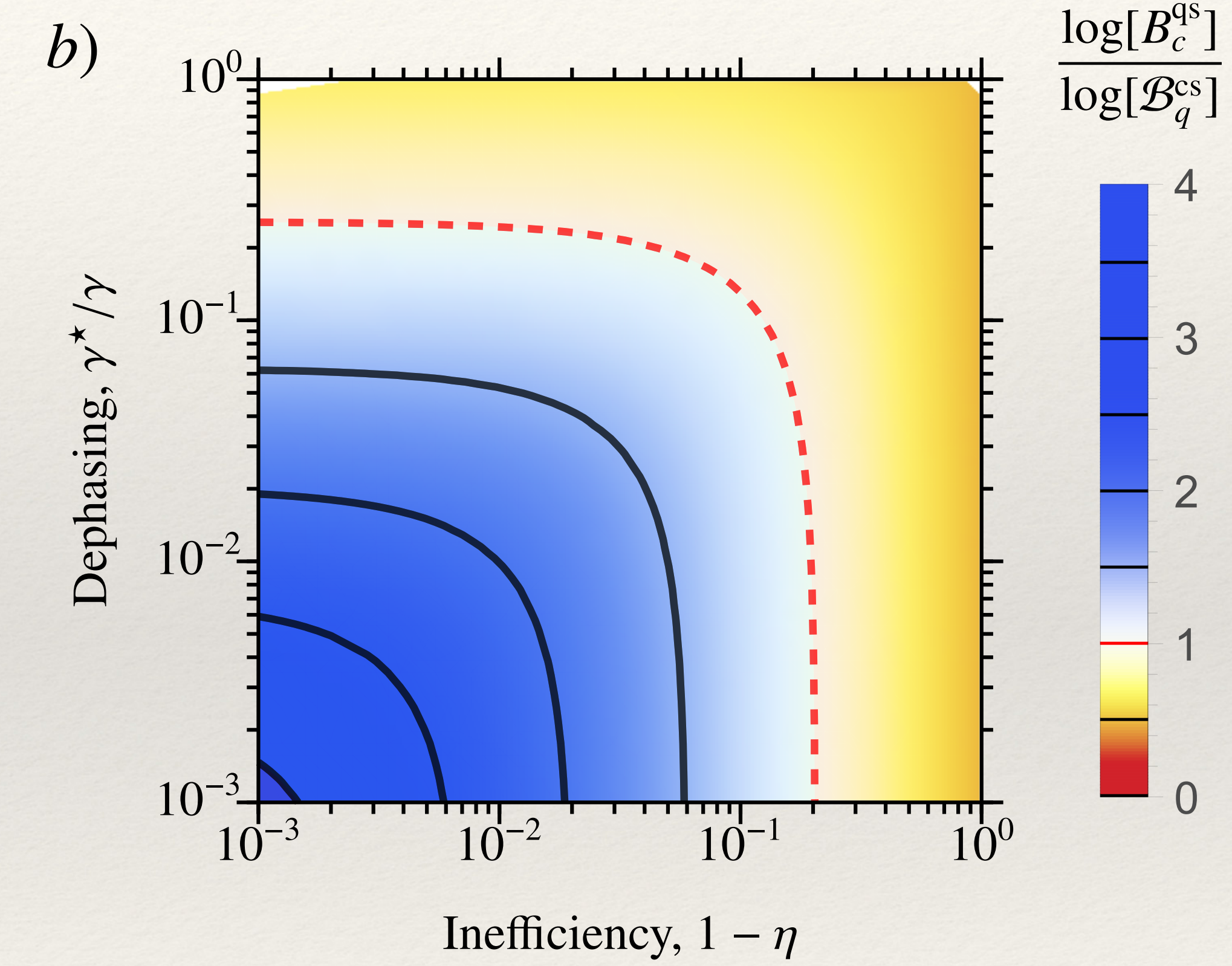
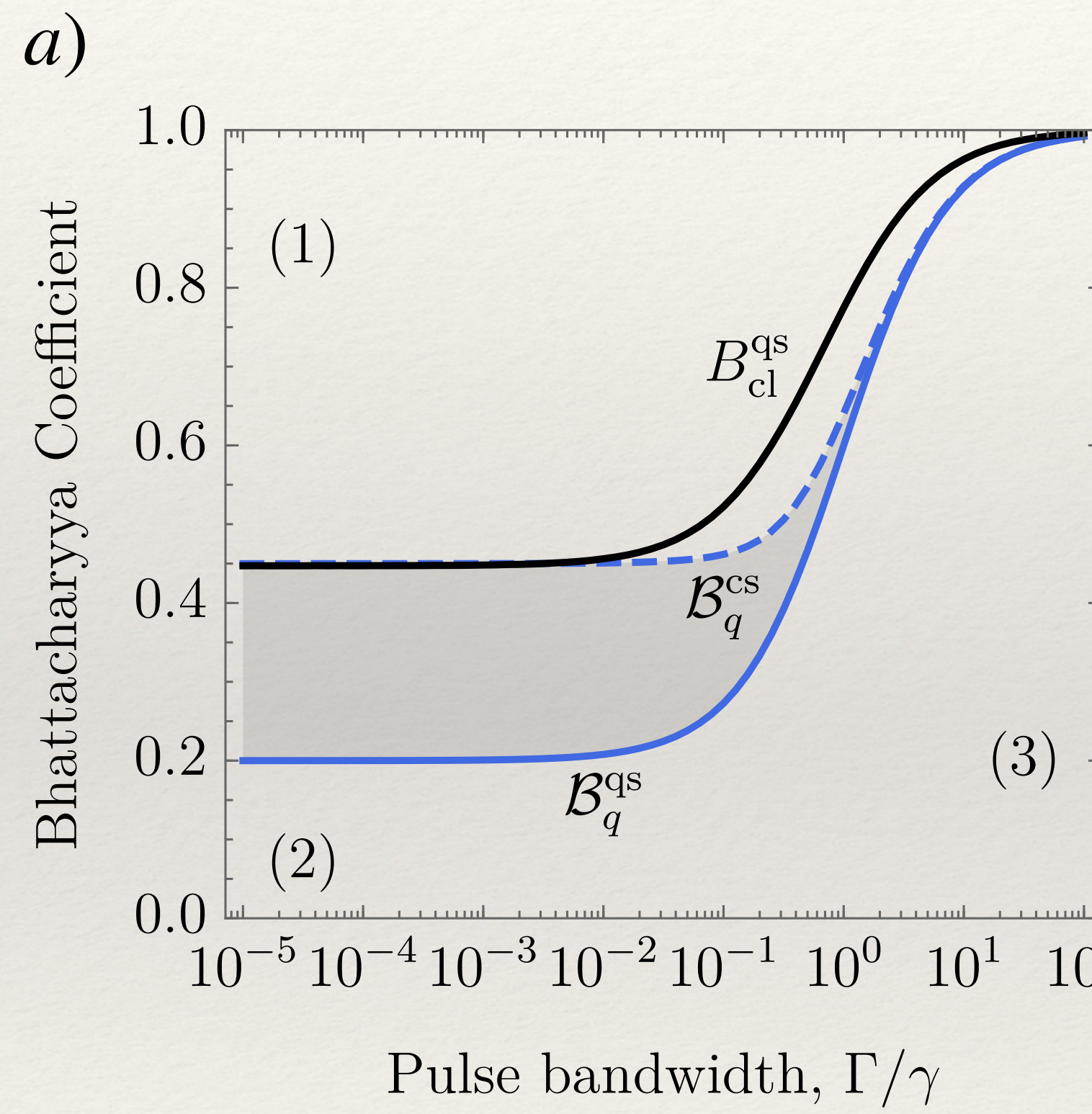
Pulsed regime: $\Gamma/\gamma = 1$



Quasi-monochromatic regime: $\Gamma/\gamma \ll 1$



Robustness of readout against dephasing



Take away messages 3

- ❖ **Low-energy regime** → restricted budget: one excitation on average
 - ❖ Compared coherent field with quantum superposition of zero and single photon states
- ❖ **Quantum advantage 1:** superposition of zero and single photon produces **better entanglement**
- ❖ **Quantum advantage 2:** maintained when spin state information extracted at classical level
- ❖ Relevant for technological applications such as **photon-photon gate** and **cluster states**.
- ❖ With the von Neumann measurement model & collisional model solution

Chapter 4: phase gate

3rd main result: possible to implement the c-phase gate, and access to the coherent error associated with the finite pulse duration

Gate action for $| \uparrow \rangle$:

Ideal	Real
$ 00\rangle \xrightarrow{G_{\uparrow}^{[1]}} 00\rangle$	$ 00\rangle \xrightarrow{G_{\uparrow}^{[1]}} 00\rangle$
$ 01\rangle \xrightarrow{G_{\uparrow}^{[1]}} - 01\rangle$	$\xrightarrow{\tilde{m} \neq 1} 01\rangle \xrightarrow{G_{\uparrow}^{[1]}} -\tilde{m} 01\rangle \equiv -e^{i\varepsilon_{\uparrow}}$
$ 10\rangle \xrightarrow{G_{\uparrow}^{[1]}} 10\rangle$	$ 10\rangle \xrightarrow{G_{\uparrow}^{[1]}} 10\rangle$
$ 11\rangle \xrightarrow{G_{\uparrow}^{[1]}} 11\rangle$	$ 11\rangle \xrightarrow{G_{\uparrow}^{[1]}} \frac{1}{2}(\tilde{m}^2 + 1) 11\rangle \equiv e^{i\delta_{\uparrow}}$

Gate errors:

$$\varepsilon_{\uparrow} = 2\pi - i \text{Log} \left\{ -\frac{(\tilde{m}^2 + 2\tilde{m} - 1)}{2} \right\}$$

$$\delta_{\uparrow} = 2\pi - i \text{Log} \left\{ \frac{\tilde{m} + 1}{2} \right\}$$

Gate action for $| \downarrow \rangle$:

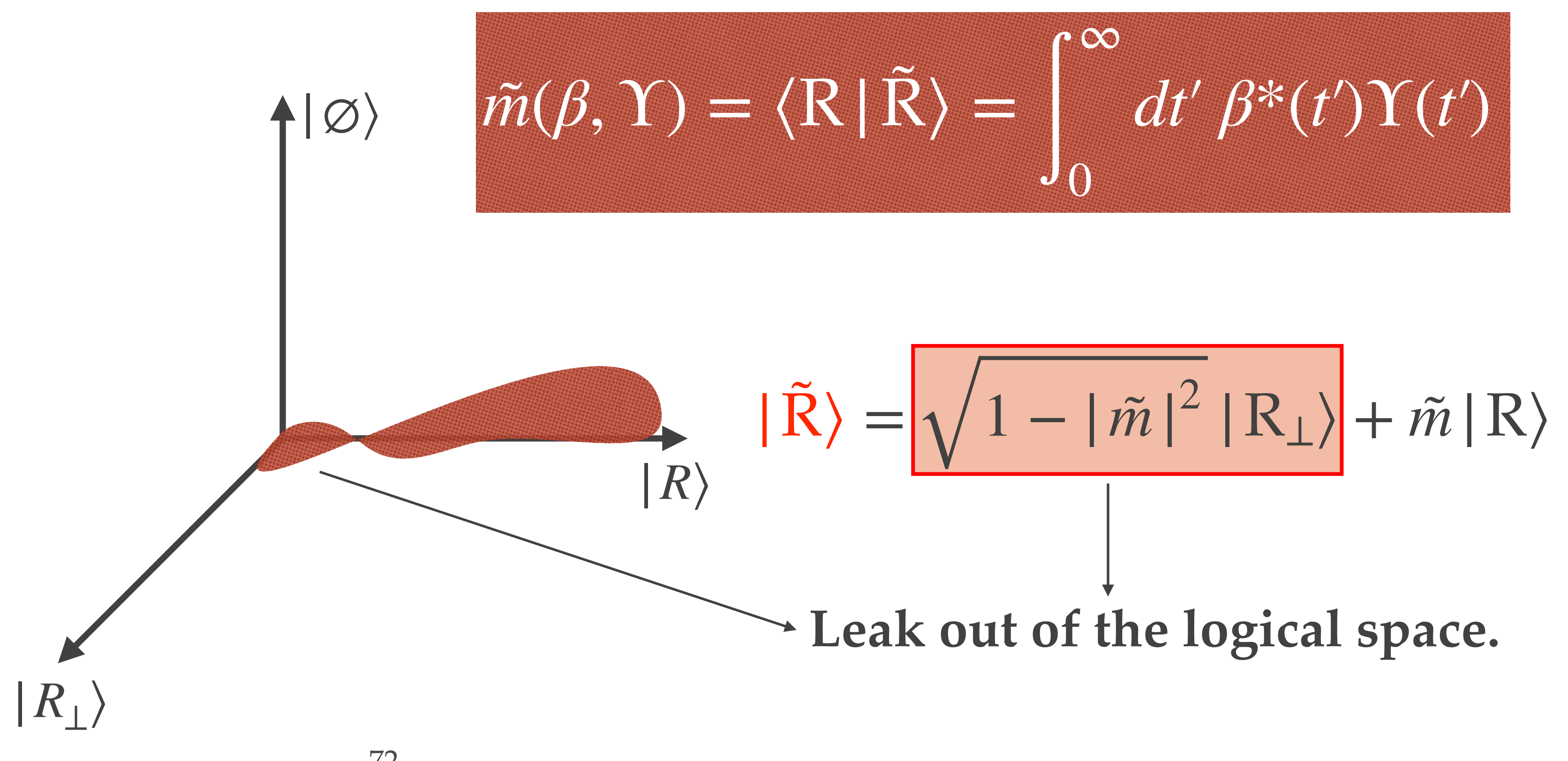
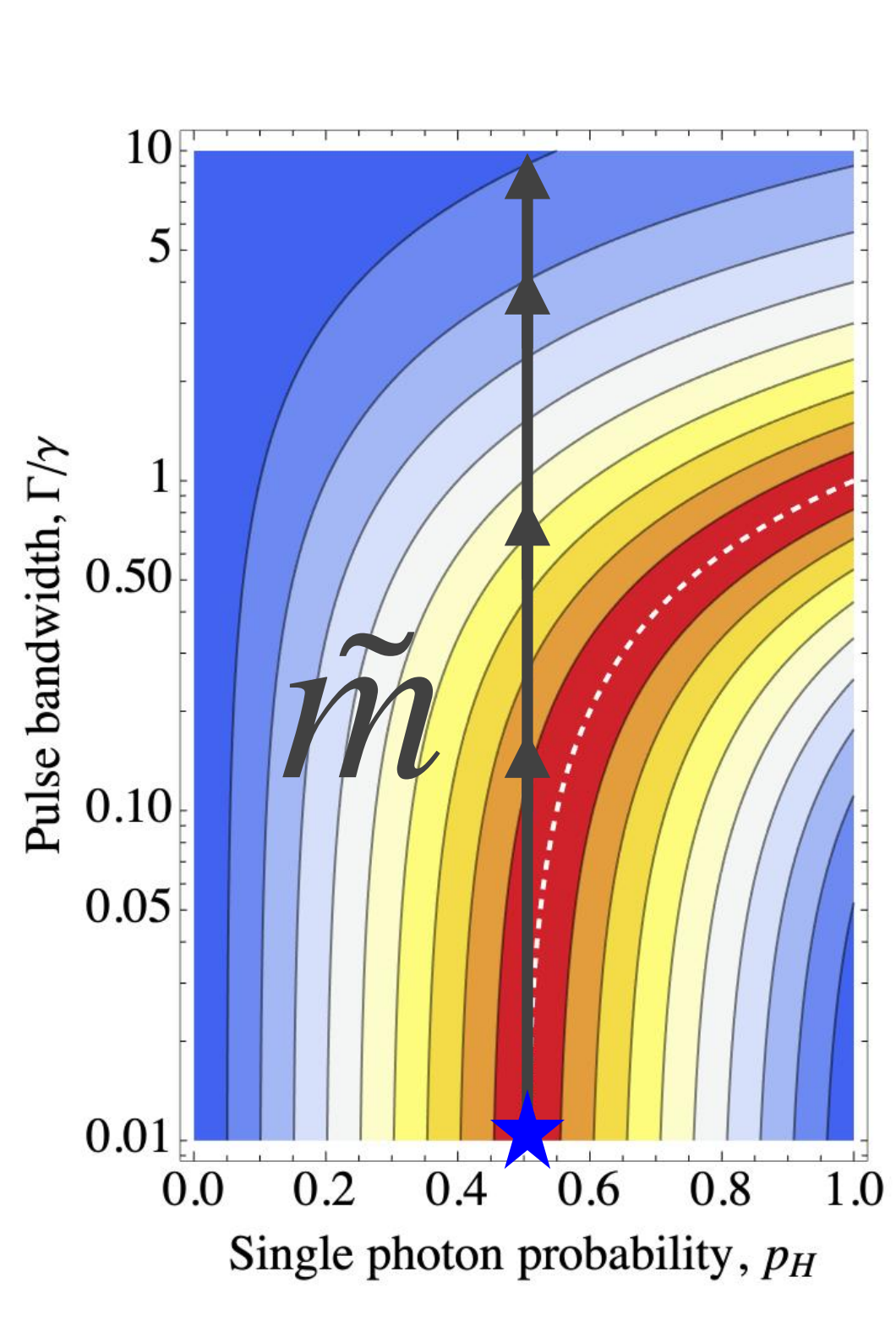
Ideal	Real
$ 00\rangle \xrightarrow{G_{\uparrow}^{[1]}} - 00\rangle$	$ 00\rangle \xrightarrow{G_{\uparrow}^{[1]}} - 00\rangle$
$ 01\rangle \xrightarrow{G_{\uparrow}^{[1]}} - 01\rangle$	$ 01\rangle \xrightarrow{G_{\uparrow}^{[1]}} - 01\rangle$
$ 10\rangle \xrightarrow{G_{\uparrow}^{[1]}} - 10\rangle$	$\xrightarrow{\tilde{m} \neq 1} 10\rangle \xrightarrow{G_{\uparrow}^{[1]}} - 10\rangle$
$ 11\rangle \xrightarrow{G_{\uparrow}^{[1]}} 11\rangle$	$ 11\rangle \xrightarrow{G_{\uparrow}^{[1]}} \frac{1}{2}(\tilde{m}^2 + 2\tilde{m} - 1) 11\rangle \equiv -e^{i\varepsilon_{\downarrow}}$

Gate error:

$$\varepsilon_{\downarrow} = 2\pi - i \text{Log} \{-\tilde{m}\}$$

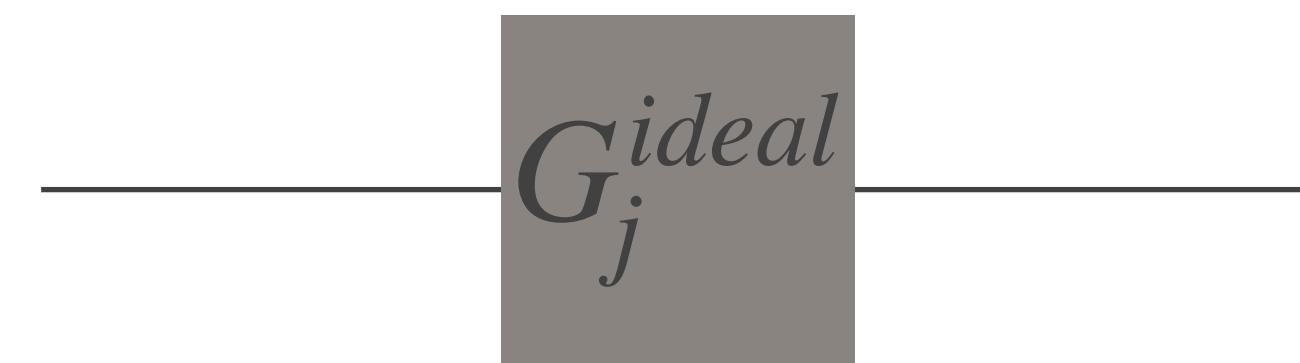
Leakage out of the logical basis due to pulse finite duration

- ❖ The protocol works in the quasi-monochromatic regime.
- ❖ What is the effect of a finite pulse duration?

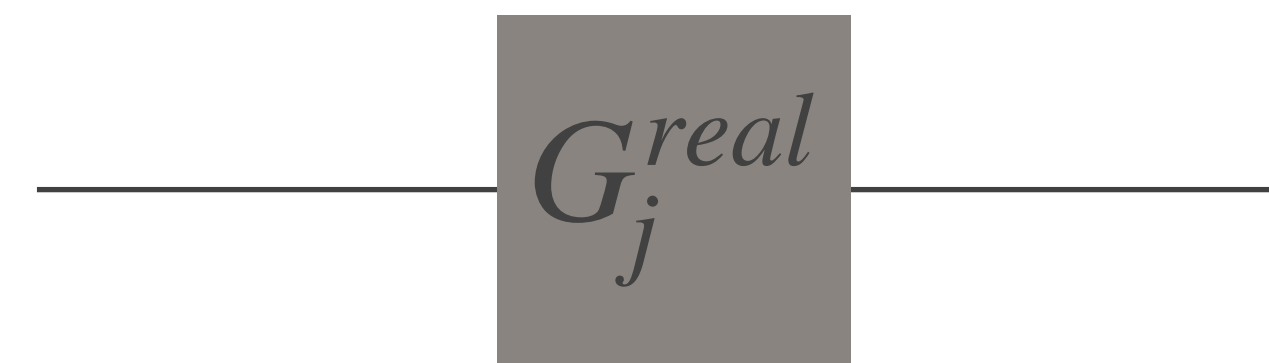


Coherent errors

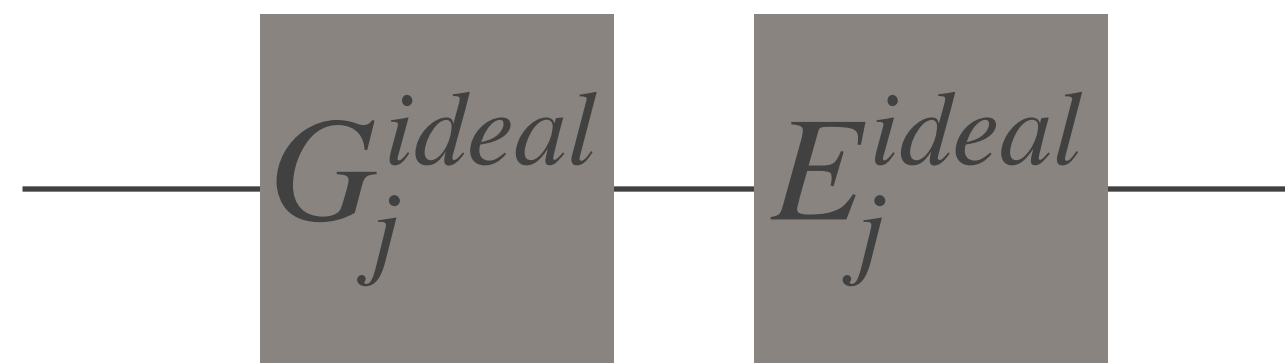
Ideal gate



Noisy real gate



||



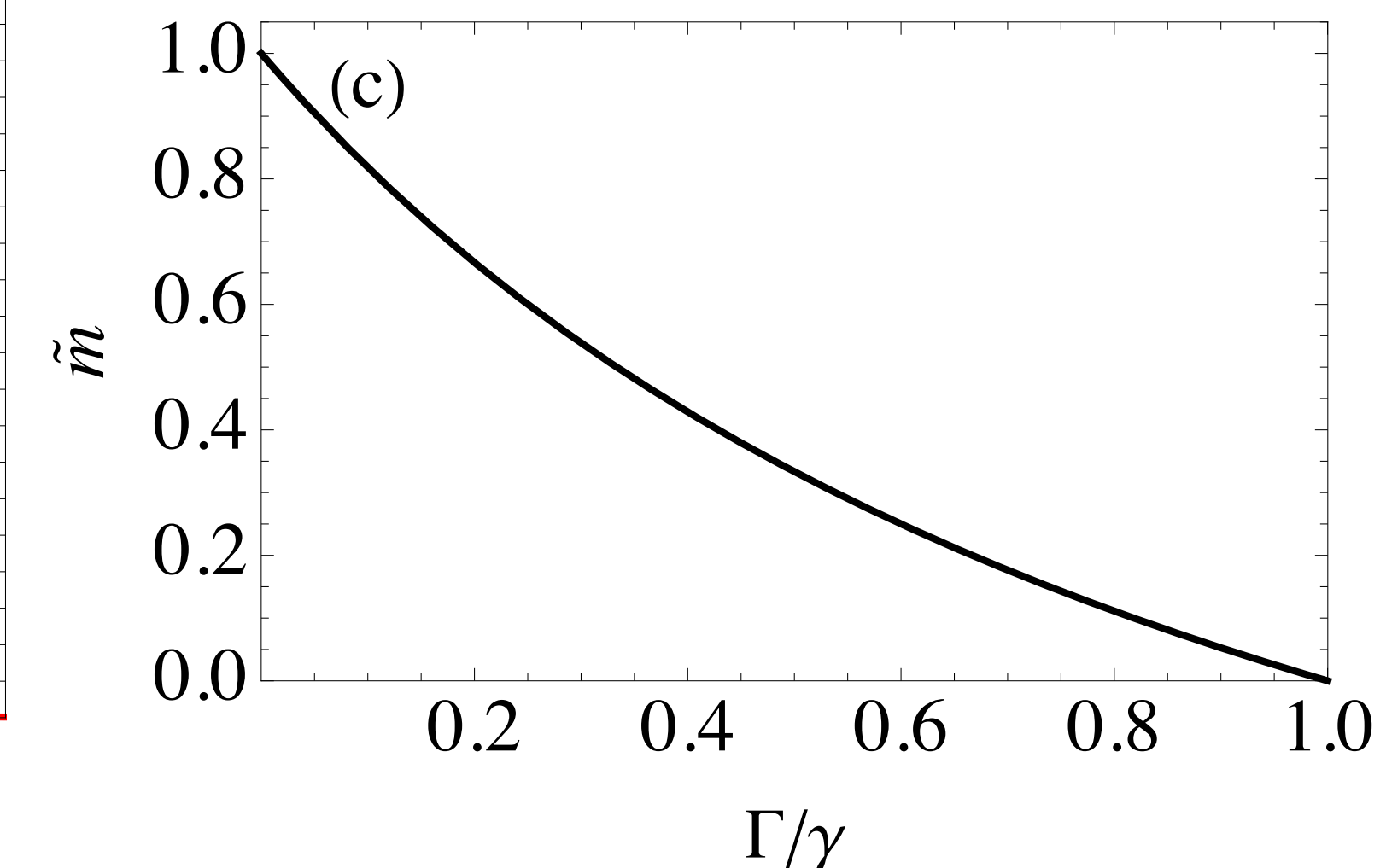
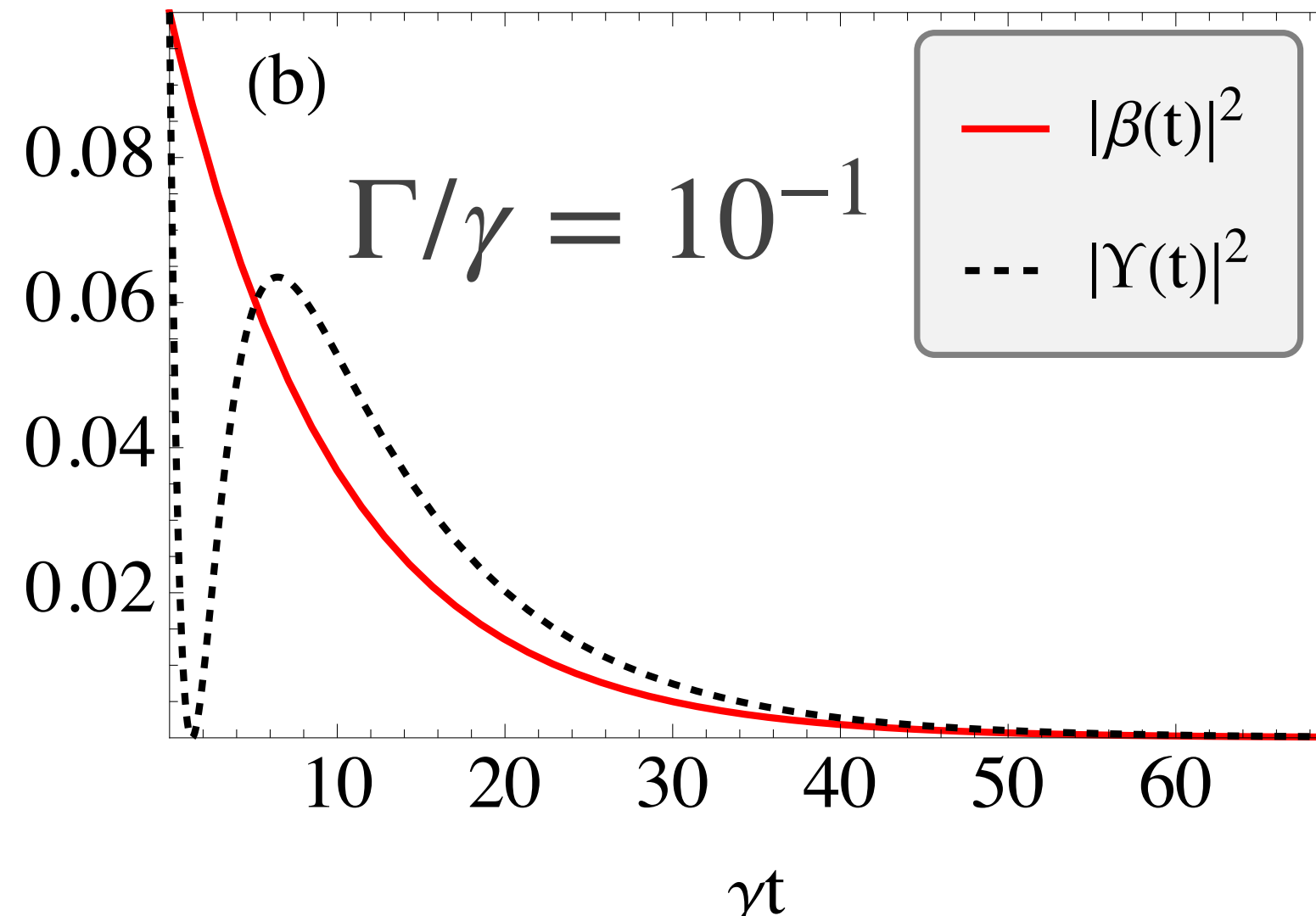
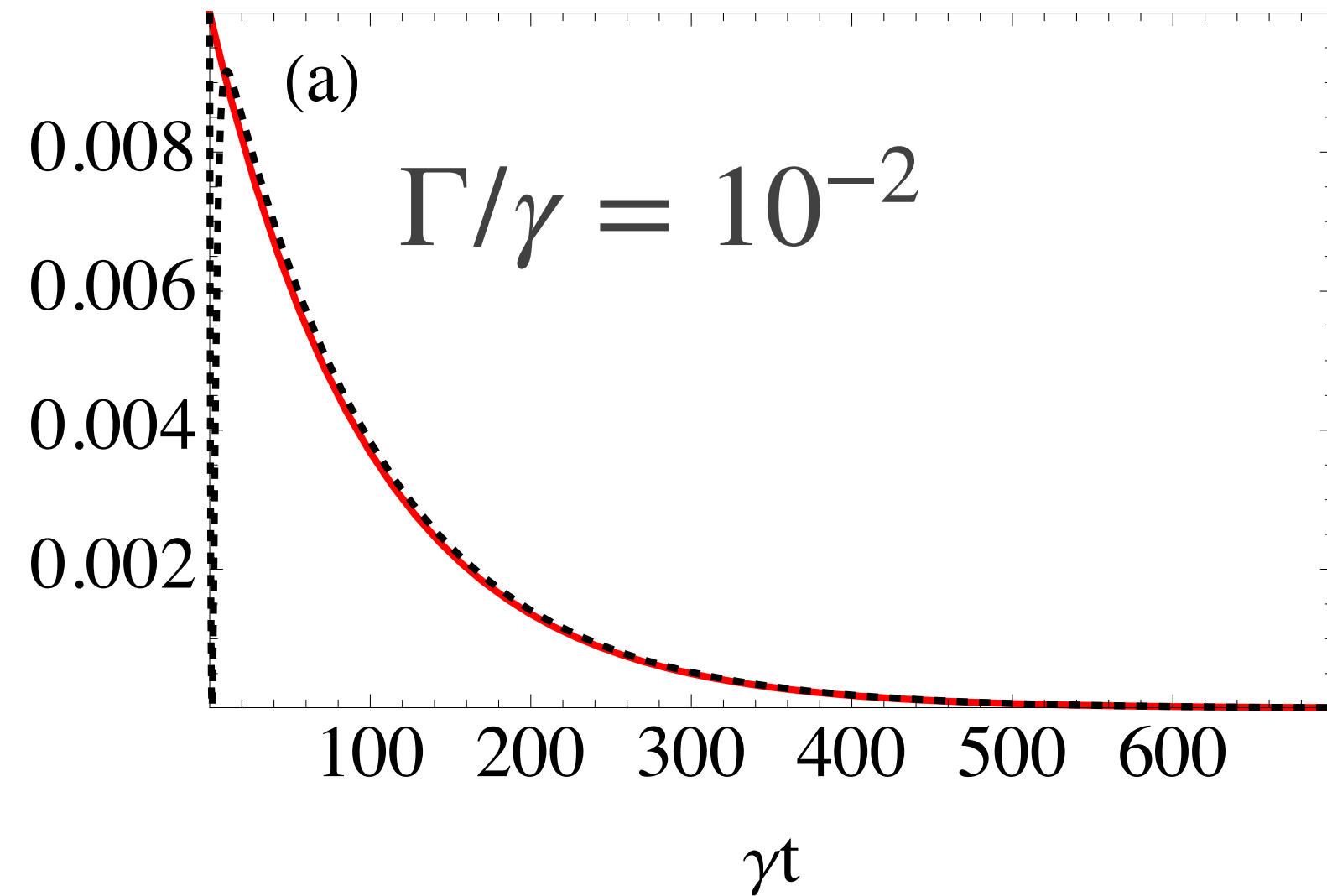
Quantifying the non-monochromaticity

- ❖ “Non-monochromaticity” of the scattering process:

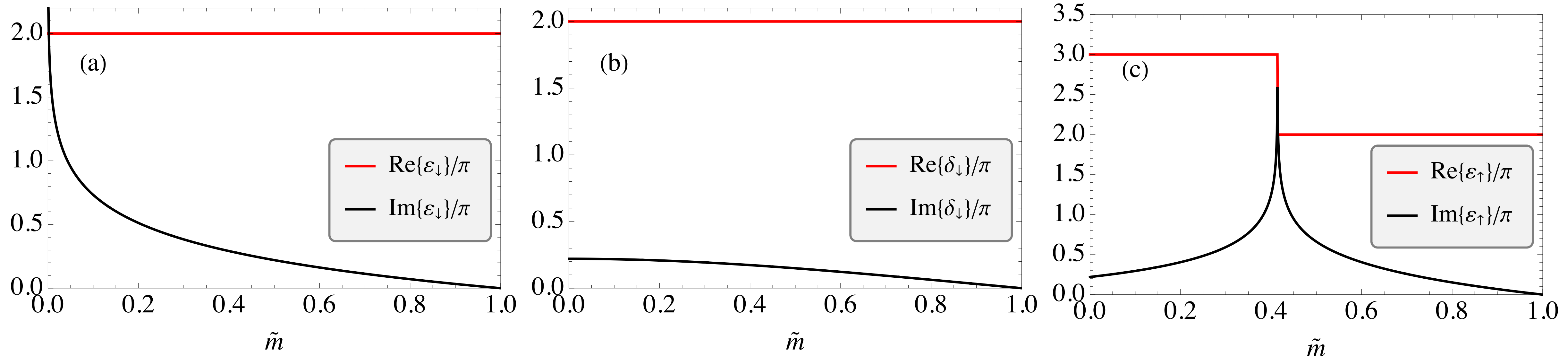
$$\diamond \tilde{m} = \langle R | \tilde{R} \rangle$$

$$|R\rangle = \int dt \beta(t) b_R^\dagger(t) |0\rangle \rightarrow |\tilde{R}\rangle = \int dt \Upsilon(t) b_R^\dagger(t) |0\rangle$$

$$\tilde{m}(\beta, \Upsilon) = \int_0^\infty dt' \beta^*(t') \Upsilon(t')$$



Error analysis: Gate errors



Error matrix

$$G_j^{\text{real}} = E_j G_j^{\text{ideal}} \rightarrow E_j = G_j^{\text{real}} \left(G_j^{\text{ideal}} \right)^{-1}$$

Pauli error model

$$\mathcal{B}_P = \left\{ 1 \equiv I, \sigma_x \equiv X, \sigma_y \equiv Y, \sigma_z \equiv Z \right\}$$

Decompose the error in a Pauli basis

$$\mathcal{B}_2 = (\mathcal{B}_P)^{\otimes 2}$$

Initial photonic state $\rho_0^{\text{photonic}} \rightarrow \sum_{B \in \mathcal{B}_2} p_B B \rho B^\dagger$

Pauli error probabilities

Take away messages 4

- ❖ It is possible to realize a controlled phase gate using the spin in the QD as the non-linear feature.
- ❖ Our detailed modeling of the gate also allowed us to analyze the **gate's error** using the Error matrix formalism.
- ❖ We accomplished this leveraging the collisional model solution.

Chapter 5

5th main result: spontaneous emission wave function obtained from the collisional model featuring the parameters

$$\begin{aligned}
|\Psi^\zeta(t)\rangle &= \left(\exp \left\{ -\frac{\gamma}{2}t \right\} \langle \uparrow_z | \mathcal{R}_e | \zeta \rangle \right) |e\rangle |\uparrow_z\rangle |\emptyset\rangle |\emptyset\rangle \\
&+ \left(\exp \left\{ -\frac{\gamma}{2}t \right\} \langle \downarrow_z | \mathcal{R}_e | \zeta \rangle \right) |e\rangle |\downarrow_z\rangle |\emptyset\rangle |\emptyset\rangle \\
&+ \left(\int_0^t du \langle \uparrow_z | \mathcal{R}_g(t-u) | \uparrow_z \rangle \sqrt{\gamma} b_R^\dagger \exp \left\{ -\frac{\gamma}{2}u \right\} \langle \uparrow_z | \mathcal{R}_e(u) | \zeta \rangle \right) |g\rangle |\uparrow_z\rangle |\emptyset\rangle |\emptyset\rangle \\
&+ \left(\int_0^t du \langle \uparrow_z | \mathcal{R}_g(t-u) | \downarrow_z \rangle \sqrt{\gamma} b_L^\dagger \exp \left\{ -\frac{\gamma}{2}u \right\} \langle \downarrow_z | \mathcal{R}_e(u) | \zeta \rangle \right) |g\rangle |\uparrow_z\rangle |\emptyset\rangle |\emptyset\rangle \\
&+ \left(\int_0^t du \langle \downarrow_z | \mathcal{R}_g(t-u) | \uparrow_z \rangle \sqrt{\gamma} b_R^\dagger \exp \left\{ -\frac{\gamma}{2}u \right\} \langle \uparrow_z | \mathcal{R}_e(u) | \zeta \rangle \right) |g\rangle |\downarrow_z\rangle |\emptyset\rangle |\emptyset\rangle \\
&+ \left(\int_0^t du \langle \downarrow_z | \mathcal{R}_g(t-u) | \downarrow_z \rangle \sqrt{\gamma} b_L^\dagger \exp \left\{ -\frac{\gamma}{2}u \right\} \langle \downarrow_z | \mathcal{R}_e(u) | \zeta \rangle \right) |g\rangle |\downarrow_z\rangle |\emptyset\rangle |\emptyset\rangle
\end{aligned}$$

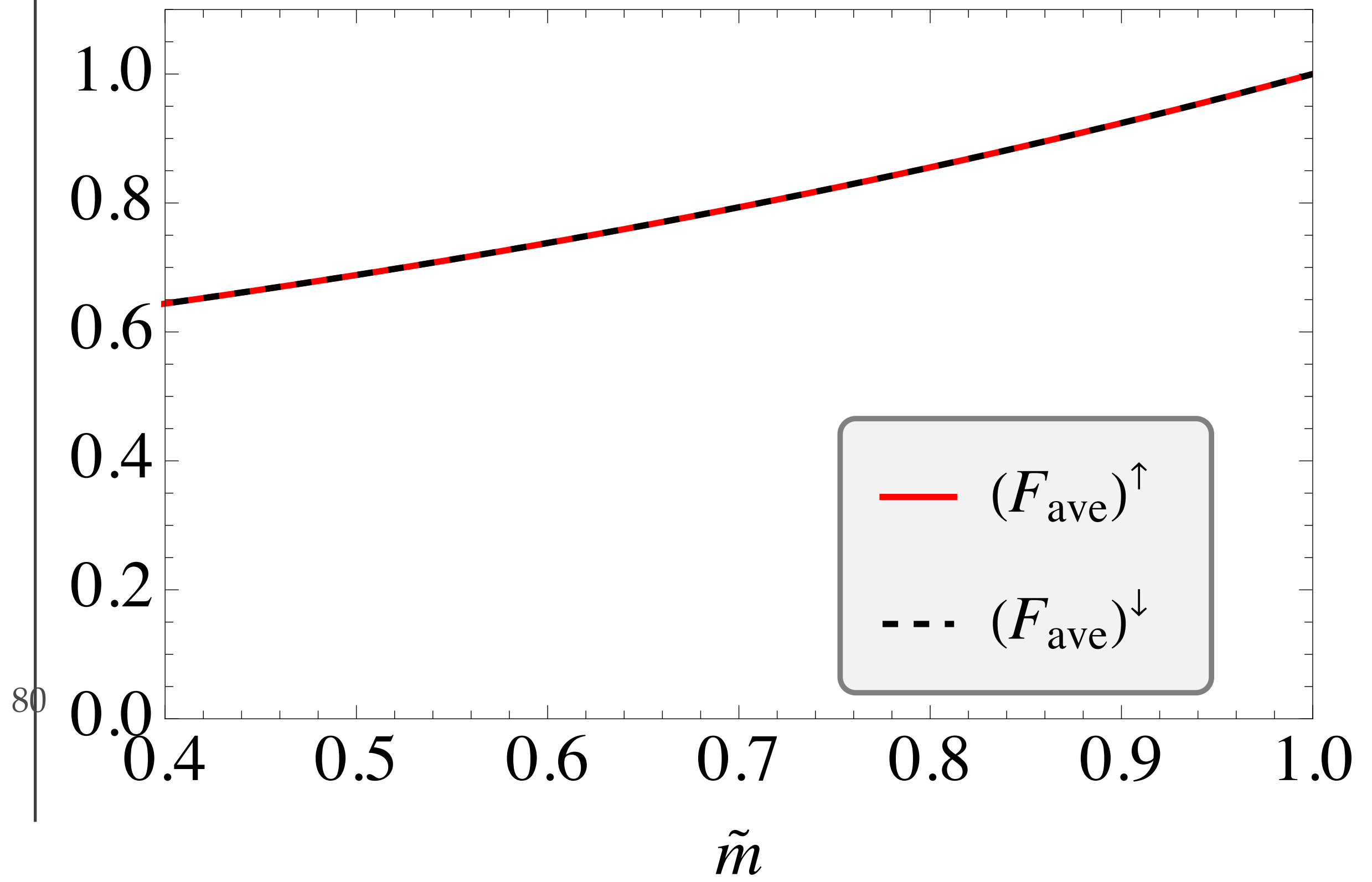
Notation

$$\begin{aligned}
|\uparrow\uparrow(\downarrow\downarrow)\rangle &= |\uparrow_z(\downarrow_z)\rangle |e\rangle \\
|\uparrow\downarrow(\downarrow\uparrow)\rangle &= |\uparrow_z(\downarrow_z)\rangle |g\rangle
\end{aligned}$$

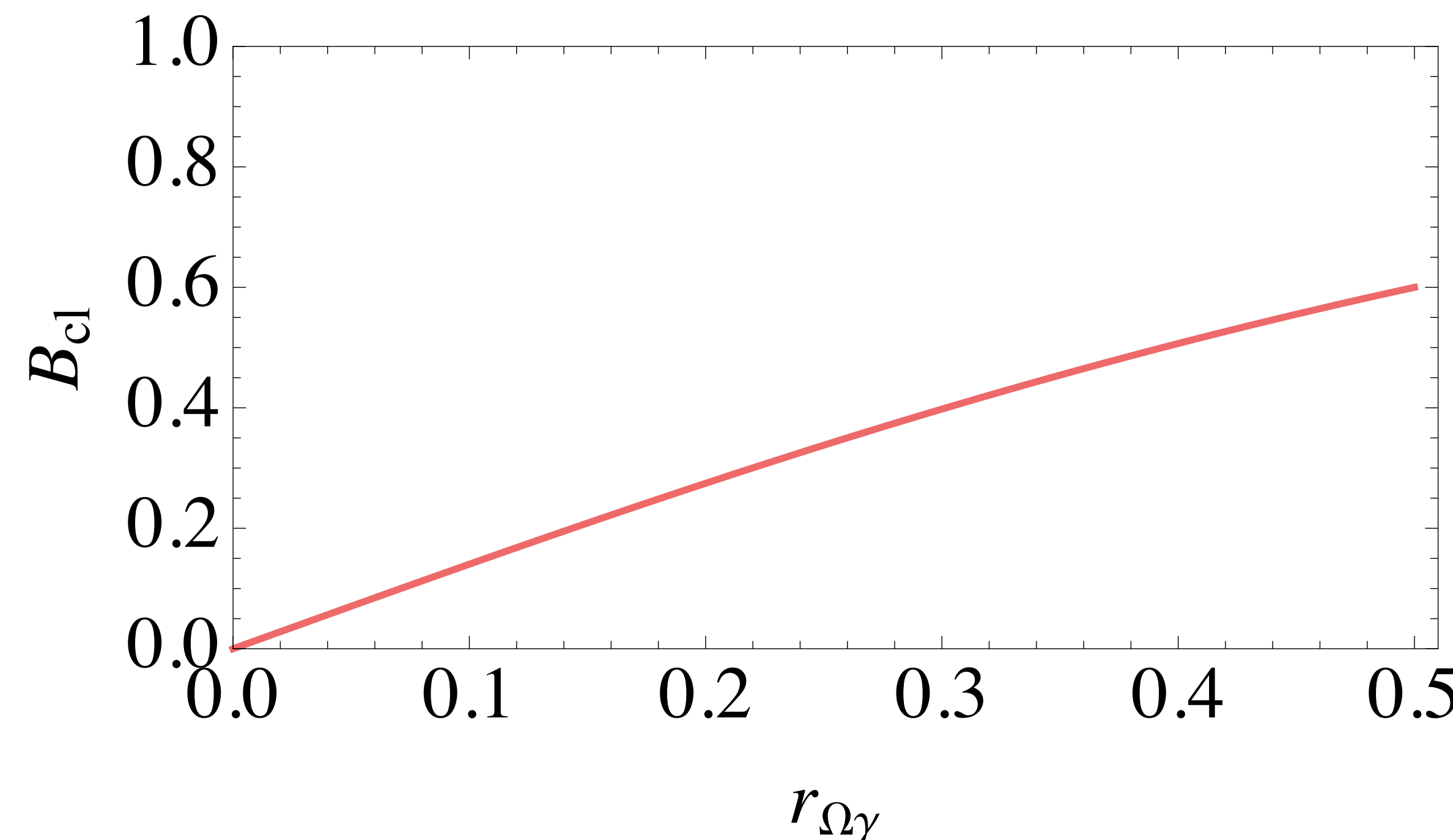
Error analysis: Gate fidelity

$$F_{\text{ave}}^j(G_j^{\text{real}}, G_j^{\text{target}}) \equiv \frac{\text{tr} \left\{ (G_j^{\text{real}})^\dagger G_j^{\text{real}} \right\} + |\text{tr} \left\{ (G_j^{\text{target}})^\dagger G_j^{\text{real}} \right\}|^2}{20}$$

$$F_{\text{ave}}^j = \frac{1}{20} \left(4 + \frac{1}{4} (5 + \tilde{m}(2 + \tilde{m}))^2 \right)$$



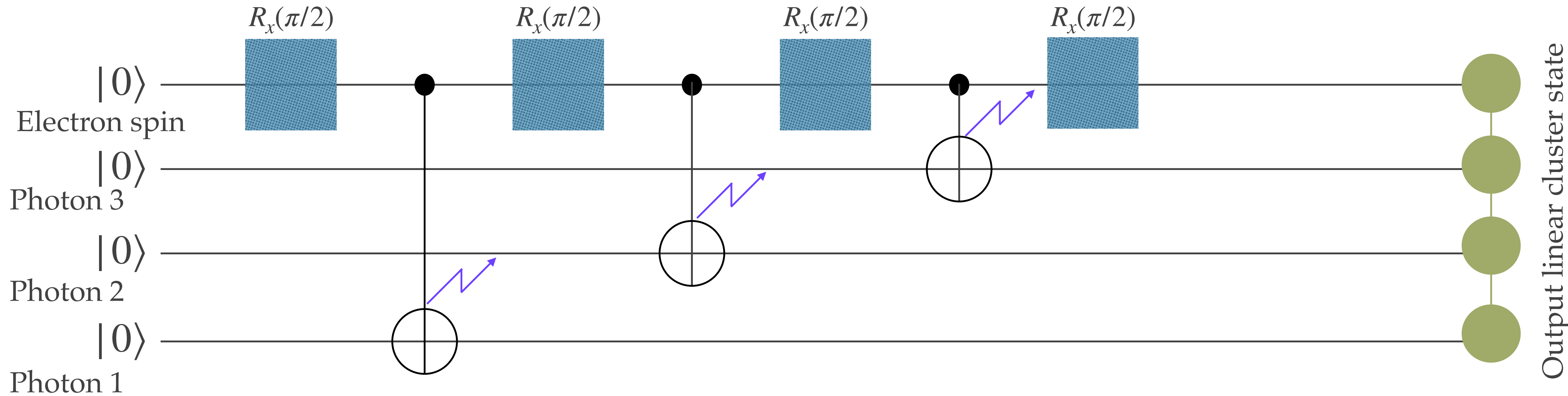
Spin read-out benchmark vs. $r_{\Omega\gamma}$



What is the LRP and how does it work?

- ❖ Two ingredients:
 - ❖ π -pulses
 - ❖ Spin rotations

$$\frac{1}{\sqrt{2}} \left(| \uparrow \rangle \left(\frac{| 1_R \rangle_1 - i | 1_L \rangle_1}{\sqrt{2}} \right) | 1_R \rangle_2 - i | \downarrow \rangle \left(\frac{| 1_R \rangle_1 + i | 1_L \rangle_1}{\sqrt{2}} \right) | 1_L \rangle_2 \right)$$



[1] Lindner, N. H. & Rudolph, T. Proposal for Pulsed On-Demand Sources of Photonic Cluster State Strings. Phys. Rev. Lett. 103, 113602 (2009).

Take away messages 5

- ❖ We extended the collisional model solution for the SPI introducing a in-plane magnetic field.
- ❖ The model's solution matches experimental data.
- ❖ We used it to study the fidelity of the emitter state
- ❖ We may also obtain the fidelity of the generated cluster state.

Coherent field & Single photon solutions

Coherent input field

$$|\Psi_{CS}(0)\rangle = \bigotimes_{n=0}^N D(\beta_n) |\emptyset\rangle \otimes |\zeta\rangle, \zeta = g, e$$

$$|\Psi_{\beta}^{\zeta}(t_N)\rangle = \sqrt{P_g(t)} |g\rangle |\phi_g(t)\rangle + \sqrt{P_e(t)} |e\rangle |\phi_e(t)\rangle$$

$$|\phi_e\rangle = \frac{1}{\sqrt{P_e(t)}} \left[\sqrt{p_{0,e}} \tilde{f}_{\varepsilon,\zeta}^{(0)}(t) + \sum_{m=1}^{\infty} \sqrt{p_{m,e}(t)} \int_0^t ds_m \tilde{f}_{\varepsilon,\zeta}^{(m)}(t,s) \prod_{i=1}^m b_i^\dagger \right] |\emptyset\rangle$$

Suffices to find the coefficients: possible to do analytically.

Single photon input field

$$|\Psi_{SP}(0)\rangle = \sum_{n=0}^{\infty} \sqrt{\Delta t} \beta(t_n) b_n^\dagger |\emptyset\rangle \otimes |g\rangle \quad \sum_{n=0}^{\infty} \Delta t |\beta(t_n)| = 1$$

$$|\Psi_{SP}(t_N)\rangle = \left(\sqrt{\gamma \Delta t} e^{-\frac{\gamma}{2} t_N} \sum_{n=0}^{N-1} \sqrt{\Delta t} e^{(\frac{\gamma}{2} + i\omega_0)t_n} \xi(t_n) |\emptyset\rangle \right) \otimes |e\rangle$$

$$+ \left(\sum_{n=0}^{N-1} \sqrt{\Delta t} \Upsilon(t_n) b_n^\dagger |\emptyset\rangle \right) \otimes |g\rangle$$

$$+ \left(\sum_{n=N}^{\infty} \sqrt{\Delta t} \beta(t_n) b_n^\dagger |\emptyset\rangle \right) \otimes |g\rangle.$$

Already interacted.

Part that is yet to interact.